STRUCTURAL STUDIES ON THE ANTIBIOTICS VANCOMYCIN, RISTOCETIN A AND TRIOSTIN A

by

David Walter Butcher

of

Churchill College

A dissertation submitted for the degree of Doctor of Philosophy in the University of Cambridge

PREFACE

This dissertation is a summary of research carried out in the University of Cambridge between October 1978 and August 1981, and represents the results of the author's original work except where otherwise stated.

I gratefully acknowledge the following:

Dr D.H.Williams for his help and encouragement throughout the course of my studies at Cambridge. Drs O.Kennard and W.B.T.Cruse for their advice on crystallisation techniques and for the crystallographic data presented in this dissertation. Dr J.Feeney (National Institute for Medical Research, Mill Hill, London) for the generous allocation of time on a 270MHz nmr machine. Steve Hammond for proof-reading this text and Mike Williamson and Drs Eva Hyde and Dave Reid for many fruitful discussions. Gustav Bojesen for performing mass spectral analyses and Eric Liddell and Brian Crysell of the Chemical Laboratories nmr unit who were ever patient when all around was collapsing. The Science Research Council for invaluable financial assistance.

Finally, I give a special thank you to my wife Jan, whose help and support greatly facilitated the eventual production of this dissertation.

D.W.BUTCHER

September 1981

SUMMARY

The work described in this dissertation concerns the three antibiotics vancomycin (a potent antibiotic against Gram-positive bacteria), ristocetin A (a member of the vancomycin group of antibiotics), and triostin A (a DNA intercalating quinoxaline antibiotic).

The precise nature of the vancomycin binding site has been mapped out with reference to that of the related antibiotic ristocetin A. The bacterial cell wall analogue Ac_2-L-lys-D-ala-D-ala was synthesised by a new simple method and was then used in these studies. The solution conformations of triostin A are described in some detail. Both of these studies have involved the extensive use of high-field (270 and 400MHz) proton nmr spectroscopy and the development of associated techniques, such as difference spectra and the nuclear Overhauser effect, to determine intra and inter-molecular interactions.

An extensive crystallisation program has resulted in the first method for the reproducible crystallisation of ristocetin A. A number of solvents were found to produce crystals but only water/75% acetone produced the quality necessary for x-ray crystallography. Unfortunately these proved unstable upon bombardment by x-rays and the desired crystal structure of ristocetin A has not been obtained. Crystals were also obtained of ristocetin A complexed to the bacterial cell wall analogues Ac-D-ala-D-ala and Ac_2-L-lys-D-ala-D-ala, although crystal structures were not determined because of the large unit cell of the complex with the former and the instability of the complex with the latter. Attempted crystallisations of derivatives of ristocetin A and of vancomycin were completely without success.

CONTENTS

1. INTRODUCTION 1

1.1 VANCOMYCIN 1

1.2 RISTOCETIN A 2

1.3 TRIOSTIN A 3

2. PREVIOUS STRUCTURAL STUDIES 5

2.1 VANCOMYCIN 5

2.2 RISTOCETIN A 8

2.3 TRIOSTIN A 10

3. THE BACTERIAL CELL WALL 14

3.1 INTRODUCTION 14

3.2 PEPTIDOGLYCAN STRUCTURE 15

3.3 PEPTIDOGLYCAN BIOSYNTHESIS 15

4. NUCLEAR MAGNETIC RESONANCE SPECTROSCOPY 17

4.1 PULSED FT NMR 17

4.2 DOUBLE IRRADIATION TECHNIQUES 19

4.2.1 SPIN-DECOUPLING 20

4.2.2 THE NUCLEAR OVERHAUSER EFFECT 20

4.2.3 DIFFERENCE SPECTRA 21

4.3 CHEMICAL EXCHANGE 22

4.3.1 TRANSFER OF SATURATION 22

5. PREVIOUS BINDING STUDIES ON VANCOMYCIN-TYPE ANTIBIOTICS 24

5.1 VANCOMYCIN 26

5.2 RISTOCETIN A 29

6. PRESENT STUDIES 32

6.1 VANCOMYCIN - REFINEMENT OF STRUCTURE AND BINDING SITE 32

6.1.1 SYNTHESIS OF AC_2-L-LYSYL-D-ALANYL-D-ALANINE 37

6.1.2 VANCOMYCIN/AC-D-ALA-D-ALA BINDING STUDIES 40

6.1.3 VANCOMYCIN/AC_2-L-LYS-D-ALA-D-ALA BINDING STUDIES 51

6.1.4 CRYSTALLISATION STUDIES 57

6.1.5 EPILOGUE 57

6.2 RISTOCETIN A - CRYSTALLISATION STUDIES 58

6.3 TRIOSTIN A 60

7. CONCLUSIONS 70

7.1 VANCOMYCIN 70

7.2 RISTOCETIN A 71

7.3 TRIOSTIN A 72

7.4 NMR SPECTROSCOPY 73

8. EXPERIMENTAL 74

8.1 PREPARATIONS 75

8.1.1 AC-D-ALA-D-ALA 75

8.1.2 N-HYDROXYSUCCINIMIDE 75

8.1.3 t-BUTYLOXYCARBONYL-D-ALANINE 76

8.1.4 D-ALANINE BENZYL ESTER - 1 76

8.1.5 D-ALANINE BENZYL ESTER p-TOLUENE SULPHONIC ACID SALT 77

8.1.6 D-ALANINE BENZYL ESTER - 2 78

8.1.7 D-ALANYL-D-ALANINE BENZYL ESTER - 1 78

8.1.8 D-ALANYL-D-ALANINE BENZYL ESTER
p-TOLUENE SULPHONIC ACID SALT 79

8.1.9 D-ALANYL-D-ALANINE BENZYL ESTER - 2 80

8.1.10 L-ALANINE BENZYL ESTER HYDROCHLORIDE 80

8.1.11 N,N′-DI-ACETYL-L-LYSINE 80

8.1.12 DI-t-BOC-L-LYSINE 81

8.1.13 DI-t-BOC-L-LYSINE SUCCINIMIDE ESTER 82

8.1.14 N,N′-DI-CBZ-L-LYSINE SUCCINIMIDE ESTER 82

8.1.15 N,N′-DI-CBZ-L-LYS-D-ALA BENZYL ESTER 83

8.1.16 N,N′-DI-CBZ-L-LYS-D-ALA-D-ALA BENZYL ESTER 84

8.1.17 N,N′-AC_2-L-LYS-D-ALA-D-ALA 84

8.1.18 RISTOCETIN IODIDE SALT 86

8.1.19 RISTOCETIN-Ψ-AGLYCONE 86

8.2 CRYSTALLISATION STUDIES 87

8.2.1 TECHNIQUES 87

8.2.2 VANCOMYCIN 87

8.2.3 VANCOMYCIN/AC-D-ALA-D-ALA 88

8.2.4 RISTOCETIN A 89

8.2.5 RISTOCETIN-Ψ-AGLYCONE 94

8.2.6 RISTOCETIN A/PEPTIDE 95

8.3 NMR EXPERIMENTS 96

9. REFERENCES 98

APPENDIX 1 103

1. INTRODUCTION

This dissertation describes investigations performed on the antibiotics vancomycin, ristocetin A and triostin A. For clarity and comparison certain chapters have been subdivided according to antibiotic.

1.1 VANCOMYCIN

Vancomycin was the first member of a group of structurally similar water-soluble glycopeptide antibiotics to be isolated and therefore lends its name to the class as a whole. It was elucidated by McCormick and co-workers[1] from Streptomyces orientalis and is active against Gram-positive bacteria. Other members of the group are ristocetin [1] , ristomycin[2], avoparcin[3], actinoidin[4], antibiotic A35512B[5], teichomycin[6] and antibiotic A4696[7]. Several of them are isolated as more than one variant, for example ristocetin and actinoidin in A and B forms. They are of considerable interest because bacteria do not readily develop resistance to them and no naturally resistant strain has ever been found. Vancomycin, ristocetin, avoparcin and A4696 are all effective in increasing food utilisation and for the prevention and treatment of ketosis[8] (a condition characterised by the accumulation of ketones in blood; often found with high-fat, low-carbohydrate diets, or in starvation). The potential market for animal feed additives therefore exists. Due to adverse side effects, vancomycin is the only member of the group in clinical use, even so it is only tolerable in the treatment of serious illness. It is used in the treatment of staphylococcal infections[9] (for example wound septicaemia and pneumonia) when other antibiotics are ineffective and, because it is absorbed poorly by the gastro-intestinal tract, is normally administered intravenously in doses of 2g per day for 2-3 weeks. However, recently it

---

[1] See Section 1.2

has been reported[10,11] that oral administration of vancomycin (2g/d) is effective in the treatment of post-operative diarrhoea, a symptom of antibiotic-associated colitis. This intestinal infection is due to Clostridium difficile, an organism which multiplies and produces toxins when the usual gut flora have been largely eliminated by the use of broad spectrum antibiotics. The infection is usually eliminated within 7 days of the onset of treatment with vancomycin.

The determination of the structure of vancomycin (figure 1.1) is described in section 2.1, the final details being obtained from an x-ray analysis of a crystalline degradation product (CDP-I) in which the asparagine residue of vancomycin was hydrolysed to aspartic acid with the consequent loss of ammonia.

The nomenclature shown in figure 1.1 is referred to throughout this dissertation.

1.2 RISTOCETIN A

The antibiotic ristocetin, a member of the vancomycin group of antibiotics, was first isolated by Grundy[12] from the actinomycete Nocardia lurida. Philip and co-workers[13] separated the antibiotic into two biologically active variants, termed A and B, which had identical aglycone structures but differed in the carbohydrate moieties. The A-form had six sugars whereas the B-form had only four. The structure of ristocetin (figure 1.2) has been determined with contributions from many groups of workers [2] , including studies on the antibiotic ristomycin, isolated from Proactinomyces fructifera[2], which was later proved to be identical in structure to ristocetin[14] in both variants. The apparent difference between them may have owed more to an ambiguity in classification[15] between the groups of workers than to any real genetic variation of the actinomycete producing the antibiotic. Unlike vancomycin, the structure of

---

[2] See Section 2.2

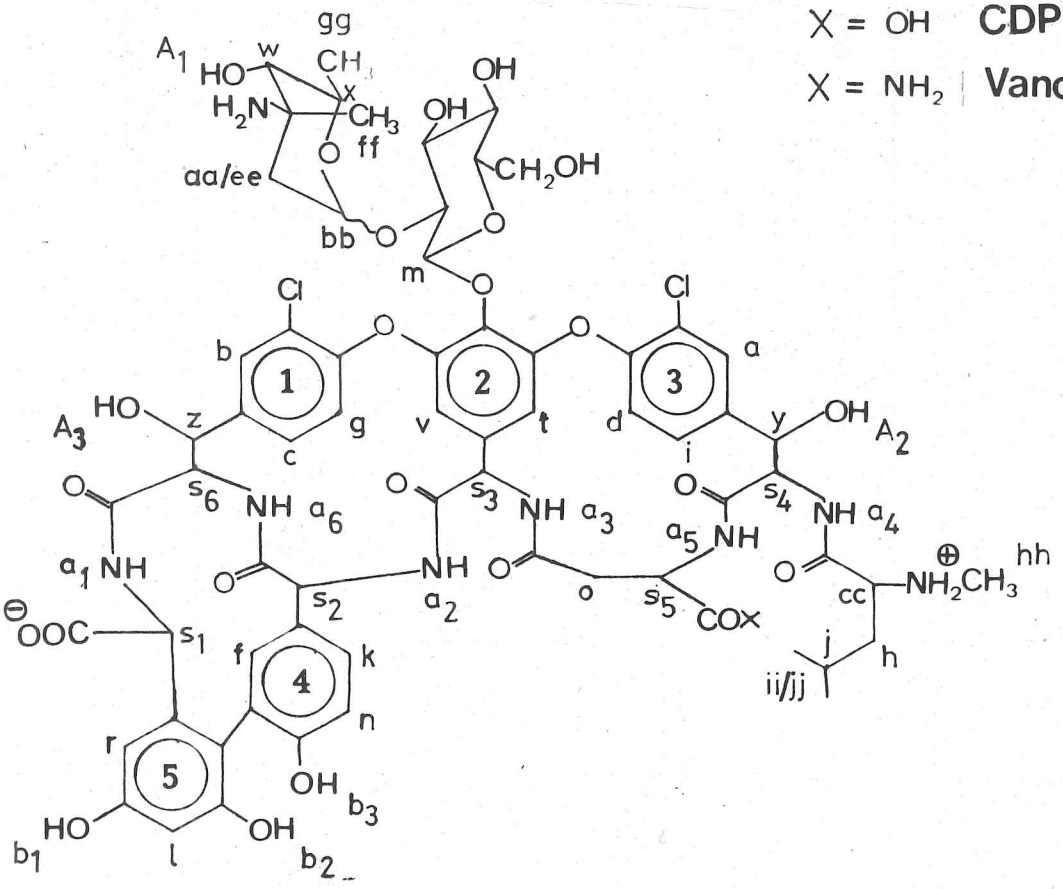

FIGURE 1·1 Vancomycin / CDP I

ristocetin has not been confirmed by x-ray analysis because of the difficulty experienced in obtaining suitable crystals.

Ristocetin B had three times the activity of the A-form[13]. Furthermore, the mild acid hydrolysates[16] (with most or all of the sugars removed) of both forms showed similarly enhanced activities compared to the parent antibiotics. Ristocetin A, like vancomycin, causes precipitation of fibrinogen and other plasma proteins. An additional effect caused by ristocetin A but not vancomycin is the aggregation of blood platelets which has led to the withdrawal of ristocetin A from clinical use[17]. However, it has found peripheral use as an important diagnostic tool in the identification of various bleeding disorders such as the Bernard Soulier syndrome[18] and von Willebrand's disease[19,20]. Recent evidence[21] has shown that mild acid hydrolysis of ristocetin A, to remove all of the sugars except for the amino sugar ristosamine, produces an antibiotic with enhanced activity (as previously noted), but more importantly with the complete removal of the platelet aggregation tendency.

The nomenclature shown in figure 1.2 is referred to throughout this dissertation and has been made as consistent as possible with that used for the related antibiotic vancomycin.

1.3 TRIOSTIN A

The quinoxaline antibiotics triostin A[22] and echinomycin[23] are members of a group of cross-bridged cyclic octadepsipeptides, characterised by the presence of quinoxaline-2-carboxylic acid moieties and are elucidated from several streptomycetes related to Streptomyces aureus (for example Streptomyces triostinius for triostin A). Recently the total synthesis of a naturally occurring quinoxaline antibiotic[24,25] (des-N-tetramethyl triostin A) was accomplished. The molecule, named tandem, only differs from triostin A in lacking the N-methylation of four peptide bonds, and is the only quinoxaline antibiotic for which an x-ray structure

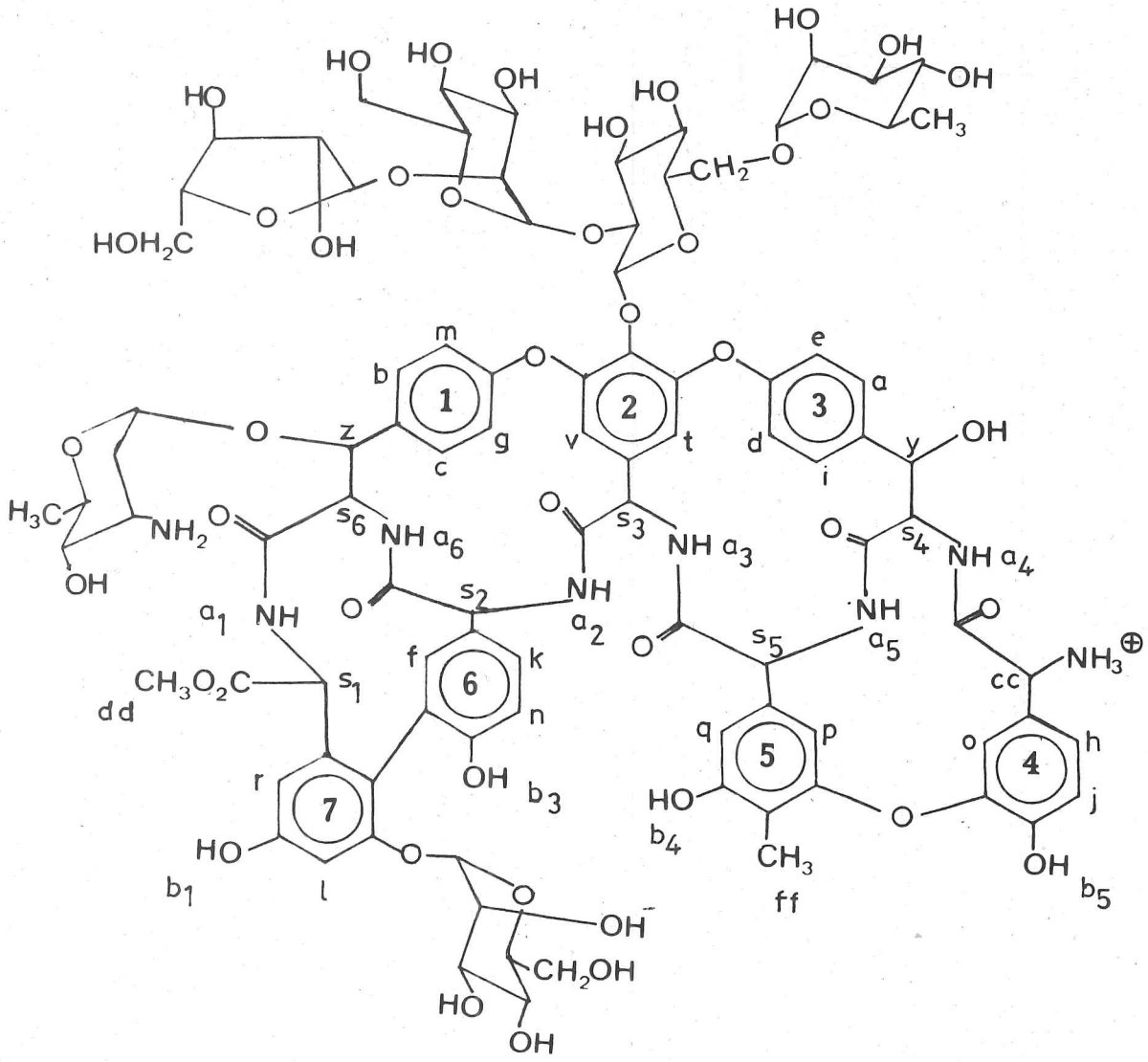

FIGURE 1·2 Ristocetin A

has been obtained[26]. The similarities in structure can readily be appreciated from figure 1.3.

The quinoxaline antibiotics are effective against Gram-positive bacteria but not against Gram-negative organisms, presumably because they fail to penetrate the outer membrane of Gram-negative bacteria [3] . In addition they are powerfully cytotoxic to mammalian cells and have some limited use as experimental anticancer agents in man. This latter action has been traced to their interaction with DNA. The binding of each triostin A molecule extends the double helix by an amount consistent with the intercalation of both of its quinoxaline rings, at locations two base-pairs apart[27]. To permit this insertion there must be preliminary local unwinding of the double helix to produce spaces between the stacked pairs into which the planar quinoxaline ring system can move. The hydrogen-bonding between the base-pairs remains undisturbed although there is some distortion of the smooth coil of the sugar phosphate backbone as the intercalated molecules maintain the double helix in a partially unwound configuration.

The integrity of the octapeptide ring and the cross-bridge are essential for intercalation with DNA. The nature of the cross-bridge is thought to account for the different affinities[28] of echinomycin, which favours poly-d(G-C), and triostin A, which favours poly-d(A-T).

---

[3] See Chapter 3

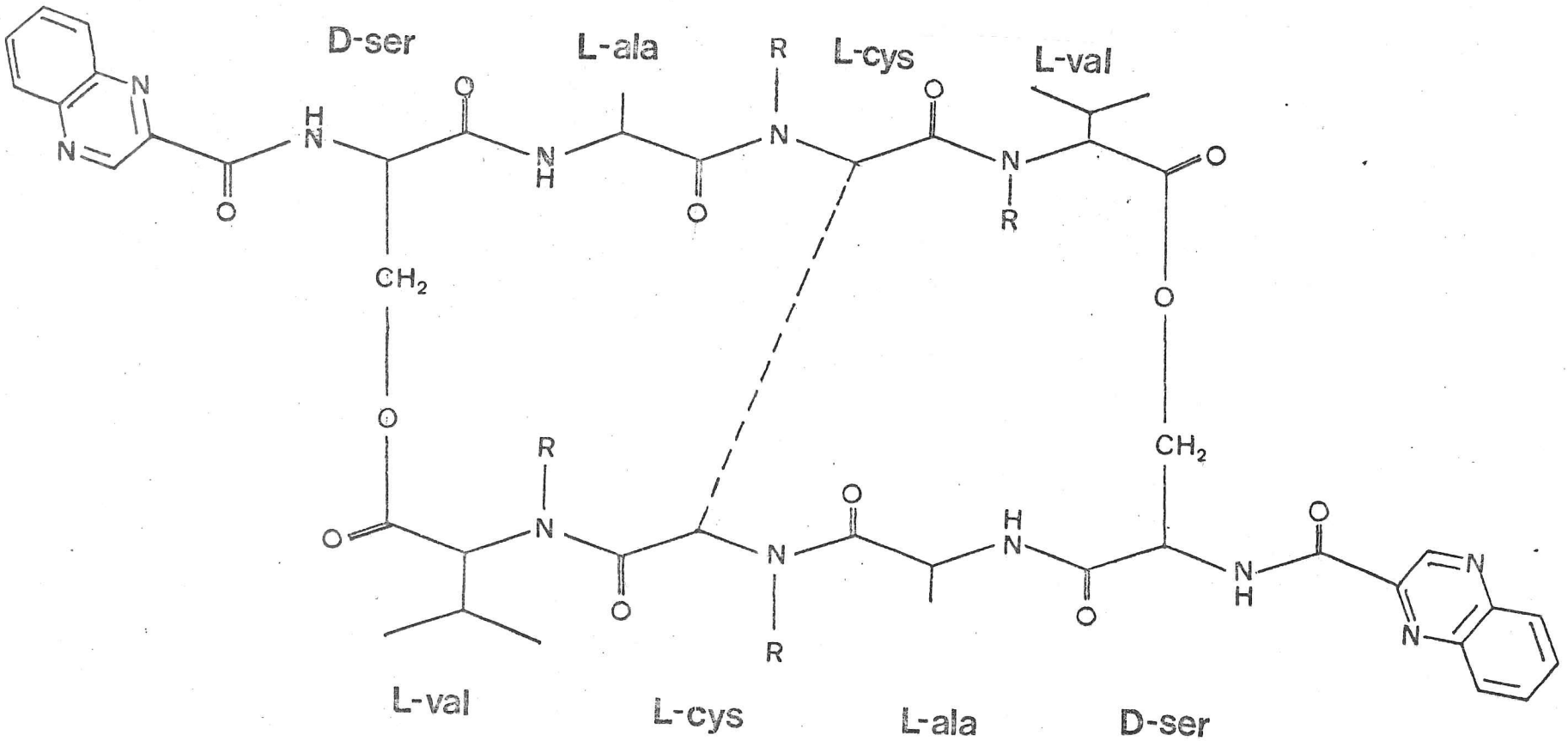

Echinomycin : $R = CH_3$

Triostin A : $R = CH_3$

Tandem : $R = H$

cross bridge: $-CH_2-S-\underset{\underset{SCH_3}{|}}{CH}-$

$\left.\begin{matrix} \| & \| \\ \| & \| \end{matrix}\right\} -CH_2-S-S-CH_2-$

FIGURE 1·3 Quinoxaline antibiotics

2.1 VANCOMYCIN

Early studies on vancomycin[29] suggested the presence of aromatic, aliphatic hydroxyls, phenolic hydroxyls, amino and carboxylic groups in addition to peptide bonds. A molecular weight of approximately 3300 Daltons was proposed by McCormick[1] but Johnson[30] later suggested that this value was due to dimerisation of the antibiotic in solution and the actual molecular weight was around 1560 Daltons. This was later confirmed[31,32] and in due course the molecular weight was established as 1448 Daltons, corresponding to a molecular formula of $C_{66}H_{75}Cl_2N_9O_{24}$. Hydrolysis of vancomycin by boiling in 0.6M hydrochloric acid for 2 minutes produced a white precipitate termed aglucovancomycin and liberated the sugars glucose[29] and vancosamine[33,34] (2.1). Large amber crystals of another derivative, called CDP-I, were formed when an aqueous solution (pH 4.2) of vancomycin was heated at 70°-80°C for 1-2 days. One mole of ammonia was lost during the reaction due to the conversion of a primary amide group to a carboxylate[31]. Treatment of CDP-I with hydrochloric acid under the same conditions as those used for the preparation of aglucovancomycin gave a white precipitate, termed CDP-II, and in addition glucose and vancosamine were liberated. The relationship between vancomycin and its derivatives is illustrated schematically in figure 2.1.

Hydrolysis of vancomycin in 6M hydrochloric acid produced L-aspartic acid, N-methyl-D-leucine and vancomycin acid (3-methyl-4-ketoheptanoic acid)[29]. Vancomycin acid was later shown to be derived from the amino sugar vancosamine[33], and N-methyl-D-leucine was identified as an N-terminal amino acid[30].

Nitration of aglucovancomycin followed by permanganate oxidation produced 3-chloro-4-hydroxybenzoic acid (2.2) and 3-chloro-4-hydroxy-5-nitrobenzoic acid (2.3)[29]. However, attempts to isolate larger chlorine-

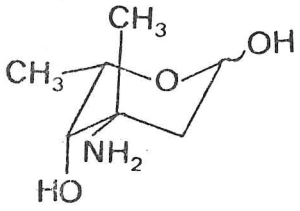

(2·1) Vancosamine (3-amino-2,3,6-trideoxy-3-c-methyl-lyxo-hexopyranose)

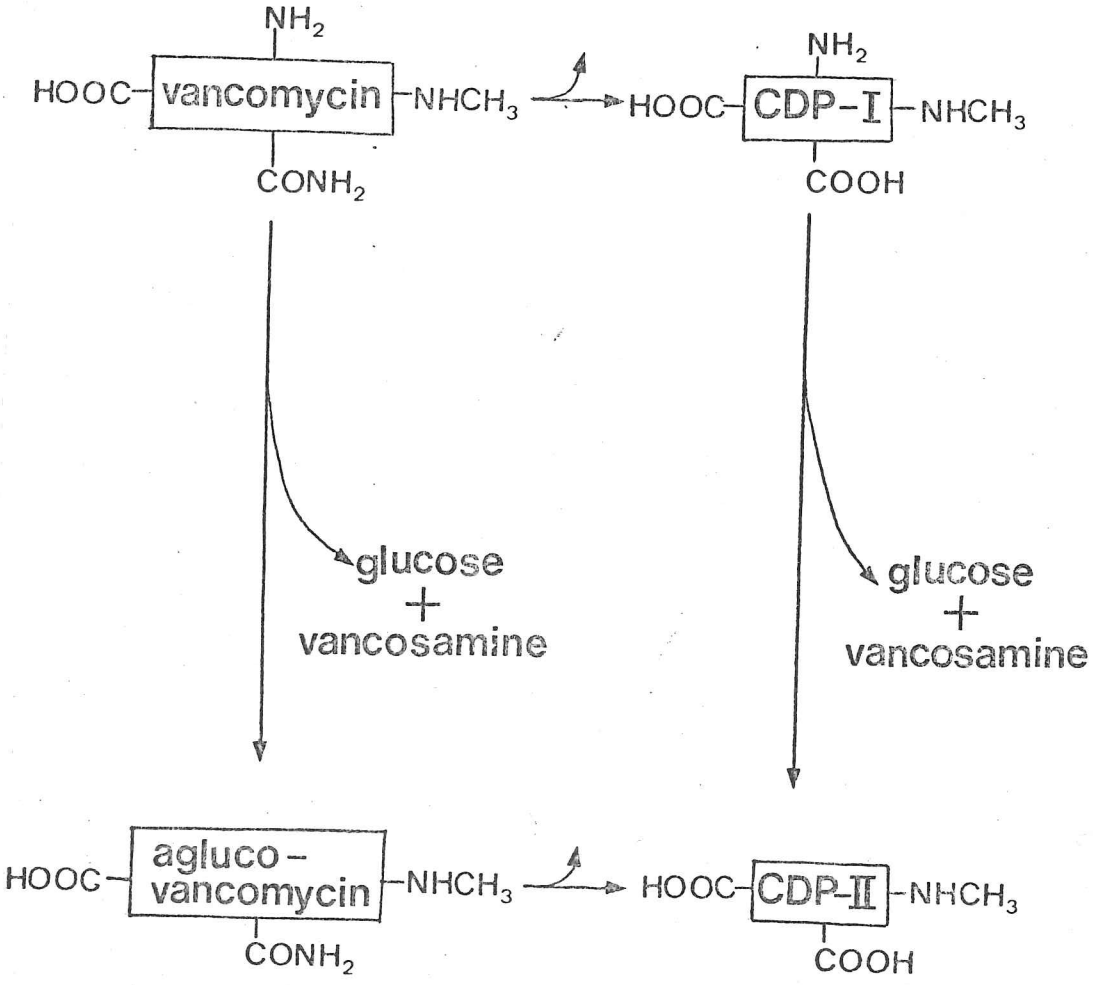

FIGURE 2·1 Derivatives of vancomycin

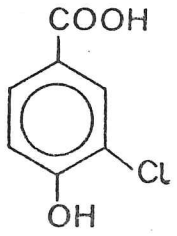

(2·2)

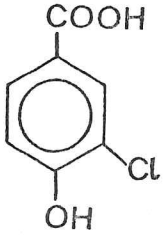

(2·3)

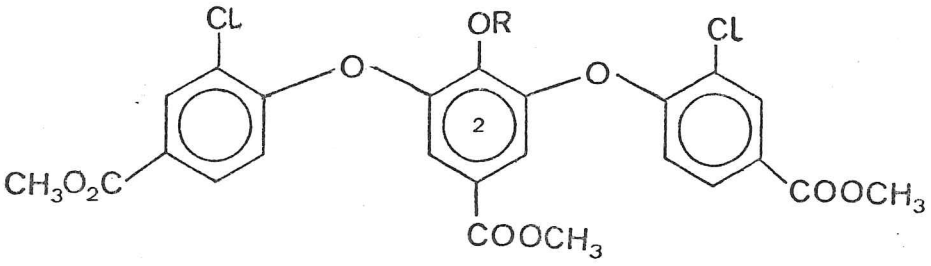

(2·4) R = CH_3

(2·5) R = CD_3

containing fragments were unsuccessful until the antibiotic was first protected by methylation of the phenols prior to oxidation[31,35]. Acidic products were isolated and methylated to yield the triester (2.4). The attachment of the sugars to the aromatic rings was determined by methylation of vancomycin, removal of the sugars by methanolysis, trideuteriomethylation, oxidation and finally methylation of the resulting carboxylic acid residues. Fragment (2.5) was isolated and established that in vancomycin a sugar was glycosidically attached to the central oxygen atom of ring 2 of (2.4). Related experiments showed that vancosamine was glycosidically attached to the C-2 of glucose, and that glucose was glycosidically linked to ring 2 of fragment (2.4)[31].

One further fragment identified from the oxidation experiments[31] was dimethyl-4-methoxyisophthalate (2.6). In addition, when vancomycin was hydrolysed with 4M sodium hydroxide under reflux and subsequently methylated, fragment (2.7) was identified[35]. It was proposed that (2.6) was derived from the 1,2,4,-trisubstituted ring of (2.7) and that the original fragment in the antibiotic was a biphenyl (2.8), the hydroxyl group being replaced by nitrogen during alkaline hydrolysis. The most probable mechanism for the formation of (2.7) from the biphenyl unit is shown in scheme 2.1.

The components described so far account for most of the molecular formula of vancomycin. However, the studies of Johnson[30] revealed that base-catalysed hydrolysis of vancomycin afforded approximately 2 moles of glycine, although this amino acid was not produced in significant amounts from acid-catalysed hydrolysis. This led to the proposal[36] that glycine may have arisen via a base-catalysed retro-aldol cleavage of a β-hydroxy amino acid ((2.9) in scheme 2.2). The products would be an aldehyde (2.10) and, by hydrolytic cleavage of the bonds indicated by wavy lines and ketonisation of the product, glycine (2.11). Two units such as (2.9) would give rise to approximately 2 moles of glycine. Since an aldehyde would be unlikely to survive the conditions necessary for alkaline hydrolysis, the reaction was performed (on methylated aglucovancomycin) in the presence of sodium borohydride (or deuterioborohydride) in situ. Fragment (2.12) was isolated by reaction with the former; and (2.13) was obtained in the presence of the latter. On the basis of these experiments, it was concluded

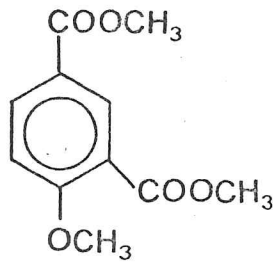
COOCH3
COOCH3
OCH3

(2·6)

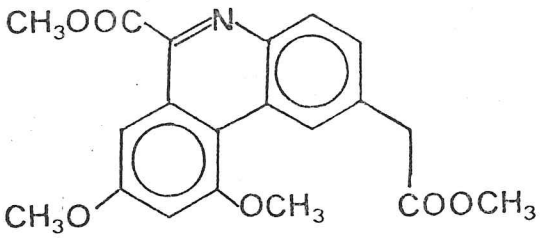
CH3OOC
N
CH3O
OCH3
COOCH3

(2·7)

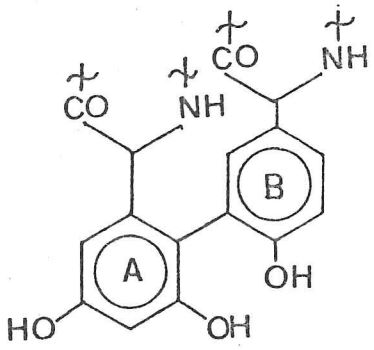
CO
NH
CO
NH
B
A
OH
HO
OH

(2·8)

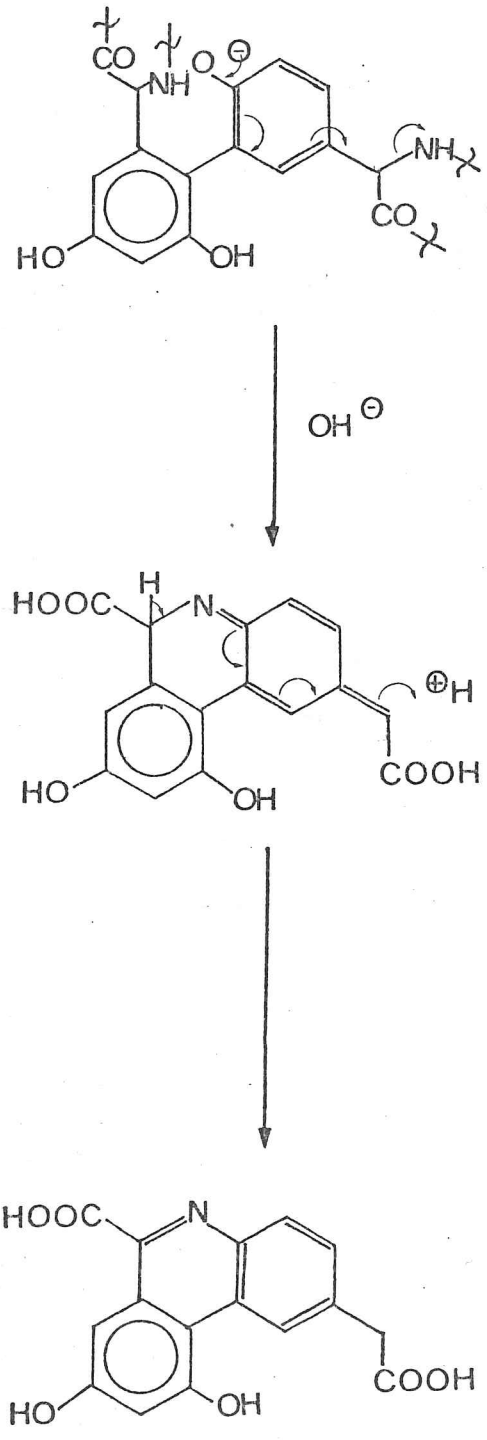

SCHEME 2·1

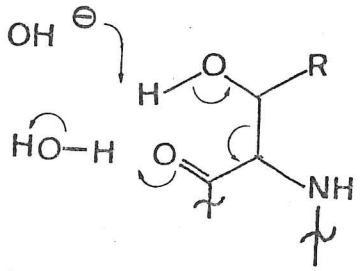

(2·9)

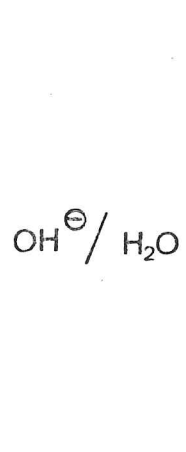

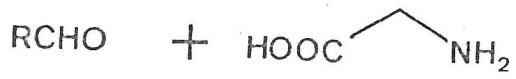

(2·10) (2·11)

SCHEME 2·2

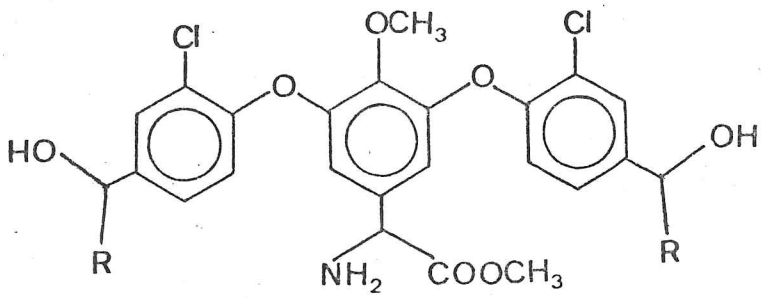

(2·12) R = H

(2·13) R = D

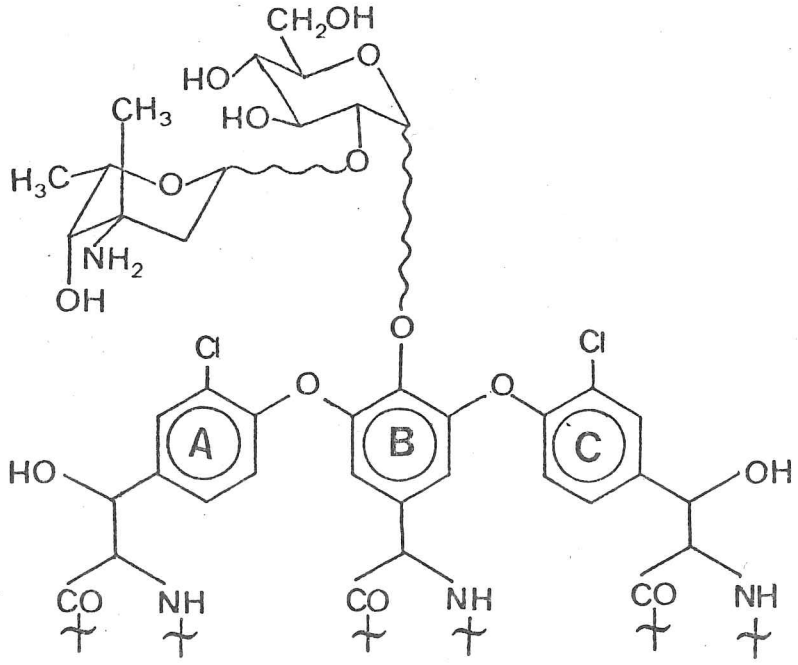

(2·14)

that vancomycin contained the major structural component (2.14).

Having identified the four structural units as N-methyl-D-leucine, L-aspartic acid, the biphenyl unit (2.8), and the disaccharide triaryl ether unit (2.14), the problem remained of establishing the six interconnecting peptide bonds in such a manner as to leave free one carboxylate and one primary amide group. In addition, the stereochemistry of seven of the nine asymmetric carbon atoms (the other two centres having already been identified as L-aspartic acid and N-methyl-D-leucine) was unsolved. Mass spectroscopic analysis[36] identified that one of the potential glycine units in vancomycin was attached via a secondary amide bond to the C-terminus of N-methyl-D-leucine. Nuclear magnetic resonance studies at 270MHz[37] established from coupling constant data that vancosamine and glucose were present as α- and β- anomers respectively. In addition, lanthanide shift experiments identified the carbonyl of ring A in (2.8) as being the position of the free carboxylate group of vancomycin. The application of the nuclear Overhauser effect (nOe)[37], which monitors the interaction of the magnetic fields of nuclei that are close in space [1] , established the relative orientation of all the structural units of vancomycin. The nOe also provided evidence for the attachment of the carbonyl group of ring C of (2.14) to the amino group of aspartic acid in vancomycin[37]. Since the stereochemistry at seven asymmetric centres remained unknown it proved impossible to establish a total structure. The final details of the molecule (figure 2.2) were provided by x-ray analysis of CDP-I[38].

---

[1] Full description in Section 4.2.2

that vancomycin contained the major structural component (2.14).

Having identified the four structural units as N-methyl-D-leucine, L-aspartic acid, the biphenyl unit (2.8), and the disaccharide triaryl ether unit (2.14), the problem remained of establishing the six interconnecting peptide bonds in such a manner as to leave free one carboxylate and one primary amide group. In addition, the stereochemistry of seven of the nine asymmetric carbon atoms (the other two centres having already been identified as L-aspartic acid and N-methyl-D-leucine) was unsolved. Mass spectroscopic analysis[36] identified that one of the potential glycine units in vancomycin was attached via a secondary amide bond to the C-terminus of N-methyl-D-leucine. Nuclear magnetic resonance studies at 270MHz[37] established from coupling constant data that vancosamine and glucose were present as α- and β- anomers respectively. In addition, lanthanide shift experiments identified the carbonyl of ring A in (2.8) as being the position of the free carboxylate group of vancomycin. The application of the nuclear Overhauser effect (nOe)[37], which monitors the interaction of the magnetic fields of nuclei that are close in space [1] , established the relative orientation of all the structural units of vancomycin. The nOe also provided evidence for the attachment of the carbonyl group of ring C of (2.14) to the amino group of aspartic acid in vancomycin[37]. Since the stereochemistry at seven asymmetric centres remained unknown it proved impossible to establish a total structure. The final details of the molecule (figure 2.2) were provided by x-ray analysis of CDP-I[38].

---

[1] Full description in Section 4.2.2

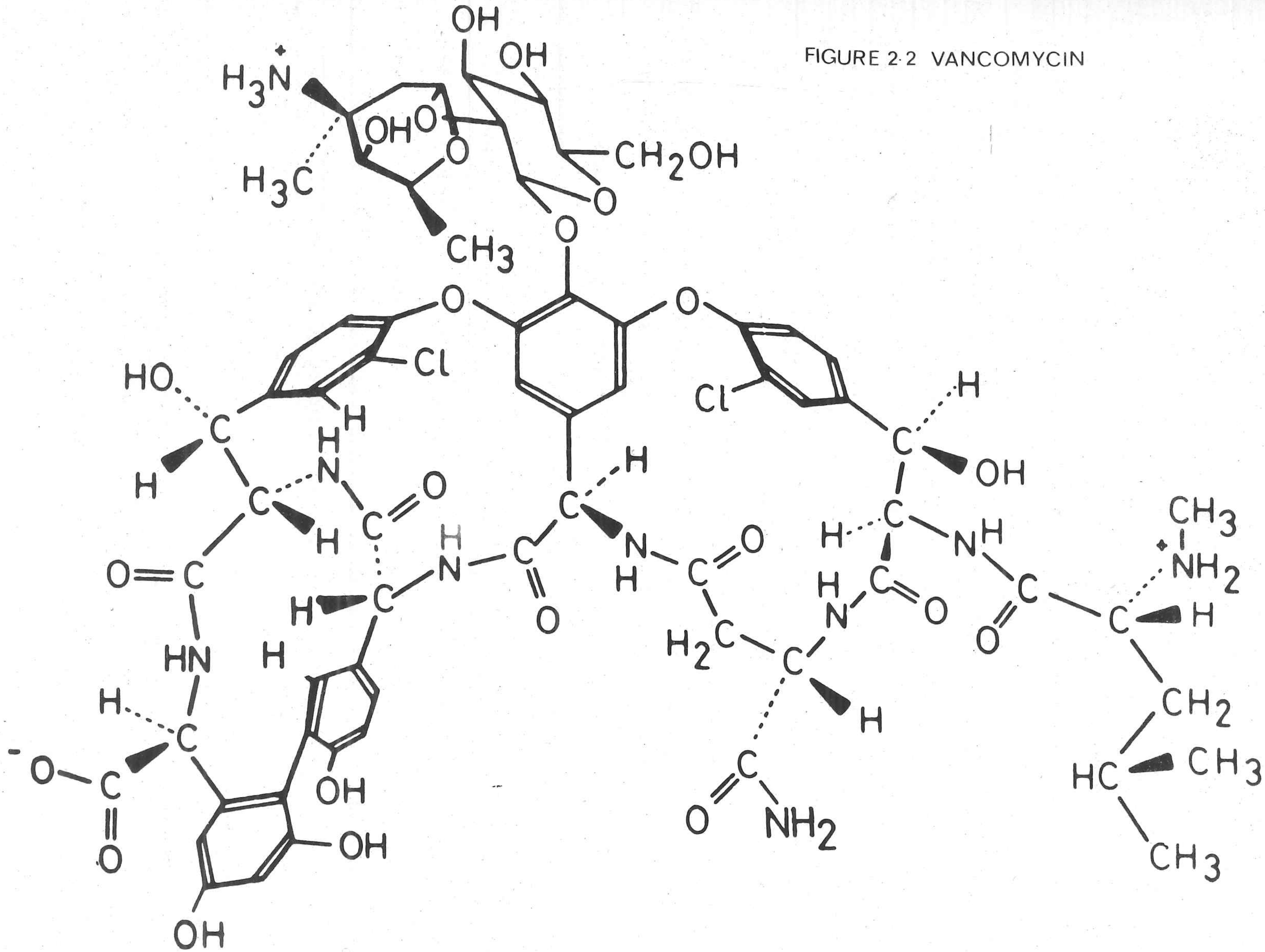

FIGURE 2·2 VANCOMYCIN

2.2 RISTOCETIN A

As stated previously ristocetin A and B are believed to be identical to ristomycin A and B[14] respectively, thus data pertaining to the latter pair of antibiotics can be directly assimilated with the former pair of antibiotics.

Mild acid hydrolysis of ristomycin A[39] liberated D-arabinose, D-mannose (2.15), L-rhamnose, D-glucose and an amino sugar ristosamine (2.16), in the ratio 1:2:1:1:1. The B-form of the antibiotic contained only L-rhamnose, D-mannose and D-glucose as the neutral sugars[39], in the ratio 1:1:1. Lomakina and co-workers[40] deduced the sequence of the sugars in ristomycin A and B by identifying the oligosaccharides formed in a series of mild acid hydrolyses. The nature and positions of the sugar linkages in a tetrasaccharide unit (2.17) was established by Sztaricskai and co-workers[41], although only recently has the ring size of the arabinose unit been confirmed[42,43] as that shown. The structure of ristosamine (2.16) has been confirmed by synthesis[44]. The carbohydrate portion of ristocetin A was thus accounted for by (2.15), (2.16) and (2.17); each sugar component being attached via glycosidic bonds at three separate points of the aglycone[45].

The aglycone moiety of ristocetin (identical in both A and B forms[39]) was initially studied by chemical degradation (acid and base hydrolyses, and oxidation) followed by isolation and characterisation of the fragments. The identified structural units were then assembled as the complete aglycone entity using high-field ^{1}H and ^{13}C nmr studies.

Strong acid hydrolysis (6M hydrochloric acid, 105°C, 18h) of ristocetin had been known for some time to produce several aromatic amino acids but it was not until the work of Tarbell and co-workers[46,47] that the structure of one of the components was identified as (2.18). Further work[14,47] identified the presence of (2.19), which had already been shown to be present in vancomycin [2].

---

[2] See Section 2.1

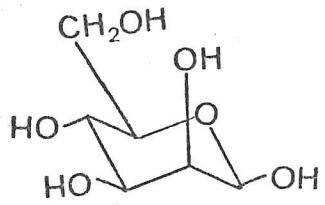
CH2OH
OH
HO
O
HO
OH

(2·15)

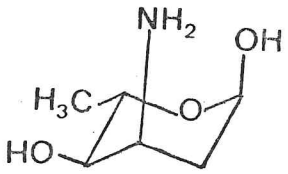
NH2
OH
H3C
O
HO

(2·16)

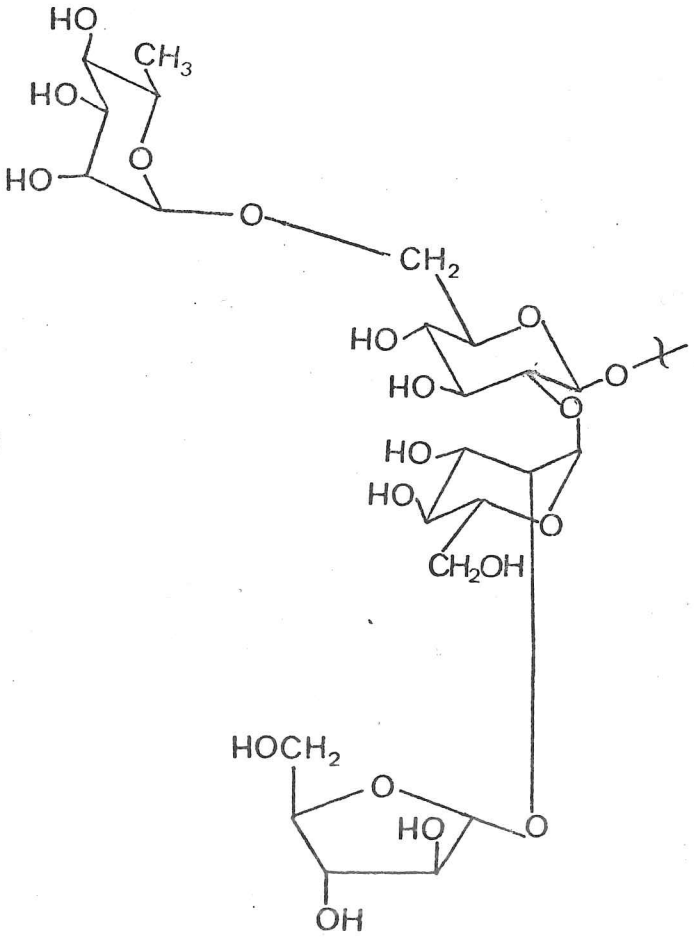
HO
CH3
HO
O
HO
O
CH2
HO
O
HO
O
HO
HO
O
CH2OH
HOCH2
O
HO
O
OH

(2·17)

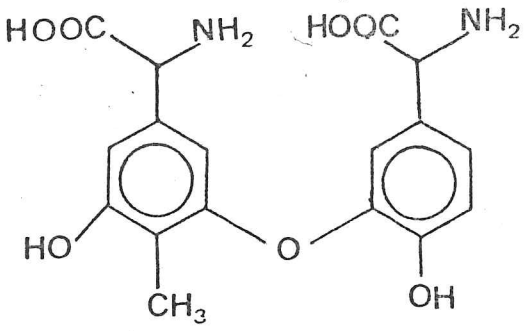

(2·18) Ristomycin acid

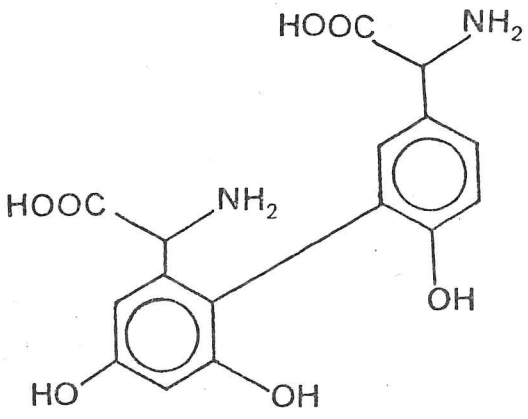

(2·19) Actinoidinic acid

Oxidative degradation of the protected ristocetin aglycone, followed by methylation of the acidic products led to isolation and characterisation of the triaryl ether residue[47] (2.20). On the basis of obvious structural analogy between the fragments of ristocetin and the structure of vancomycin, it was reasonable to suppose that ristocetin contained the structural unit (2.21), and indeed this was confirmed using reductive alkaline hydrolysis experiments[48,49], similar to those carried out on vancomycin.

The molecular weight of ristocetin A was determined[14] by californium plasma desorption mass spectroscopy (2063 ± 5 Daltons) and in conjunction with ^{1}H and ^{13}C nmr studies[14] the structural units (2.15), (2.16), (2.17), (2.18), (2.19) and (2.21) were identified as constituting essentially all of the ristocetin A molecule. However, the problem remained of deducing the manner in which the components were coordinated and the stereochemistry of the nine asymmetric centres. Fortunately the structural similarities between vancomycin (as determined by x-ray studies) and ristocetin A, and the fact that both were able to bind to peptidoglycans terminating in -D-ala-D-ala, indicated that the similarities were likely to extend to stereochemical detail. Further studies using ^{1}H nmr proved this to be the case and allowed the complete structure to be established.

The 270MHz ^{1}H nmr spectrum was assigned completely. Standard nmr methods were then used in conjunction with extensive application of negative nOe's which established the relative orientations of the various structural units, stereochemistry, and points of attachment of the substituents[50,51]. The full structure as deduced by these studies is presented in figure 2.3.

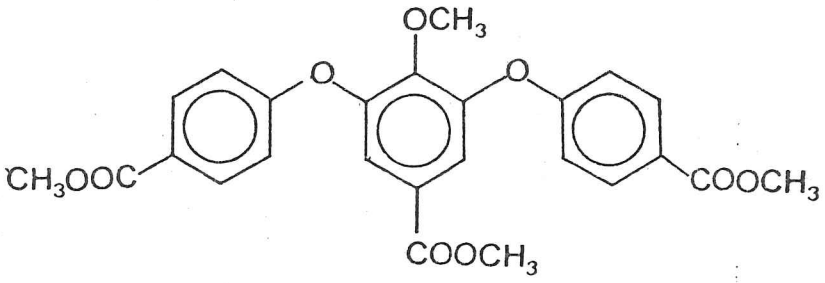

(2·20)

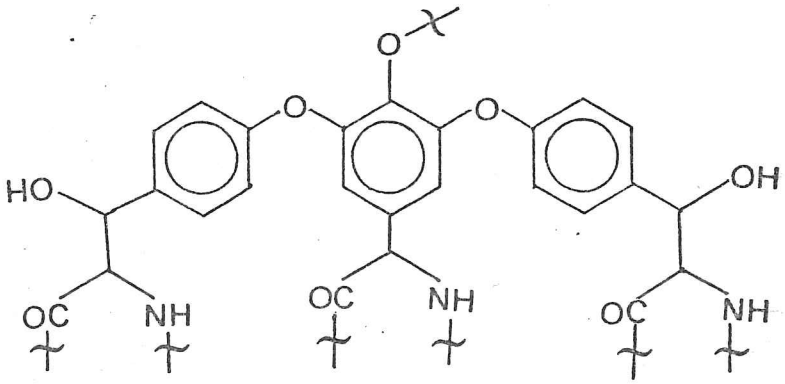

(2·21)

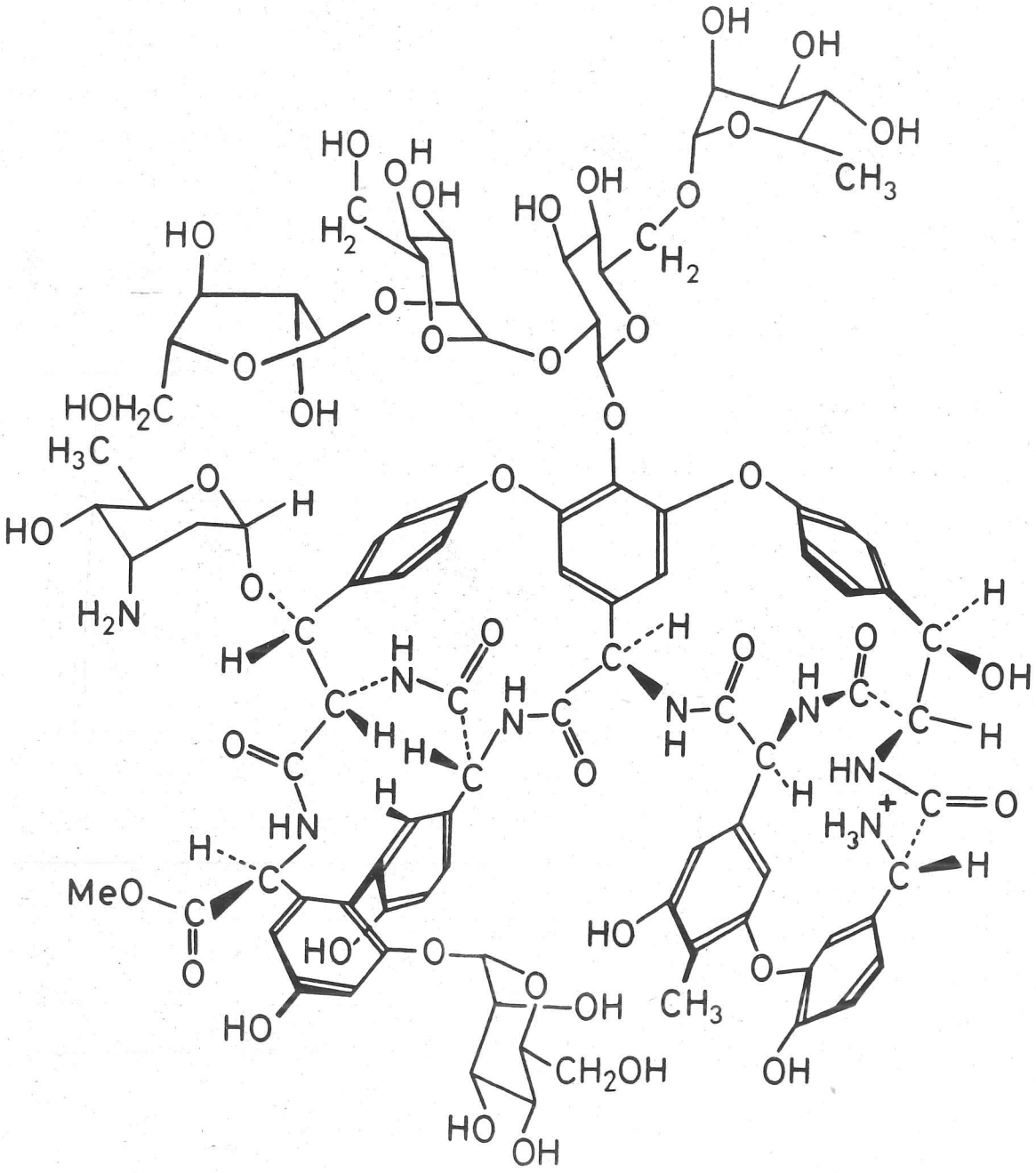

FIGURE 2-3 RISTOCETIN A

2.3 TRIOSTIN A

The structural determinations of the triostin antibiotics were considerably easier than those described in the previous two sections for vancomycin and ristocetin A. Conventional amino acid analysis, after acid hydrolysis, identified most of the antibiotic components[52], for example triostin A was composed of the following moles of amino acid per mole of antibiotic; serine 1.46, alanine 1.98, dimethylcystine 1.05, methylvaline 1.87. Ammonia (0.29 moles) was also isolated. In addition, UV absorption identified the presence of quinoxaline-2-carboxylic acid (2 moles) in all triostins and echinomycin-type antibiotics as being the only other component[52].

In order to obtain a better understanding of the mode of action of triostin A preliminary studies to determine the conformations in solution were performed[53]. The molecule has a two-fold axis of symmetry, therefore a single resonance only was observed for identical nuclei in the two halves of the molecule. The existence of two discrete conformers, with an energy barrier of 92 $KJ.mole^{-1}$ between them, was proposed from ^1H nmr spectra. The population of the conformations was dependant upon solvent polarity and led to the conformer favoured in polar solvents (water, dmso, etc.) being labelled 'p', and that preferred in non-polar solvents (chloroform, benzene, etc.) as the n-conformer. Further extensive studies were performed[54] to identify the precise nature of the conformers and to determine the differences between them that could account for the observed energy barrier. The conformation in solution of the related antibiotic echinomycin[55] was determined using nmr spectroscopy, CPK model building and potential energy calculations. A similar approach was used for triostin A, and comparison of the nmr chemical shift and coupling constant data of the p-conformer with echinomycin produced minor differences only. A similar parallel existed for the temperature variation and solvent effects of the amide NH protons. It was therefore proposed that triostin-p and echinomycin had very similar conformations in solution. A summary of the more significant findings of Kalman and co-workers is now presented.

The quinoxaline H-3 proton chemical shifts (n, 9.61 δ ; p, 9.69 δ) of both conformers were deshielded by around 1.5ppm relative to the other

ring protons. The existence of an intramolecular hydrogen bond between the quinoxaline carbonyl group and H-3 was proposed to account for this and was based on comparable studies with model compounds. The quinoxaline system ring current was invoked as the cause for the low-field resonance positions of the ser-NH protons in both conformers. The ser $J_{\alpha,NH}$ coupling constant in triostin-p was 6.4Hz whereas for the n-form it was 8.4Hz; a significant change in orientation had occurred about the serine $C_{\alpha-N}$ bond. Model building studies for both conformers revealed that the serine α-CH and β-CH_2 groups can only point outwards from the peptide ring. A trans orientation was assumed for the ester linkage and since the serine β-CH_2 resonance chemical shifts were similar for both of the triostin conformers and for echinomycin it was assumed to be so in all three antibiotics. In the absence of $J_{\alpha,NH}$ coupling constants for the N-methylated residues, the amide bonds of both conformers were assumed to be trans on the basis of α-CH chemical shift correlations with linear peptides, diketopiperazines and other model systems. Slight differences only were proposed between the conformers for the orientation about the cys-val peptide bond. The large valine vicinal α-CH-β-CH coupling constants (p, 10.0Hz; n, 10.5Hz) were indicative of hindered rotation of the valine side-chain in both conformers. Steric interference between the val-γ-methyl groups and the val-N-methyl was proposed which suggested that both of these groups were on the same face of the molecule, possibly the upper face as in echinomycin. The deshielding of the ala-α-CH protons in both conformers was ascribed to the proximity of the ser-CO, the two groups being closer in the n-conformer which experienced larger deshielding. Trans ser-ala peptide bonds were therefore proposed for both conformers. A major change in orientation of the alanine residue was apparent from the coupling constants; for triostin-p ala $J_{\alpha,NH}$ 5.7Hz whereas for the n-conformer $J_{\alpha,NH}$ 9.0Hz.

In accordance with other studies on disulphides the cross-bridge was assumed to have a dihedral angle (the angle between the cysteine methylene groups when looking along the disulphide bond) of 80°-90°. It was not possible to discriminate between the two possible chiralities ($+90^{\circ}$ and -90°) by nmr.

The cys $J_{\alpha,\beta}$ coupling constants were calculated from an ABX analysis of the multiplets for both conformers although no single rotamer could be found for either one which fitted the data. A flexible cross-bridge was therefore proposed in each case.

Upon addition of the lanthanide shift reagent (lsr), $Eu(fod)_3$, the largest shifts were observed for triostin-n, in addition the equilibrium between the two conformers was displaced in favour of the n-conformer. The binding of Eu^{3+} to triostin-n was evidently stronger than to triostin-p. From the magnitude of the shifts the site of complexation for the n-conformer was deduced to be the ser-CO (as in echinomycin), whereas in triostin-p multiple binding sites for Eu^{3+} prevented detailed analysis.

Having appraised the data for each residue of the antibiotic, in each conformer, Kalman and co-workers were in a position to postulate the changes that would be necessary to account for the energy barrier of $92KJ.mole^{-1}$. Three possibilities were considered.

(1) Rotation of a trans-N-methylated peptide unit through the ring. Two such conversions would be necessary to conserve the molecular symmetry.

(2) Conversion of a trans amide bond to cis, again two such interconversions would be necessary.

(3) Reversal in chirality of the disulphide bond.

Molecular models were constructed using the partial conformational information derived earlier and including the additional constraints imposed by cyclisation and cross-bridge formation. The nmr spectra of triostin-p and echinomycin were so similar (although the lanthanide induced shift, LIS, data was at variance) that the overall ring conformation for these two antibiotics was concluded to be the same. Similarly, despite considerable variations between the nmr spectra of triostin-n and echinomycin, on the basis of the LIS data it was concluded that these too had the same overall ring conformation. It was therefore proposed that the main difference between the two triostin conformers was the chirality of the disulphide bond. Additionally, in triostin-n an

intramolecular hydrogen bond between the quinoxaline-CO and the ala-NH, forming a seven-membered ring, was invoked to account for the low-field ala-NH resonance. Other differences observed between the two conformers were considered to be due to small conformational changes associated with the interconversion noted above.

Although it was not possible to determine whether either of the conformers studied was actually involved in binding to DNA it was observed that the proposed conformations placed the quinoxaline rings 10Å apart; a distance suitable for simultaneous intercalation with DNA. It was further speculated that the ala-NH of triostin-p may be involved in determining the specificity of binding by hydrogen bonding to groups in the groove of DNA. This also accounted for the observed differences in specificity of binding between echinomycin and triostin-p which differ in the orientation of the ser-ala portion of the antibiotic.

3. THE BACTERIAL CELL WALL

3.1 INTRODUCTION

The vancomycin-type antibiotics function by inhibiting synthesis of peptidoglycan[56] (also called mucopeptide), the major structural component of the cell-walls of Gram-positive bacteria. These outer layers of a bacterium determine its response to the Gram stain which has been used as the basis for the classification of bacteria.

The individual components of the bacterial envelope can be differentiated both structurally and functionally. The innermost layer, the cytoplasmic membrane, is the permeability barrier across which substrates must be transported, and is also the site of oxidative phosphorylation and chromosome attachment; it is responsible for the biosynthesis of wall and membrane polymers. The peptidoglycan is responsible for the mechanical strength of the bacterium. In Gram-positive bacteria the teichoic acids are the antigenic determinants, provide some of the sites of attachment for bacteriophages and may also play a role in ion-binding and transport. In Gram-negative bacteria the lipopolysaccharides have these functions. Both Gram-positive and Gram-negative bacteria have the same basic structure of an inner cytoplasmic membrane surrounded by a wall containing the peptidoglycan, but the additional components and their arrangement in the walls are different (figure 3.1). In addition the walls of Gram-positive bacteria are significantly thicker than those of Gram-negative species.

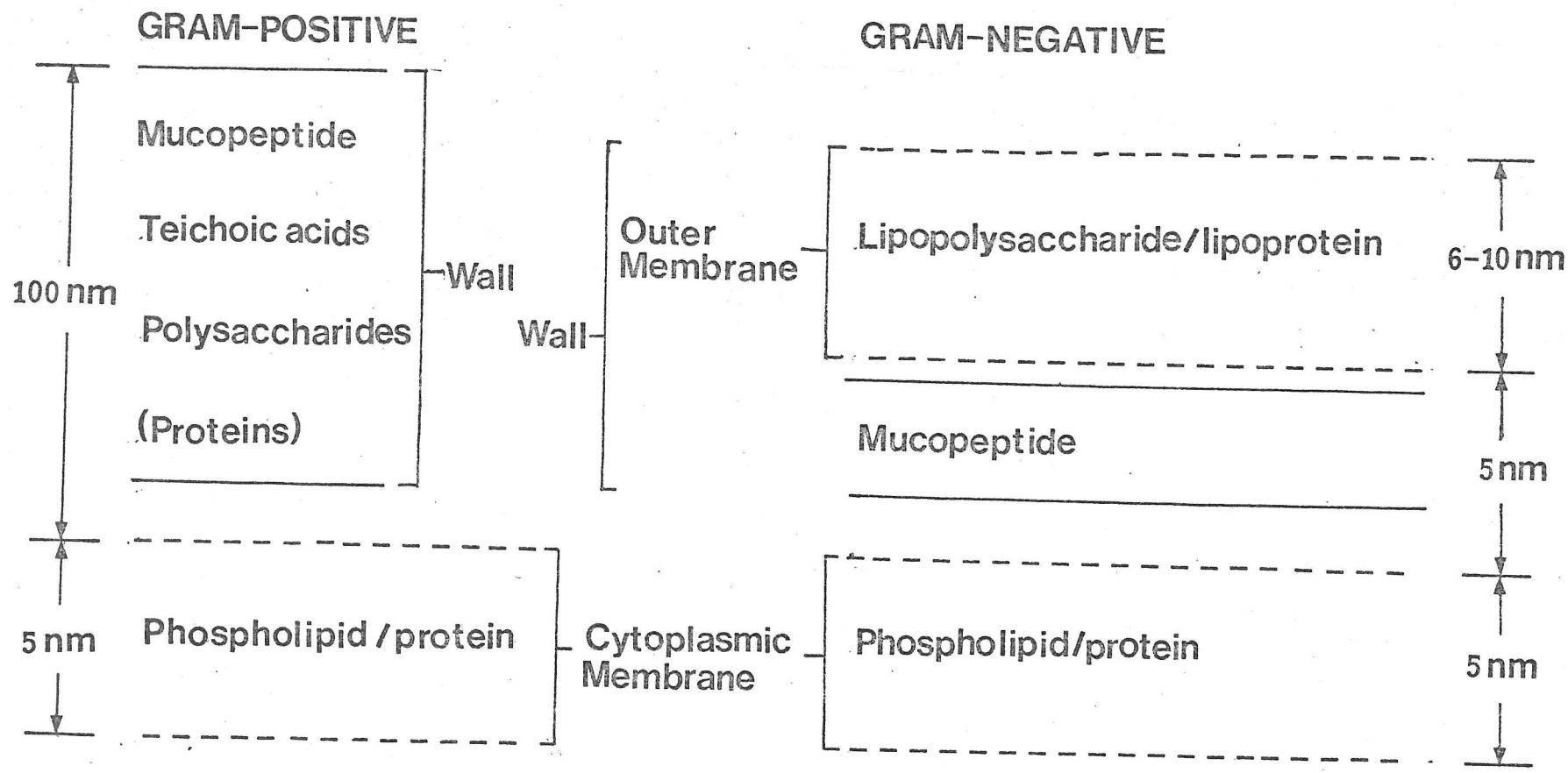

FIGURE 3·1 Bacterial envelope components

3.2 PEPTIDOGLYCAN STRUCTURE

In all bacterial species the peptidoglycan consists of a backbone of β-1,4-linked alternating units of the amino sugars N-acetyl-glucosamine (GlcNAc) and its O-lactyl ether, N-acetyl-muramic acid (MurNAc). Projecting from the amino sugar backbone are short peptide chains in a species specific sequence. The most common of these consists of the four amino acids, L-alanine, D-glutamic acid, a diamino acid and finally D-alanine (figure 3.2). In staphylococci the diamino acid is L-lysine while in Escherichia coli and all Gram-negative bacteria it is meso-diaminopimelic acid (DAP). In some species the γ-carboxylate of glutamic acid is amidated or substituted with an additional amino acid. The peptide chains are cross-linked from the carboxylate group of the terminal D-alanine to the free amino group of the diamino acid either directly or by a short peptide bridge. The overall structure of a typical peptidoglycan is shown in figure 3.3.

3.3 PEPTIDOGLYCAN BIOSYNTHESIS

Synthesis of peptidoglycan can be divided conceptually into three stages. The first stage, catalysed on the inside of the cell by cytoplasmic enzymes, is the synthesis of the soluble peptidoglycan precursor uridine 5′-diphosphate-N-acetyl-muramylpentapeptide (figure 3.4).

This step is followed by transfer of the N-acetyl-muramylpentapeptide (MurNAc-pentapeptide) and N-acetyl-glucosamine (GlcNAc) to a lipid carrier, C_{55}-isoprenyl alcohol (figure 3.5) in the membranes, forming a subunit of the glycan polymer (figure 3.6). The membrane-bound disaccharide pentapeptide is now modified in a species specific fashion. Such modification may include substitution of a carboxyl group on glutamic or diaminopimelic acid residues, or attachment of a peptide side chain (for example the pentaglycine chain attached to the lysine residue of the pentapeptide in Staphylococcus aureus (figure 3.6). In the last stage, the modified disaccharide-pentapeptide residue is

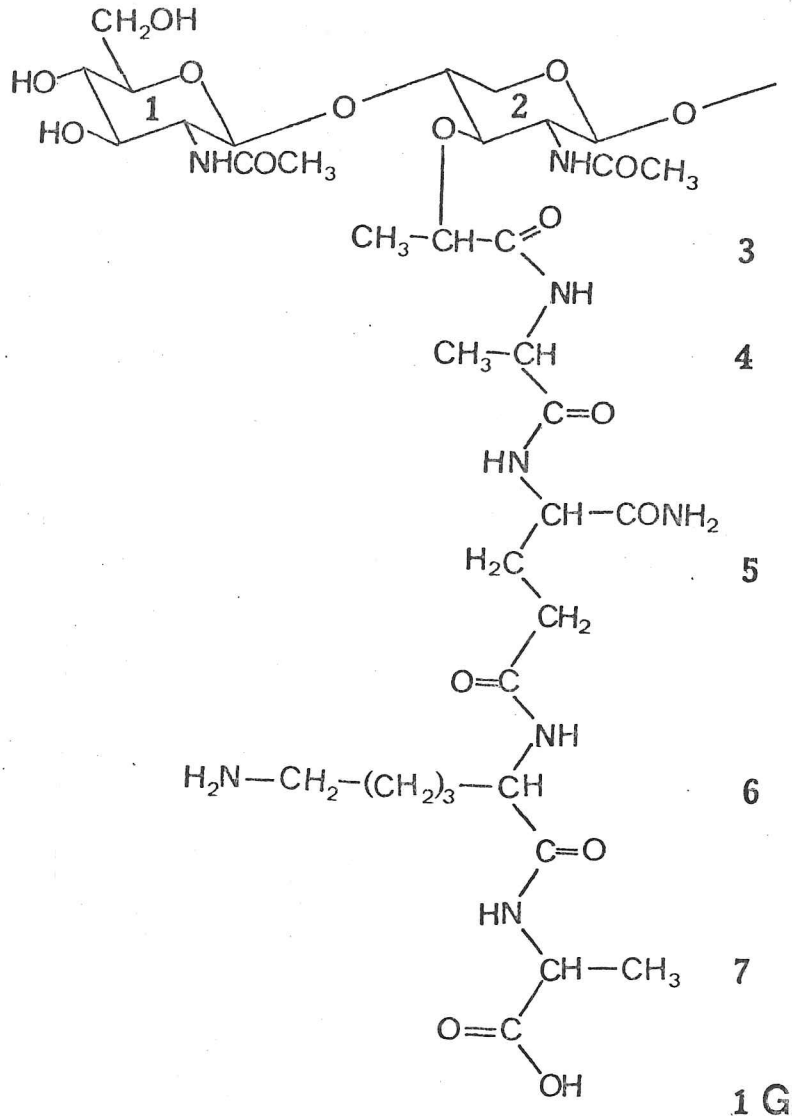

1 GlcNac

2 MurNAc

3 O-lactyl ether

4 L-ala

5 D-isoglu-NH_2

6 L-lys

7 D-ala

FIGURE 3·2 Recurring peptidoglycan subunit (S.aureus)

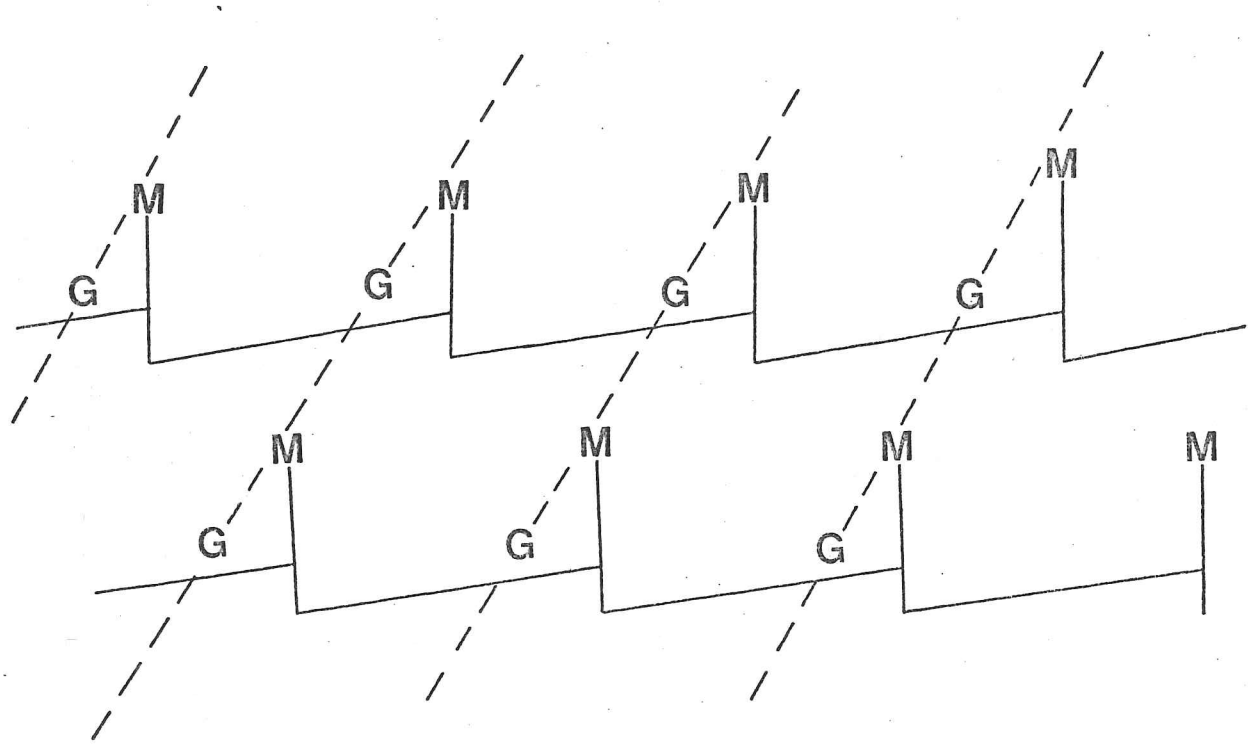

FIGURE 3·3 Structure of a typical peptidoglycan

Dotted lines ≡ polysaccharide chains

Bold lines ≡ peptide chains

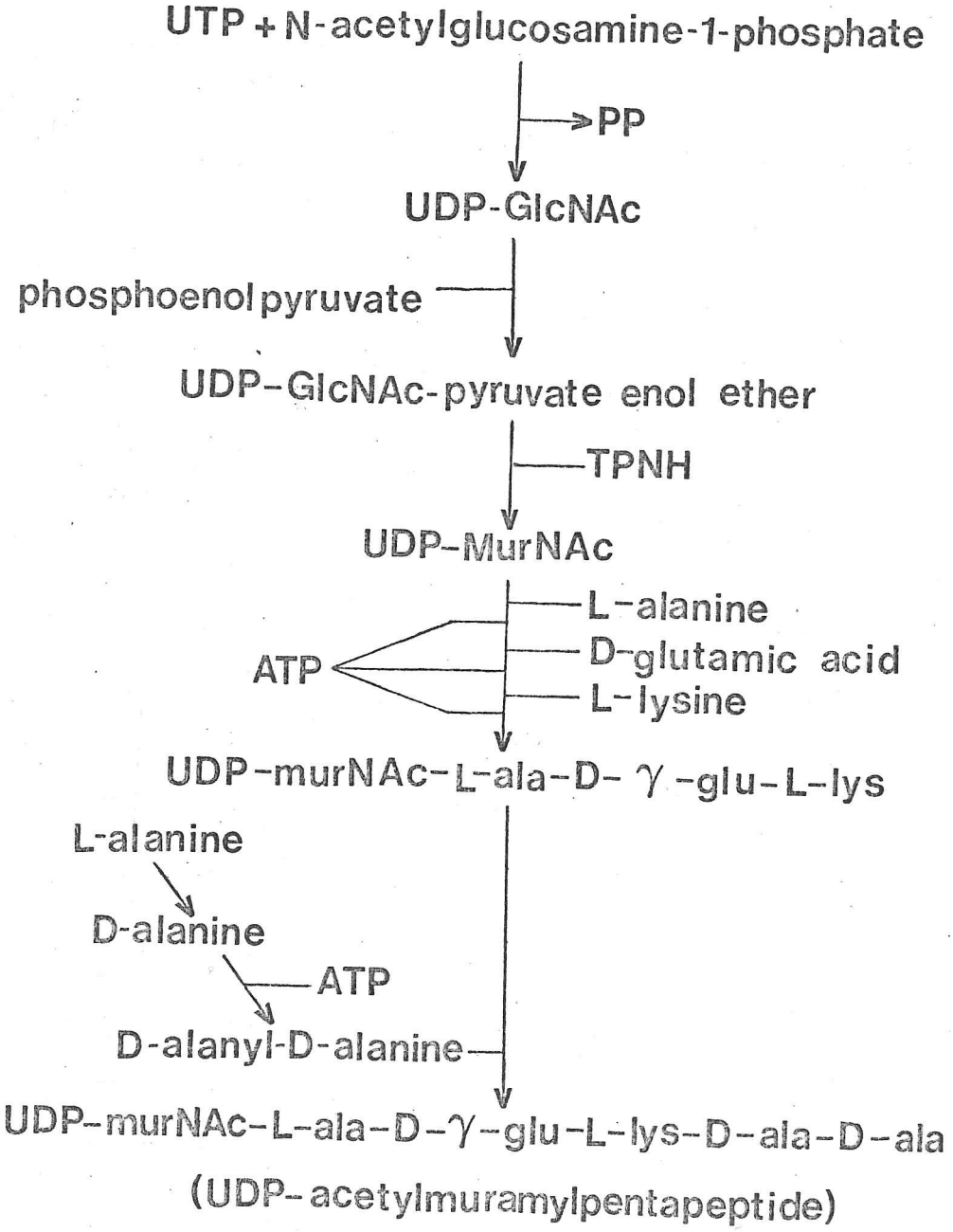

FIGURE 3·4 Cell wall synthesis - stage 1

Formation of UDP-N--acetylmuramyl-pentapeptide

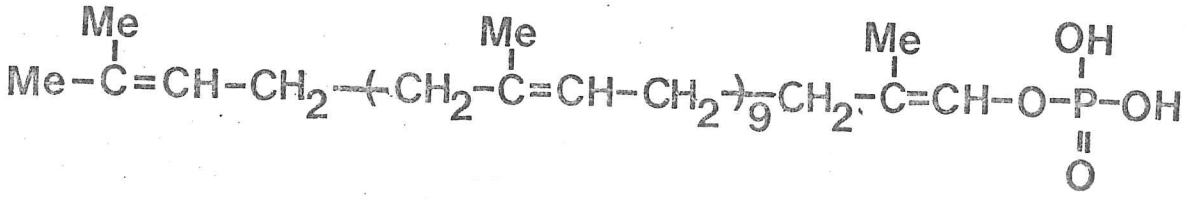

FIGURE 3·5 Structure of lipid carrier, C_{55}-iso-prenyl alcohol

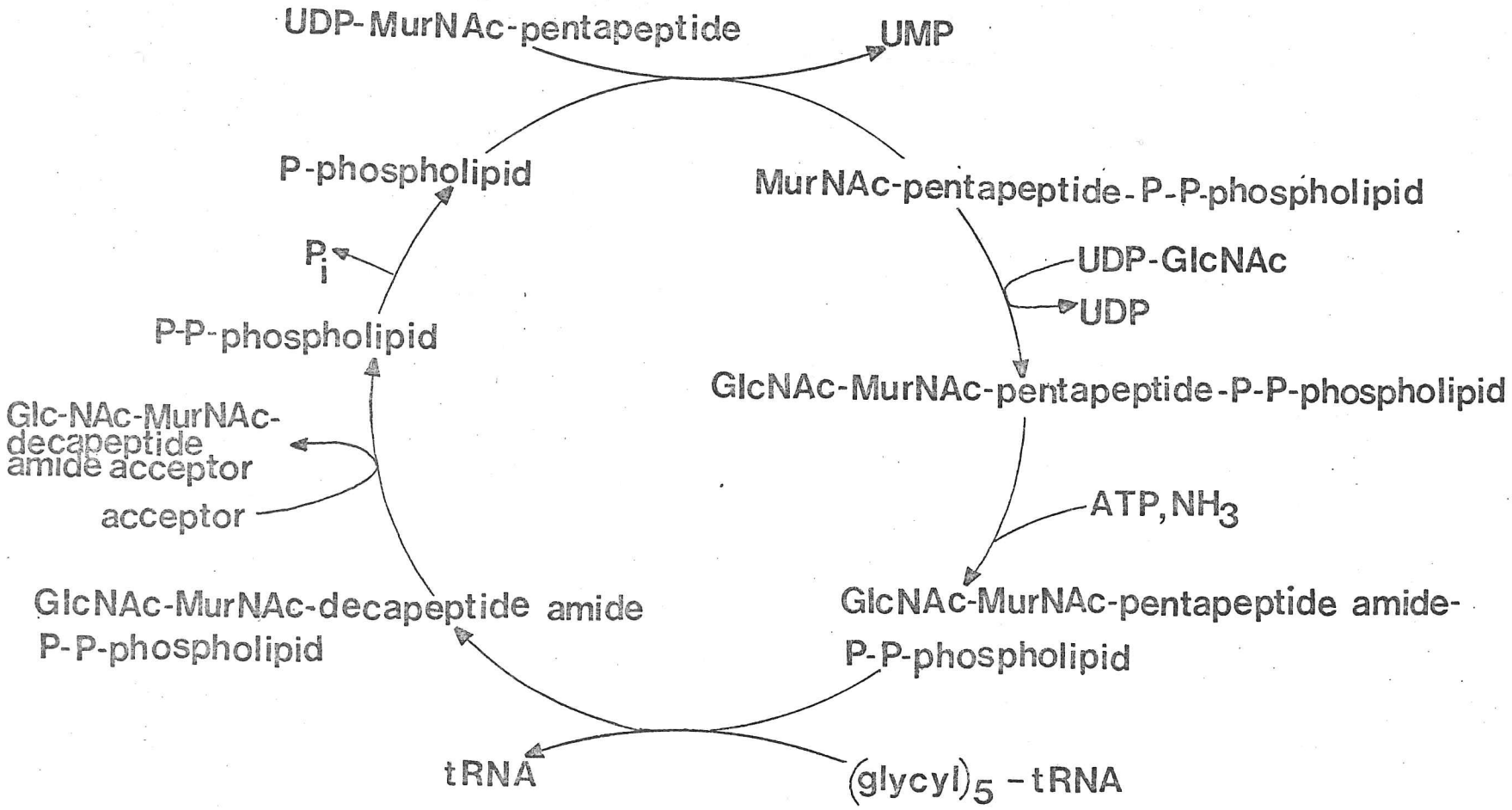

FIGURE 3·6 Cell wall synthesis–stage 2 (S.aureus)

transferred to a glycan acceptor on the outside of the cell to form a linear peptidoglycan.

Finally, the peptide chains of the linear peptidoglycan are cross-linked in a reaction catalysed by a transpeptidase. The cross-bridge is formed between the carboxyl group of the penultimate D-alanine in the pentapeptide on one chain and an amino group in a nearby chain, for example that of the DAP residue (figure 3.7a). The analogous step for Gram-positive bacteria is shown in figure 3.7b.

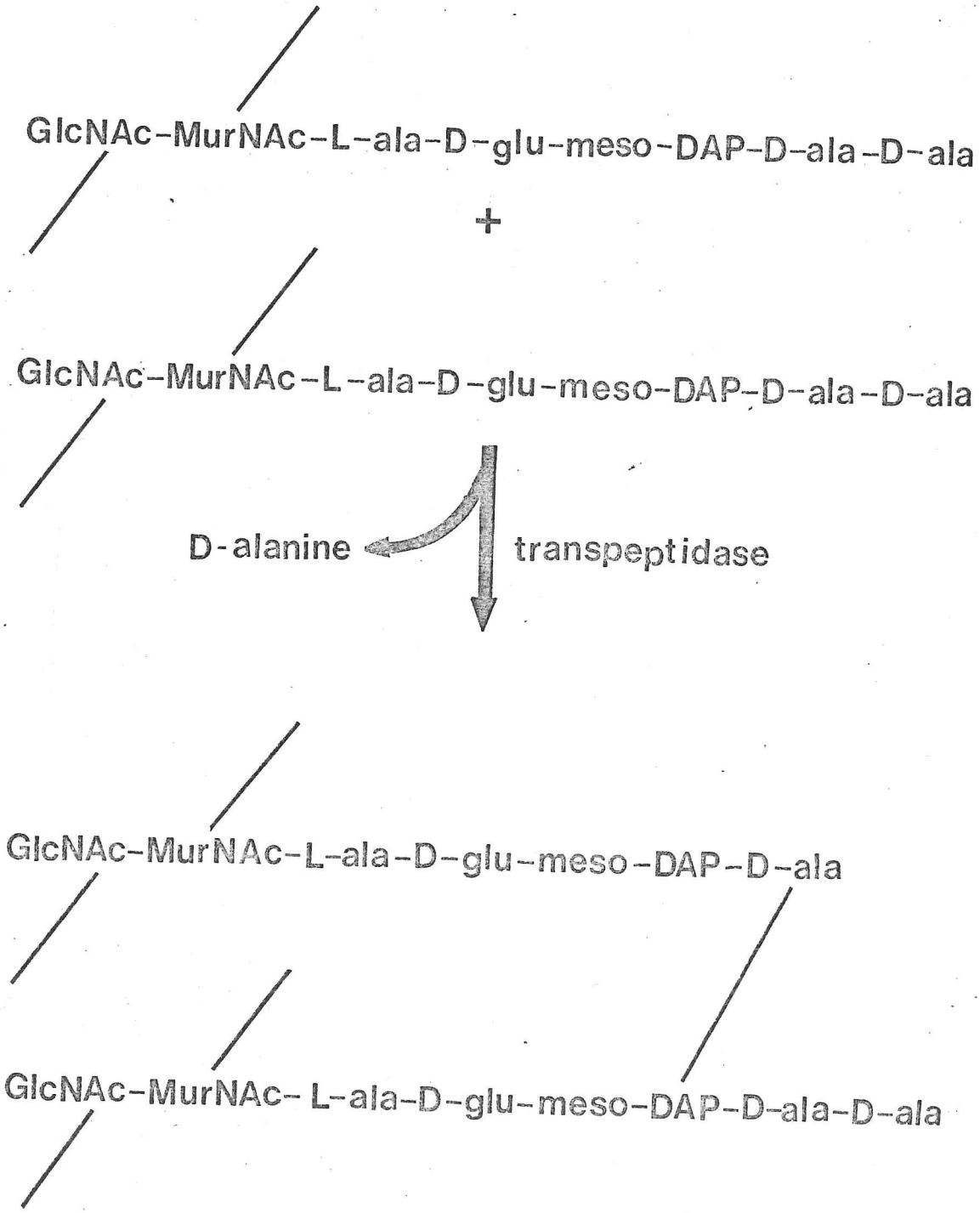

FIGURE 3·7 (a) Cell wall synthesis – stage 3 (Gram-negative)
Cross-linking of (E. coli)

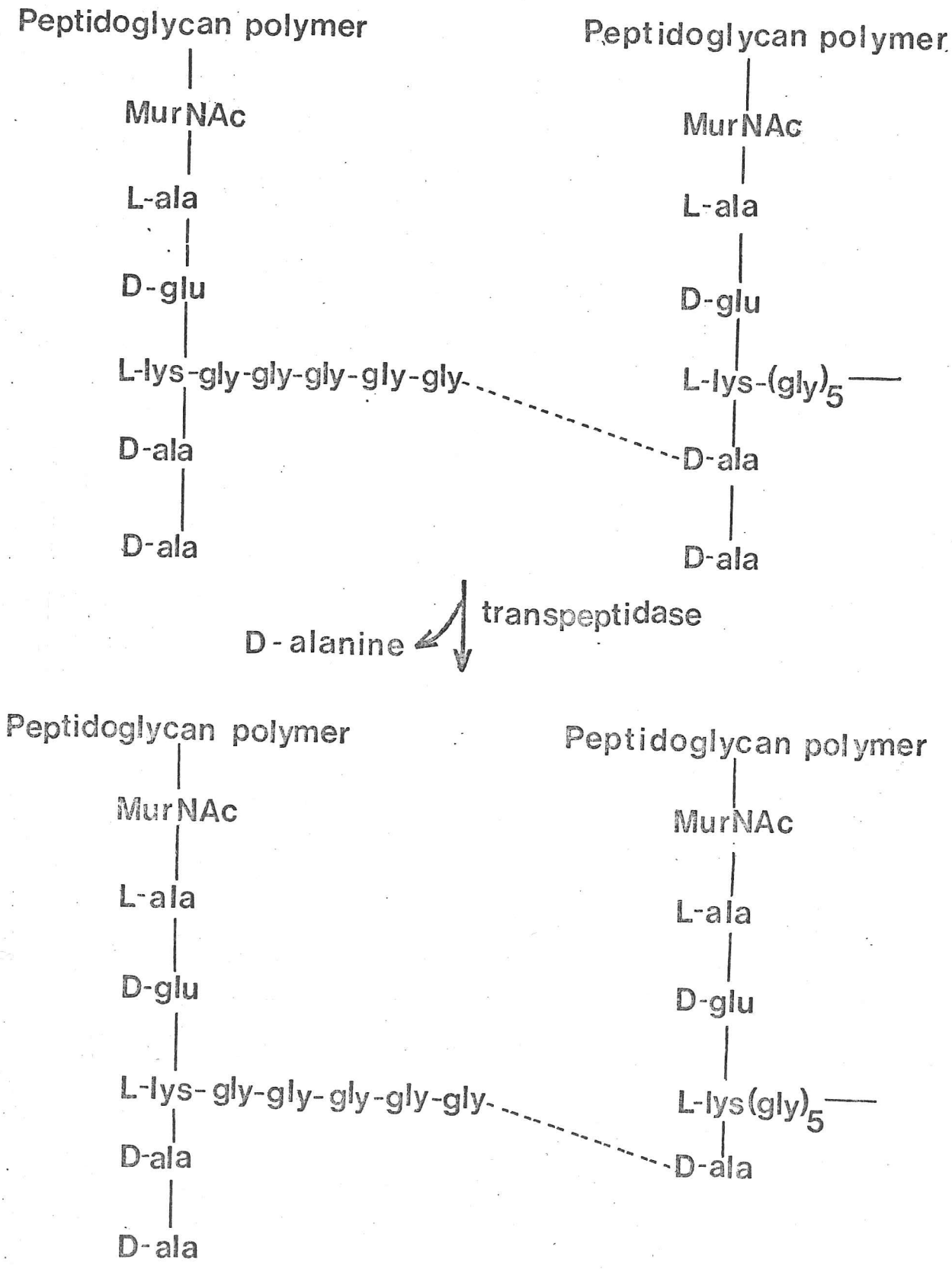

FIGURE 3·7(b) Cell wall synthesis–stage 3 (Gram-positive)

Cross-linking of S. aureus

4. NUCLEAR MAGNETIC RESONANCE SPECTROSCOPY

An understanding of the nuclear magnetic resonance (nmr) phenomenon can be gained by reference to any suitable standard text [1] . However, it is worth emphasising certain points, especially relating to high-field pulsed Fourier transform nmr which has been extensively used in the studies described later [2] .

4.1 PULSED FT NMR

Pulsed nmr involves the simultaneous excitation of all the protons in a molecule. A stronger radio-frequency is used for irradiation than that for conventional continuous wave nmr and to avoid total saturation of the energy levels it is applied for a very short time (typically microseconds). The return to equilibrium of the excited nuclear spins gives rise to what is termed free induction decay (FID) which corresponds to the nmr spectrum along a time axis instead of the usual frequency axis. Conversion to the latter is effected by application of the mathematical process of Fourier transformation. It is important to realise, therefore, that the FID and the conventional nmr spectrum are two representations of the same data set. Pulsed FT nmr has the advantage of enormous savings in time over continuous wave nmr and, since the data is accumulated rapidly in a digital form, many successive experiments may be performed on the same sample and the data from each one added together to provide significant improvements in the signal to noise ratio.

By convention, the magnetic field direction, B_o, is termed the z-axis, the radio-frequency pulse is applied along the x-axis, and the

---

[1] See Appendix 1
[2] See Chapter 6

remaining dimension, in which the observe receiver is situated, is termed the y-axis. Thus only magnetization in the x-y plane can be detected with this arrangement. The Boltzmann distribution describes the equilibrium situation in which a slight excess of nuclei are in the lowest energy level which therefore produces a net magnetization along the direction of the magnetic field (the z-axis). The maximum signal therefore corresponds to a 90^{o} perturbation of these nuclear magnetic vectors to the y-axis (figure 4.1).

In optical spectroscopy an excited molecule returns by spontaneous emission to the ground state almost instantaneously, the excess energy being dissipated into the surroundings (the lattice) as heat. This process is not favourable for a nuclear spin, which is effectively insulated from the lattice. Instead they return to the ground state by an emission process (relaxation) taking seconds and involving interaction with the lattice and other magnetic fields. From the uncertainty principle the existence of the excited state for a long time produces sharp lines and enables equalisation (saturation) of the ground and excited levels to be attained by application of a strong secondary exciting field.

The spin-populations return to equilibrium either by interaction with the environment, which is called spin-lattice or longitudinal relaxation and has a time constant T_1, or by interaction of proximal nuclear spins through a dipole-dipole effect, which is termed spin-spin or transverse relaxation and has a time constant T_2. Short T_1 values indicate the efficient return of the nuclear spins to equilibrium and T_2 values are never greater than T_1. In order to relate these effects to the magnetization diagrams shown in figure 4.1 it is desirable to use what is known as the rotating frame of reference. With the conventional cartesian axes the magnetization vectors are rotating in the x-y plane about the z-axis at the Larmor frequency. If instead one considers the frame of reference (viz. the axes) rotating about the magnetic field at the Larmor frequency the magnetization vectors appear stationary. The spin-lattice relaxation can now be identified as the return of the vector from the y-axis to the z-axis in the y-z plane. Similarly, the spin-spin relaxation can be considered as a dephasing of the magnetization vectors in the x-y

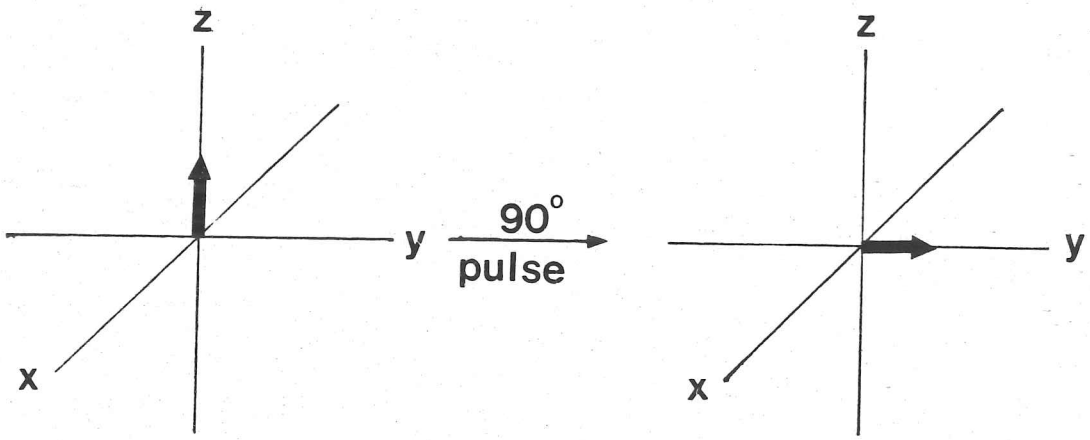

FIGURE 4·1 The observe pulse

plane which produces a reduction in the net effect observed in the y-direction. Obviously these effects do not occur in isolation but both influence the return to equilibrium by varying degrees. The situation can be schematically represented as shown in figure 4.2.

Finally, high-field nmr machines of 6.34 and 9.40T (270 and 400MHz H^1) were extensively used for the studies described in Chapter 6, in preference to lower-field machines which were more accessible, because of a number of advantages associated with their use. The coupling constant is invariant with magnetic field strength, unlike the chemical shift. For example, upon comparing spectra taken at 100MHz and 400MHz a four-fold increase in the spectral width in Hz is involved for an equivalent chemical shift (ppm) range. Since multiplets occupy the same range in Hz at any field strength, assuming that undue resonance broadening has not occurred at increased field, it can clearly be seen that the spectrum will be significantly spread-out at higher field. Thus, spectral simplification is an important consequence of higher field instruments. In addition, chemical exchange studies [3] can benefit at higher field because the rate of exchange is proportional to the chemical shift difference in Hz between the resonances of the exchanging species. High field also produces increased sensitivity since signal strength is proportional to the square of the magnetic field. One major disadvantage is that the wider spectral widths used at high field necessarily reduce the digitization; coupling constants are therefore currently most accurately measured at lower field.

4.2 DOUBLE IRRADIATION TECHNIQUES

Apart from the non-selective pulse discussed above, the application of a selective second pulse can provide additional information. Resonances which are scalar-coupled can be identified, as can dipolar-coupled resonances. The pulse power can be varied according to the experiment and elaborate pulse sequences may be necessary in order to differentiate

---

[3] See Section 4.3

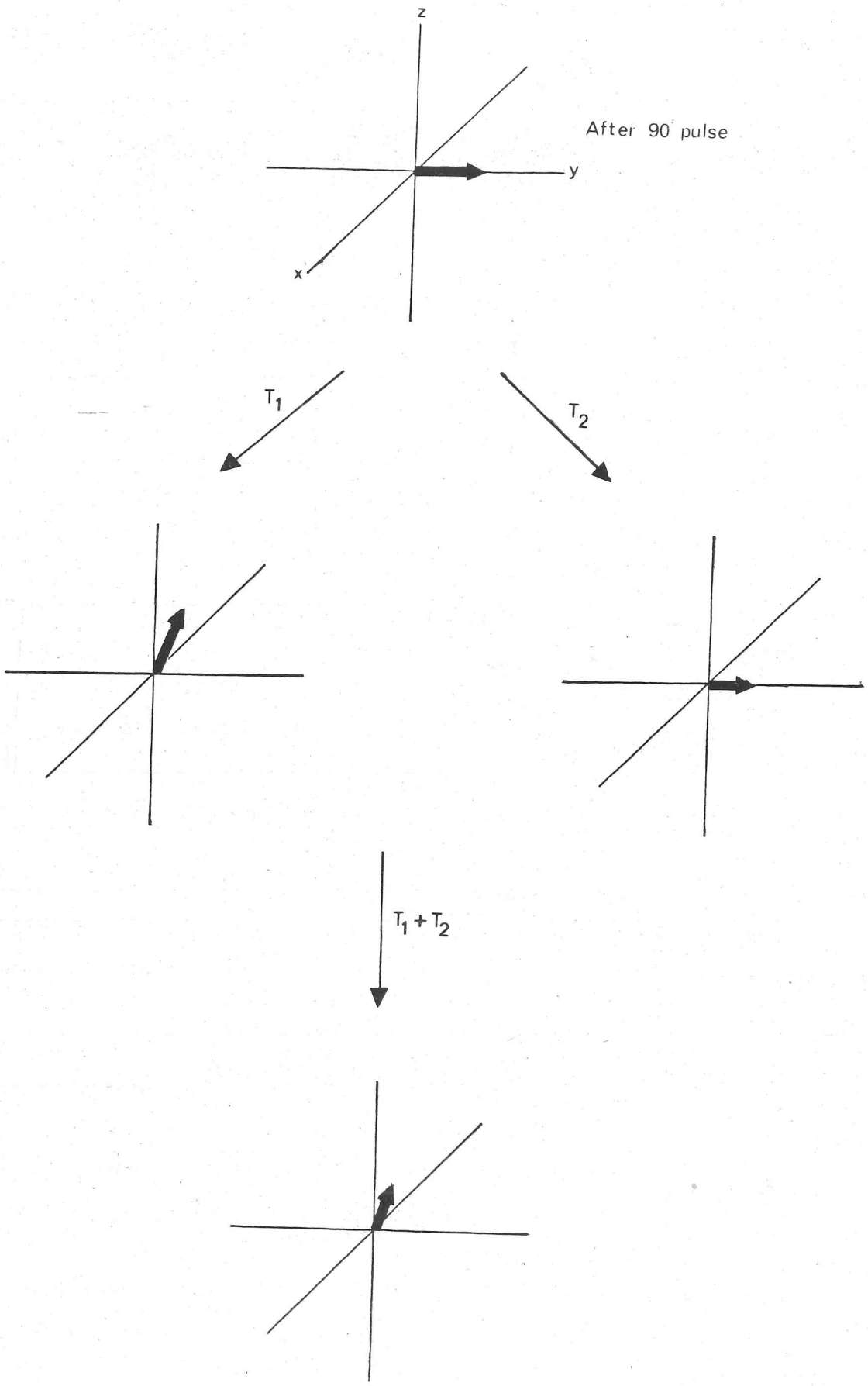

FIGURE 4·2 Relaxation processes

between different effects.

4.2.1 SPIN-DECOUPLING

Spin-decoupling is by far the most common double irradiation technique. High pulse powers, greater than those necessary for saturation, are used in order to selectively remove spin-coupling effects. A simple decoupling pulse can also give rise to effects such as transfer of saturation between chemically exchanging species, and nOe's, both of which are discussed below.

4.2.2 THE NUCLEAR OVERHAUSER EFFECT

The nOe is manifested by a change in peak intensity when two nuclei are close in space, and therefore dipolar-coupled, and one of them is saturated. If one considers two such nuclei which are not scalar-coupled the equilibrium situation can be represented by figure 4.3a. The direction of the nuclear spins are shown by the arrows and the transitions for each nucleus, A and X, which give rise to the resonance lines are indicated by W. At equilibrium the populations of energy levels 2 and 3 are considered to be equal (p), with a slight excess of population in level 1 (p+q) and a slight deficit in the highest energy level 4 (p-q). Peak intensity is proportional to the population differences of the energy levels between which transitions occur. Thus before perturbation of the spin system both nuclei have an intensity of 2q. Saturation of spin A causes equalisation of the populations between which transitions giving rise to the A resonance line occur. In other words levels 1 and 2 (p+1/2q), and levels 3 and 4 (p-1/2q) are equalised. However, at this stage the intensity of nucleus X is still 2q (figure 4.3b). The system as a whole is now perturbed compared to the equilibrium situation; the degenerate levels 2 and 3 are separated by a population difference of q, and the separation between levels 1 and 4 has been reduced from 2q to q. The system attempts to return to equilibrium, the usual single quantum transitions are too inefficient therefore the double quantum (level $4 \rightarrow 1$) or zero quantum (level $2 \rightarrow 3$) transitions are used. Considering the double quantum transition, W_2, first (figure 4.3c); an amount of spin density, d, is transferred from level 4 to the ground state. The intensity of the X-resonance is now increased to

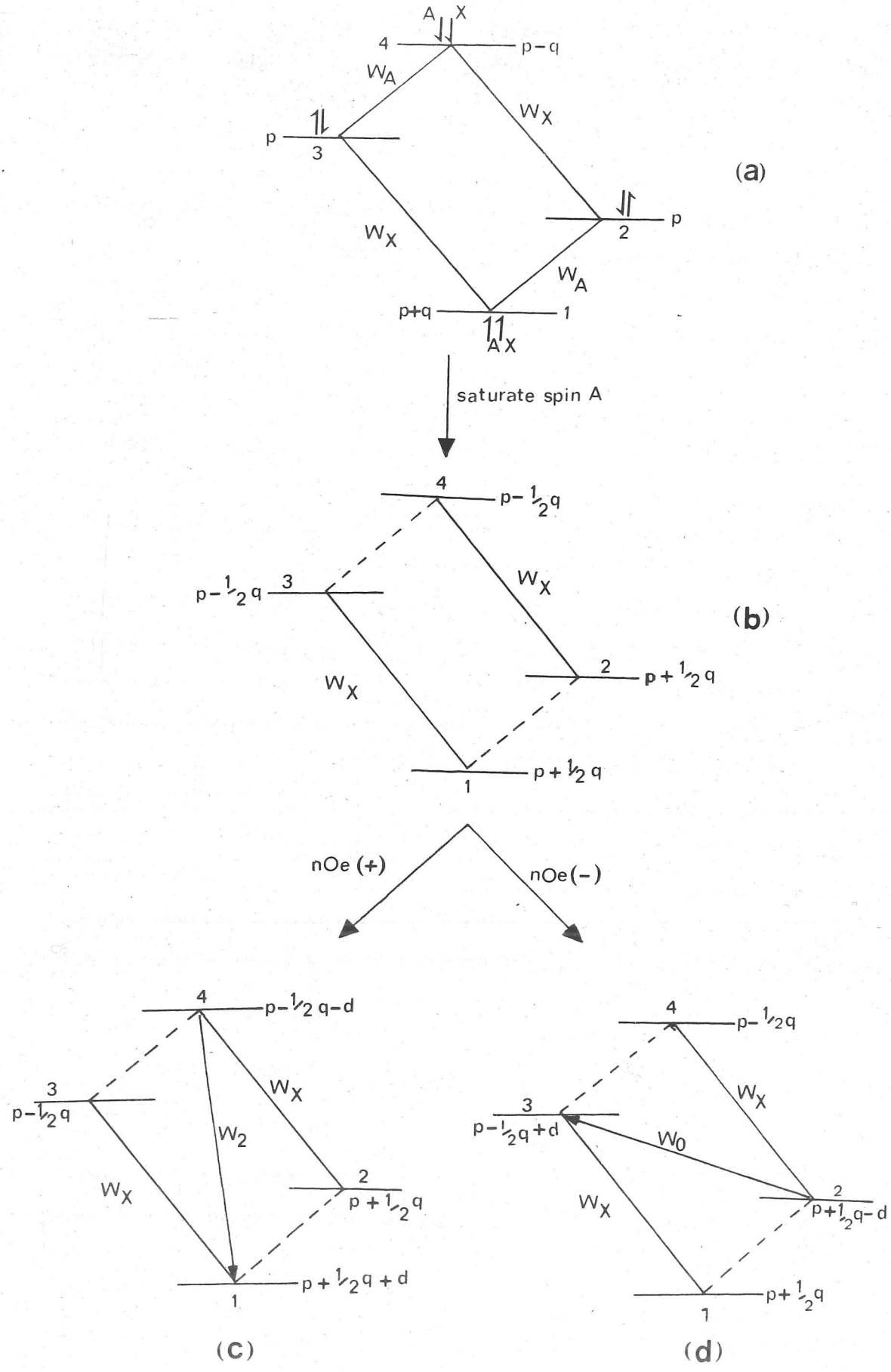

FIGURE 4·3 The nuclear Overhauser effect

2q+2d, thus it is enhanced by 2d and is termed a positive nOe. Conversely, if the spin density, d, is transferred from level 2 via the zero quantum transition, W_o, to level 3 (figure 4.3d) then the intensity of the X-resonance is reduced to 2q-2d. Thus it is decreased by 2d and is termed a negative nOe.

The rate of build-up of an nOe has an r^{-6} dependence. The maximum homonuclear positive nOe is 50% whereas the maximum negative nOe is 100%. The nOe is critically dependent on the function Wt_c, where $W=2\pi\nu$ Hz (the Larmor frequency) and t_c is the rotational correlation time (effectively the tumbling time). If the value of this function is above 1.12 a negative nOe is observed whereas below 1.12 a positive nOe is observed. At exactly $Wt_c=1.12$ no nOe is observed. In general large molecules, or small molecules in viscous solvents, exhibit negative nOe's whereas small molecules usually produce a positive effect. The magnitude and sign of the nOe can be manipulated by varying the temperature (larger and more positive nOe's at higher temperatures) or the solvent system (larger and more negative nOe's in viscous solvents). For Wt_c far greater than 1.12 an effect termed spin diffusion becomes important. At long t_c, especially with large molecules, excitation applied to one nucleus is no longer dissipated through molecular motion, but is instead transferred to neighbouring nuclei, causing their signals to decrease or disappear. Hence this effect is only observed in the negative nOe regime. In addition, spin diffusion can be rapidly spread throughout a molecule if either the irradiated proton, or one of the neighbouring protons is exchangeable with protons in other distant parts of the same molecule. However, the initial decay of magnetization is much more dependent on the local environment than the overall decay.

4.2.3 DIFFERENCE SPECTRA

Subtle changes in spectra are frequently difficult to monitor because of the initial complexity of the spectrum. A simple and rapid method of removing unnecessary information is to make use of difference spectra. A reference spectrum is accumulated in one block of computer memory whilst in another block the perturbed spectrum is collected. Subtraction of one set of data from the other produces a spectrum solely

of perturbed resonances which is far easier to interpret. Figure 6.16 is an example of an nOe difference spectrum, and figure 6.27 is that of a decoupling difference spectrum.

4.3 CHEMICAL EXCHANGE

The line shape of nmr signals is sensitive to chemical exchange processes and such spectra are also temperature dependent. The effect depends upon the rate of exchange compared with the nuclear spin time scale. If the exchange is slow, then the spectra of the separate species is observed. If the exchange is fast then a spectrum corresponding to the weighted mean of the individual spectra is observed but without significant line broadening. However, in the intermediate region broadened and averaged spectra are obtained.

Quantitative kinetic and thermodynamic information can be obtained from line shape analysis of a slow exchanging species which is slowly converted to the fast exchanging species, usually by an increase in temperature. The temperature at which the resonance lines, corresponding to the same nucleus in two environments, merge is called the coalescence temperature. The relatively complex nature of line shape analysis has prompted a number of approximate solutions, most of which require a knowledge of the coalescence temperature, T_c, and the shift difference, $\delta\nu$Hz, between the resonances in question in the slow exchange region. The most useful of these are shown in figure 4.4. The energy barrier obtained from figure 4.4b is temperature dependent.

4.3.1 TRANSFER OF SATURATION

If a nuclear species exists in two environments which are non-equivalent then one would expect a change in the magnetization of site A to also be detectable at site B. The effect is observed only if the T_1 in site B is not negligible compared with the lifetime of the nucleus in site B.

$$K_{coal} = \frac{\pi \delta \nu}{\sqrt{2}} = 2{\cdot}22\,\delta\nu \qquad \text{(a)}$$

K_{coal} is the rate constant at the coalescence temperature

$$\Delta G^{\ddagger} = 19{\cdot}14\,T_c\,(9{\cdot}97 + \log\frac{T_c}{\delta\nu})\ \text{J mole}^{-1} \qquad \text{(b)}$$

$\Delta G^{\ddagger}$ is the energy barrier for the process at the coalescence temperature

FIGURE 4·4 Approximate equations for chemical exchange phenomena

5. PREVIOUS BINDING STUDIES ON VANCOMYCIN-TYPE ANTIBIOTICS

The site of action of vancomycin-type antibiotics had been known for some time to be the cell-wall of Gram-positive bacteria[57,59] but it was not until the extensive studies of Nieto and Perkins[60-63] that the precise location of this interaction was determined. Vancomycin-type antibiotics inhibit the biosynthesis of the peptidoglycan of bacterial cell walls causing the accumulation of UDP-N-acetylmuramyl-peptide precursors. Using various peptidoglycan precursors and systematically changing each residue in turn Nieto and Perkins were able to identify the conditions necessary for complex formation as follows:

(1) Residue 1 (C-terminal) must have D-configuration or be glycine, the carboxyl group must be free and in the anionic form, and the optimum side-chain length is a methyl group for vancomycin but larger side-chains can be accommodated with ristocetin (presumed due to steric crowding around the chlorine atom of ring 1 of vancomycin).

(2) Residue 2 must also have the D-configuration or be glycine and the optimum side chain is a methyl group. The peptide N-terminus must be blocked, by acetylation or formylation, for complex formation.

(3) The L-configuration is preferred for residue 3 and the optimum affinity is found with L-lysine or L-ornithine.

On the basis of their experimental evidence [1] it became clear that the primary site of attack for vancomycin-type antibiotics was the D-ala-D-ala growth point of the bacterial cell wall.

---

[1] See table 5.1

5. PREVIOUS BINDING STUDIES ON VANCOMYCIN-TYPE ANTIBIOTICS

The site of action of vancomycin-type antibiotics had been known for some time to be the cell-wall of Gram-positive bacteria[57,59] but it was not until the extensive studies of Nieto and Perkins[60-63] that the precise location of this interaction was determined. Vancomycin-type antibiotics inhibit the biosynthesis of the peptidoglycan of bacterial cell walls causing the accumulation of UDP-N-acetylmuramyl-peptide precursors. Using various peptidoglycan precursors and systematically changing each residue in turn Nieto and Perkins were able to identify the conditions necessary for complex formation as follows:

(1) Residue 1 (C-terminal) must have D-configuration or be glycine, the carboxyl group must be free and in the anionic form, and the optimum side-chain length is a methyl group for vancomycin but larger side-chains can be accommodated with ristocetin (presumed due to steric crowding around the chlorine atom of ring 1 of vancomycin).

(2) Residue 2 must also have the D-configuration or be glycine and the optimum side chain is a methyl group. The peptide N-terminus must be blocked, by acetylation or formylation, for complex formation.

(3) The L-configuration is preferred for residue 3 and the optimum affinity is found with L-lysine or L-ornithine.

On the basis of their experimental evidence [1] it became clear that the primary site of attack for vancomycin-type antibiotics was the D-ala-D-ala growth point of the bacterial cell wall.

---

[1] See table 5.1

Table 5.1 Vancomycin and Ristocetin B Binding Data[63]

Peptide	Vancomycin		Ristocetin B	
	K_A	ΔG	K_A	ΔG
Change in Residue 1				
Ac_2-L-lys-D-ala-D-ala	150	35.1	59	32.8
Ac_2-L-lys-D-ala-gly	13	29.1	2.2	24.7
Ac_2-L-lys-D-ala-D-leu	0.92	22.5	61	32.9
Ac_2-L-lys-D-ala-D-lys	1.4	23.5	10	28.4
Ac_2-L-lys-D-ala-L-ala	N/C	N/C	N/C	N/C
Ac-D-ala-D-ala	2.0	24.4	7.2	27.6
Ac-D-ala-gly	0.54	21.2	0.19	18.7
Change in Residue 2				
Ac_2-L-lys-gly-D-ala	9.4	28.3	16	29.6
Ac_2-L-lys-D-leu-D-ala	29	31.0	5.8	27.0
Ac_2-L-lys-L-ala-D-ala	N/C	N/C	N/C	N/C
Ac-gly-D-ala	1.1	23.0	4.9	26.7
Change in Residue 3				
Ac-gly-D-ala-D-ala	9.4	28.3	16	29.6
Ac-L-ala-D-ala-D-ala	31	31.1	22	30.4
N-Ac-L-tyr-D-ala-D-ala	19	30.0	29	31.1
Ac-D-ala-D-ala-D-ala	5.0	26.7	13	29.1
Free Amino Group				
L-lys-D-ala-D-ala	1.2	23.0	0.82	22.2
-Ac-L-lys-D-ala-D-ala	47	32.2	19	30.1
Other Peptides				
Ac-L-ala-gly-gly	0.49	21.7	0.25	19.3
Ac-gly-gly-gly-gly	0.15	18.0	0.08	16.5
Ac-L-ala-D-glu-gly	48	32.3	0.07	16.1

Association constants (K_A) measured in 10^4.l.mole^{-1},
free energy changes (ΔG) measured in KJ.mole^{-1}.
No combination is indicated by N/C.

In order to determine the nature of the interaction between peptidoglycan precursors and vancomycin, electrophoresis was performed in the presence of various reagents[60]. In the presence of 1M sodium chloride or 10mM Ca^{2+} or 85mM Mg^{2+} there was no sign of dissociation of the compound, which indicated that a simple ionic interaction was not involved, whereas in the presence of 8M urea almost complete dissociation of the complex occurred. Hydrogen bonding was therefore invoked as the

major interaction. The two free amino groups of vancomycin were not thought to have a significant influence on complex formation[60] since upon N-acetylation or N-formylation binding still occurred, as monitored by antibacterial activity, although to a reduced extent. Aglucovancomycin, a form of the antibiotic with the sugar moiety removed, was also found to retain antibacterial activity, indicating that the sugar moieties were not essential for activity but probably aided transport within the body.

5.1 VANCOMYCIN

The first direct study of the intermolecular interactions using nmr was performed by Brown and co-workers[64,65] who monitored the peptide resonances and the methyl resonances of vancomycin upon binding. The complexity of the spectrum at 100MHz precluded detailed analysis and assignment, thus limited information only, of methyl group shifts and pH dependence of association constants was obtained. The most stable complex was formed in the pH4.0-7.5 region, being stabilised by a favourable electrostatic interaction (ΔG^{o}=-5.9KJ.mole^{-1}) between the terminal carboxylate anionic group of the peptide with the cationic group on the N-methylleucine of vancomycin. Weaker complexes were found in the ranges pH2-4 and pH7.5-10.5. The acetyl methyl group was the only bound peptide methyl resonance to shift upon pH titration; about 7Hz at the pK of the amino groups (pK$\sim$8), which suggested that this group was proximal to the vancosamine amino group. The leucine methyl groups were shifted 13Hz in the complex and this was pH independent between pH3.7-10.5, being apparently unaffected by most ionization states of the ionic groups. However, at pH2.2, the shift was reduced to 3Hz, which suggested that these two methyl groups were close to the peptide carboxyl. The thermodynamic parameters of complex formation were calculated as ΔG^{o} -25.2KJ.mole^{-1}; ΔH^{o} -58.1KJ.mole^{-1}; ΔS^{o} -24e.u. The bound shifts were found to be temperature independent indicating that they were probably due to ring current effects rather than a conformational change. Experiments on the complex of aglucovancomycin with acetyl-D-ala-D-ala produced a similar

pattern of bound shifts but reduced by about 75% compared with the vancomycin complex, implying a slightly modified binding site. The association constant was also reduced compared with vancomycin/Ac-D-ala-D-ala by about one order of magnitude. Further confirmation of the results of Nieto and Perkins was evidenced by a series of experiments in which peptide residues were systematically changed to investigate specificity of the binding site. The position of the bound resonance of the C-terminal alanine was found to be invariant with changes in other parts of the peptide, suggesting that it was enveloped in a pocket in the receptor site, a view supported by the reduction in the association constant upon substituting a larger group for the methyl side-chain.

The first high field nmr study was performed by Williams and Kalman[37] using a 270MHz machine. The spectra of aglucovancomycin and vancomycin were assigned in dmso-d_6 in order to retain exchangeable proton resonances. By this time all of the component parts of vancomycin had been identified although there was little evidence to suggest the most probable way in which they were coordinated to one another. Using chemical shift and nOe evidence Williams and Kalman were able to tentatively suggest a structure in which all the residues were assigned approximate positions in the molecule although four of the six secondary amide bonds were not identified. Further details of their structural studies are presented elsewhere [2] . Preliminary studies using vancomycin and Ac-D-ala-D-ala (1:1) in dmso-d_6 produced a complex, as evidenced by selective shifting and broadening of certain resonances (table 5.2).

---

[2] See Section 2.1

Table 5.2 Vancomycin/Ac-D-ala-D-ala (1:1) in dmso-d_6 (270MHz) Shifts Upon Binding (70°C)

Proton	Shift(Hz)	Proton	Shift(Hz)
a_3	+51	d	-19
b	-36	hh	+18
f	+31	cc	+18
s_4	+27	a_5	+15
s_5	+23	a	-14
		s_2	+13

Downfield shifts are positive.

A binding site was sketched out on the assumption that the protons whose resonances were most perturbed and selectively broadened were those associated most closely with the complexing of Ac-D-ala-D-ala. The downfield shifts of the N-methylleucine N-Me (hh) and the α-CH resonances (s_4, s_5, cc) were ascribed to the possible formation of a zwitterionic salt bridge between the carboxyl group of the peptide and the N-methylleucine of the antibiotic. In addition, upon cooling to 45°C the N-methylleucine N-Me was shifted downfield (60Hz) to a position close to that found in aglucovancomycin, in which it was known to be protonated[64]. From the data it was also suggested that protons f,b,s_2 and a_3 were involved in the binding site which would indicate a cleft, between the triaryl system and the biphenyl system, along which the N-terminal end of the peptide substrate was bound. The previously reported[64] shielding of the C-terminal alanine methyl group was also confirmed. Shortly after this study Sheldrick and co-workers published[38] the x-ray structure of a crystalline degradation product (CDP-I) of vancomycin in which the primary amide had been hydrolysed to a carboxyl. On the basis of a CPK model, built with reference to the x-ray data and the previous nmr studies, a more precise binding site was proposed involving three hydrogen bonds between the antibiotic and the peptide. This arrangement is shown schematically in figure 5.1 and the model is shown in figure 5.2. Convert and co-workers[66] recognised that the crystal structure of CDP-I did not allow for any interaction between the peptide carboxyl and the NH_2^+Me group of vancomycin. Having previously found[64] a contribution of 5.9KJ.mole^{-1} for a

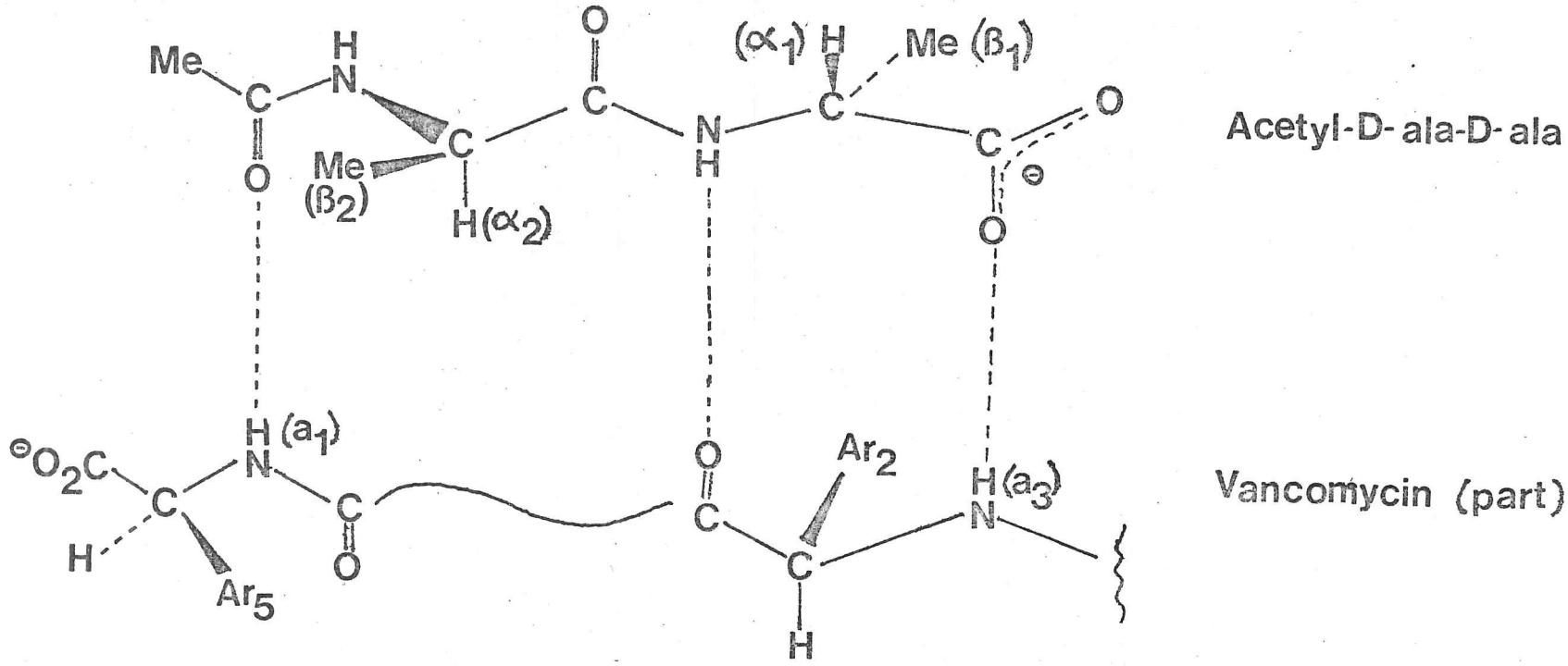

FIGURE 5·1 Vancomycin / Ac-D-ala-D-ala proposed binding site

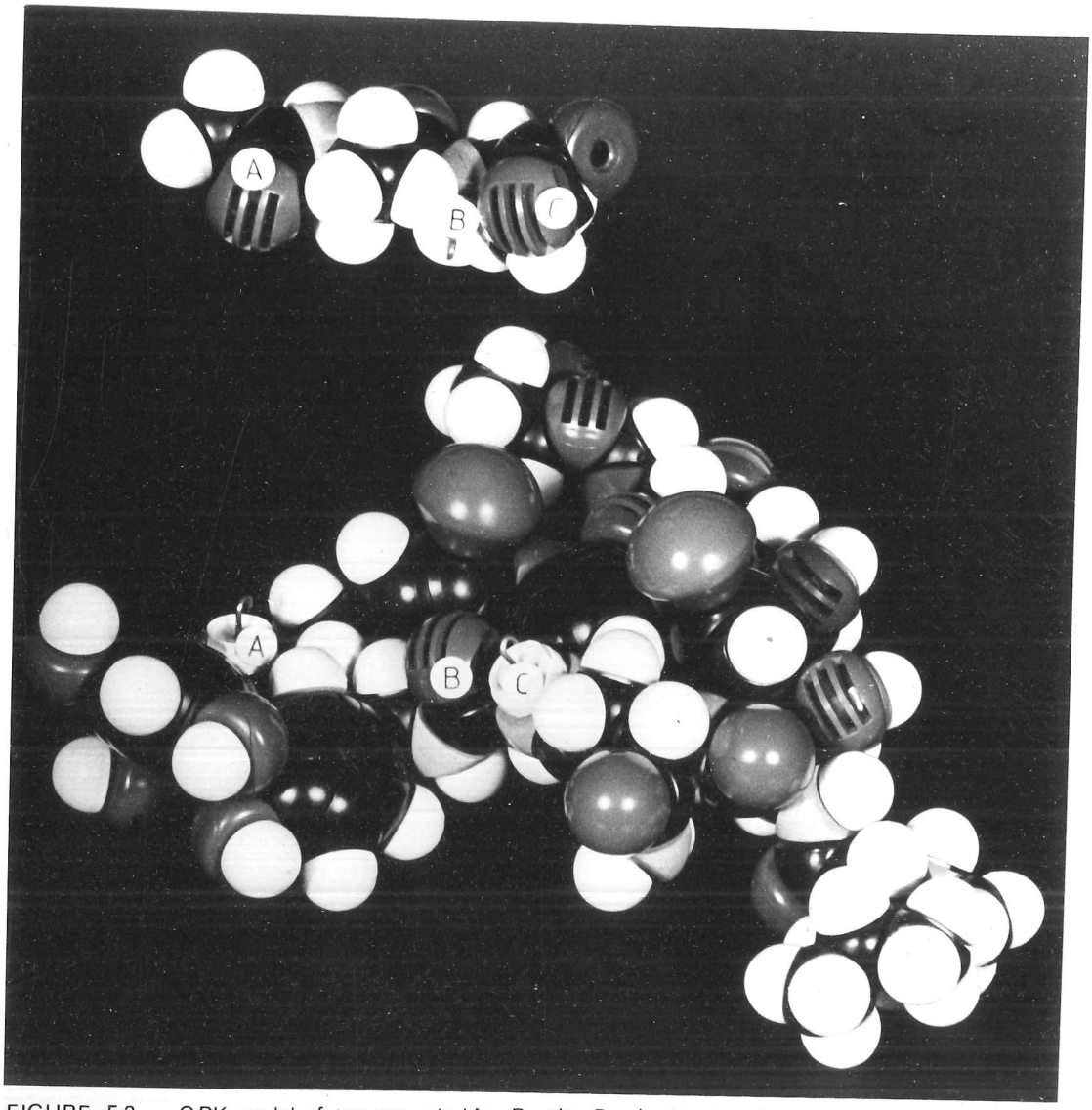

FIGURE 5·2 CPK model of vancomycin/Ac-D-ala-D-ala binding site (proposed hydrogen bonds A-A, B-B & C-C)

zwitterionic salt bridge between these two groups upon complex formation they proposed that the positively charged N-Me protons, which are about 9Å distant from the peptide carboxyl according to the x-ray study, could reasonably be moved to within 5Å of the peptide carboxyl simply by rotation about the flexible leucine side-chain (figure 5.3). Such a modification could account for the shifts of the leucine methyl groups, the aspartic-NH and aspartic methylene protons. In addition, upon increasing the length of the peptide backbone by adding a diacetylated L-lysyl residue to the N-terminal alanine of D-ala-D-ala, a significant upfield shift, of 28Hz, was observed for the C-3 methyl group of the amino-sugar vancosamine, indicating a possible sugar-peptide interaction.

5.2 RISTOCETIN A

The specific nature of the binding site of the antibiotic ristocetin A has only recently been studied, by Kalman and Williams[67] using 270 and 360MHz proton magnetic resonance spectra. Assignment of the spectrum of ristocetin A bound to Ac-D-ala-D-ala was simplified by the fact that slow exchange conditions [3] prevailed for most resonances at temperatures less than 40°C in dmso-d_6. This was due to the high barrier to dissociation[14] ($\sim$75KJ.mole^{-1}) and the large shift differences suffered by some of the protons. Addition of 0.5 molar equivalents of ristocetin A to peptide in dmso-d_6 solution gave rise to two sets of resonances due to free and bound peptide; the correlation being made between them by transfer of saturation experiments [4] . The two alanine methyl groups were found to be considerably shielded (0.35 and 0.89ppm), the C-terminal methyl being the most shielded was presumed to lie over one of the aromatic rings of the triaryl system such that it experiences a significant ring current effect. The downfield shift (0.33ppm) of the proton (cc) attached to the same carbon as the free amino group was

---

[3] See Section 4.3
[4] See Section 4.3.1

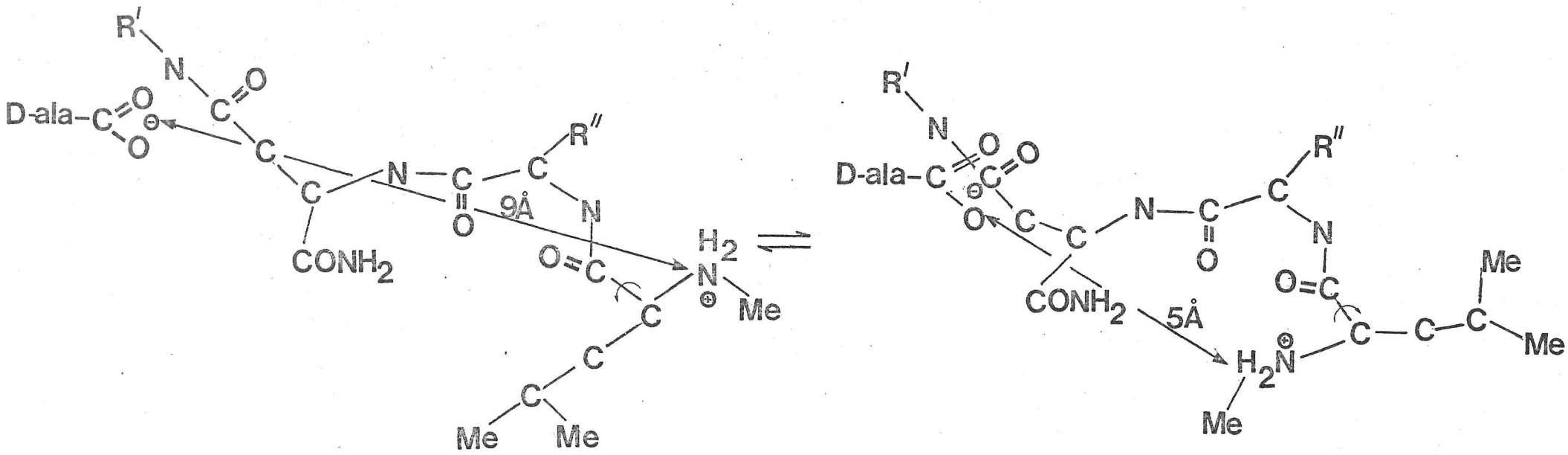

FIGURE 5·3 Proposed rotation of vancomycin leucine residue

ascribed to the protonation of this amino group after the addition of the acidic peptide (N.B. this grouping was presumed un-protonated in free vancomycin on the basis of shift analogies with aglucovancomycin upon the addition of base to deprotonate the amino group). From the small changes observed in $J_{\alpha,NH}$ for the free and bound antibiotic it was clear that no major conformational change, such as peptide bond rotation or cis-trans isomerization, had taken place upon binding. The main evidence used to map out the binding site of ristocetin A with the cell wall peptide analogue Ac-D-ala-D-ala was obtained from the temperature dependence and chemical shifts of NH resonances and intramolecular and intermolecular nOe's of the complex. From a study of the free peptide it was shown that secondary amide NH protons exposed to solvent have temperature coefficients of the order -5 to -6 X 10^{-3}. Comparing this value with the temperature coefficients of the bound NH protons it was clearly evident that the N-terminal NH proton ($\Delta\delta/\Delta T$ = -6.2 X 10^{-3}) was exposed to solvent, whereas the C-terminal NH proton ($\Delta\delta/\Delta T$ = -1.5 X 10^{-3}) was not. A hydrogen bond was therefore postulated between the latter and ristocetin A. Similarly, the reduced accessibility of the ristocetin a_1 proton to solvent, and the considerable downfield shifts of the NH proton resonances a_4 (4.64ppm), a_5 (2.42ppm) and a_3 (1.45ppm) upon binding was in accord with the existence of hydrogen bonds between these protons and the peptide. On the basis of the above data it was proposed that in the ristocetin A/peptide complex the antibiotic NH proton a_1 and the pocket of NH protons formed by a_3-a_5-a_4 act as H-bond donors to respectively the acetyl-CO and the carboxylate group of the peptide, and that the antibiotic ring 2 carbonyl is H-bonded to the peptide C-terminal NH proton . An additional interaction between the peptide carboxylate group and the antibiotic $-NH_2^+Me$ group was proposed on the grounds of the Coulombic stabilization of the complex and the additional H-bonding. The arrangement is illustrated schematically in figure 5.4 and in a CPK model in figure 5.5. Further evidence for this model was provided by the observation of intermolecular nOe's between protons of the antibiotic and the peptide in the complex (table 5.3, nOe's 1,2,3 and 7).

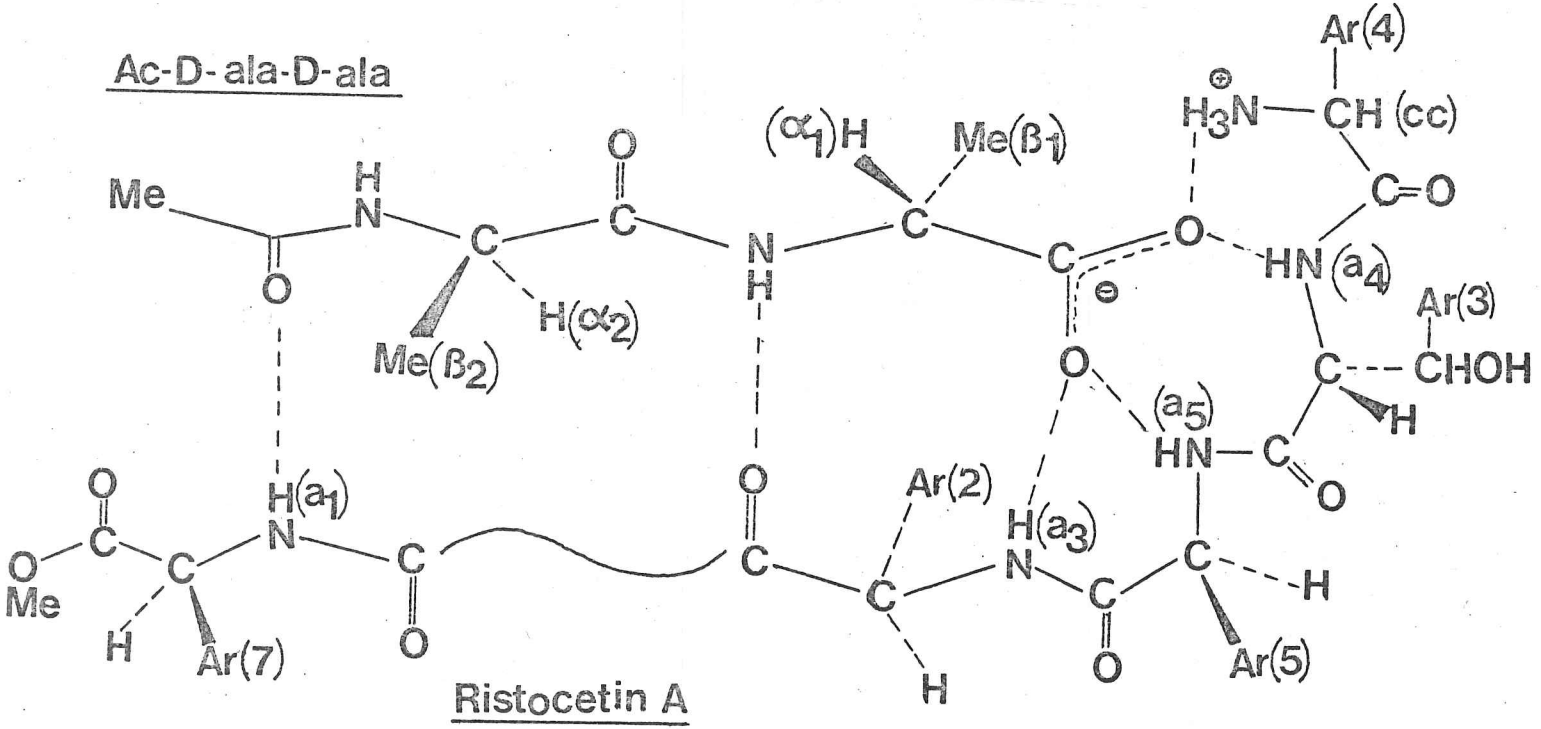

FIGURE 5-4 Ristocetin A / Ac-D-ala-D-ala proposed binding site

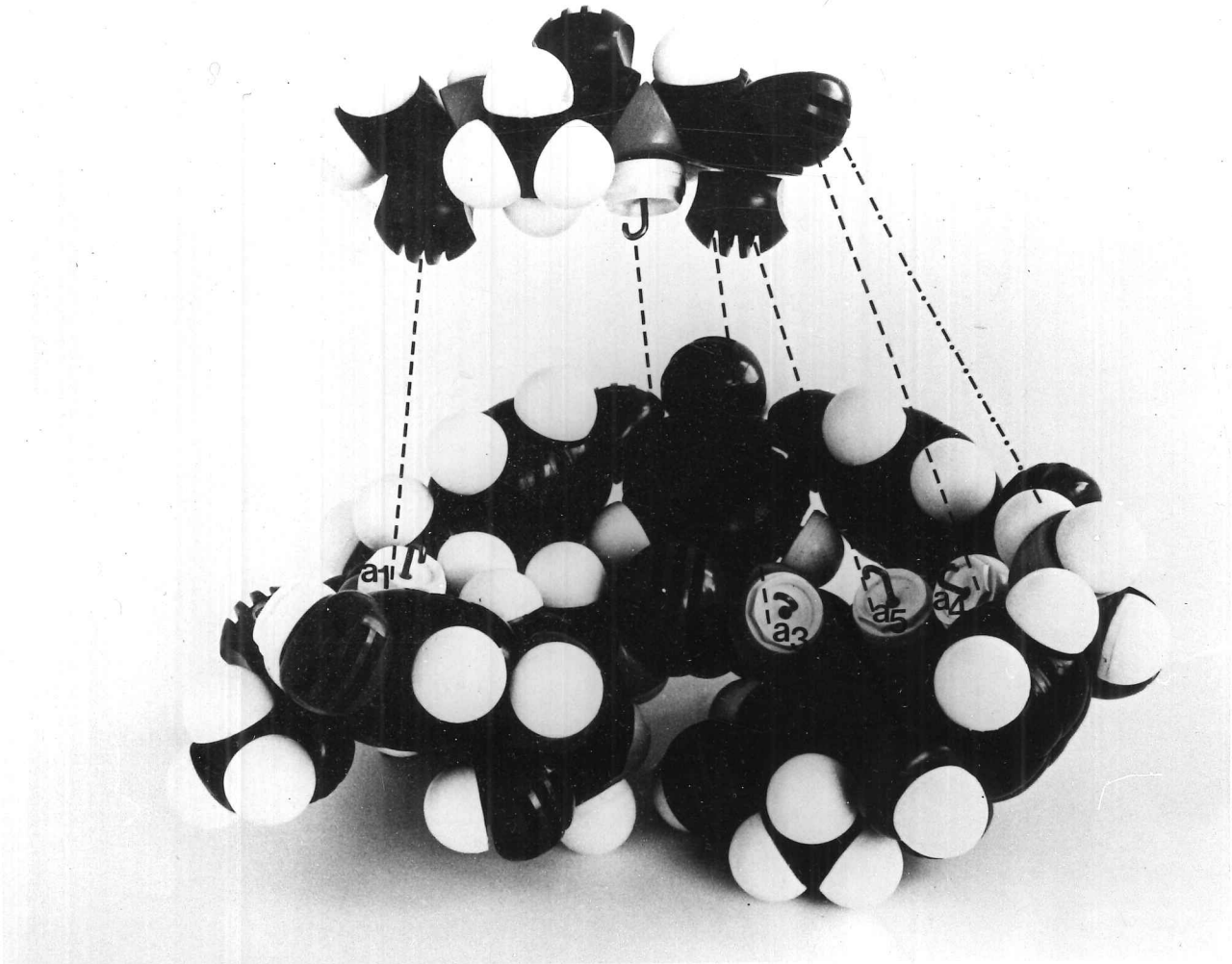

FIGURE 5·5 CPK model of ristocetin A / Ac–D–ala–D–ala binding site (proposed hydrogen bonds indicated by broken lines)

Table 5.3 Ristocetin A/Ac-D-ala-D-ala nOe's (negative)[67]

nOe no.	Proton Irradiated	nOe's Observed
1	ala_2CH_b	f,s_6
2	ala_1Me_b	d
3	ala_2Me_b	f
4	ala_1NH_b/i	ala_2CH_b
5	$ala\text{-}Ac\text{-}Me_b$	ala_2NH_b
6	a_4	i/ala_1NH_b
7	s_6	ala_2CH_b

Subscript b denotes bound resonances

From CPK models it was evident that the peptide protons involved in these intermolecular nOe's were in contact with, or close to, protons of the antibiotic, as shown in figure 5.6. This model was found to accomodate all the data, including the large upfield shift (0.89ppm) of the C-terminal alanine methyl group, which would have to reside immediately over the face of the aryl ring 2. Finally parallels were drawn between the proposed binding of ristocetin A to Ac-D-ala-D-ala and the mode of action of vancomycin [5] ; it was noted that three of the hydrogen bonds proposed in the ristocetin A model (viz. involving NH protons a_1 and a_3 of the antibiotic and the C-terminal alanine NH of the peptide) had also been proposed in the vancomycin model.

---

[5] Discussed in Section 5.1

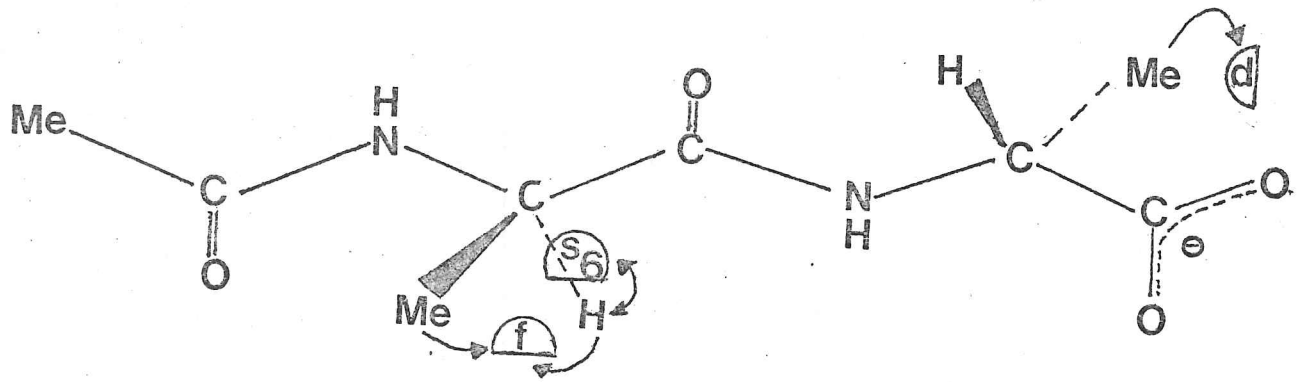

FIGURE 5·6 Ristocetin A / Ac-D-ala-D-ala intermolecular nOe's (indicated by arrows)

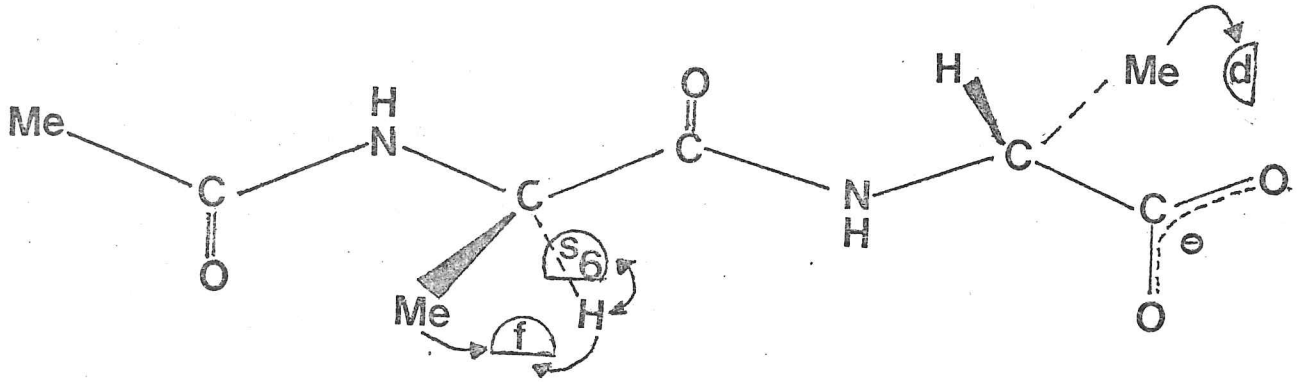

FIGURE 5·6 Ristocetin A/ Ac-D-ala-D-ala intermolecular nOe's (indicated by arrows)

6.1 VANCOMYCIN - REFINEMENT OF STRUCTURE AND BINDING SITE

The binding model (figure 5.1) of vancomycin and dipeptide proposed on the basis of x-ray data[38] of the vancomycin derivative CDP-I, independent nmr studies[37,64,65] and CPK model building[38] has been generally accepted as correct. I now propose to show that it omits further important interactions and that the structure of vancomycin, as deduced from the crystal study of CDP-I, is incorrect.

Earlier studies on vancomycin[37] had led to the assumption that commercial samples of vancomycin in dmso-d_6 were not protonated on the terminal N-methylleucine residue. This was based on the observation that a number of protons which shift upfield on deprotonation of the N-methylleucine function of aglucovancomycin also suffer an upfield shift in vancomycin relative to protonated aglucovancomycin. However, striking as these analogies in chemical shift changes are, the conclusion must be incorrect since commercial samples of vancomycin hydrochloride give aqueous solutions with pH$\sim$4. The N-methyl amino group has a $pK_a \sim 7.2$[61] and must therefore be protonated in dmso-d_6 solutions. This point has been reinforced by comparing the chemical shifts in dmso-d_6 at 70°C of the N-methyl protons hh and the α-CH proton cc respectively of the N-methylleucine residue in (a) aglucovancomycin hydrochloride (2.65 and 3.99ppm) (b) aglucovancomycin base (2.42 and 3.30ppm) and (c) commercial vancomycin hydrochloride (2.42 and 3.80ppm). Thus the same chemical shifts found for the N-methyl protons in aglucovancomycin base and commercial vancomycin are not due to a lack of nitrogen protonation in the latter case, since for this compound proton cc is much nearer in chemical shift to its position in aglucovancomycin hydrochloride than in aglucovancomycin base. The obvious conclusion, therefore, is that the chemical shift differences between cases (a) and (c) are due to a conformational change

between aglucovancomycin and vancomycin hydrochlorides which involves movement of the flexible N-methylleucine residue. Further support for the mobility of this side-chain is provided by the observation that the only large chemical shift difference ($<$0.2ppm) between aglucovancomycin and vancomycin hydrochlorides, for a CH or CONH proton, is for a_4 (8.67 and 8.00ppm respectively). Furthermore, in the spectrum of vancomycin hydrochloride, protons cc and a_4 give very broad resonances relative to those found in the spectrum of aglucovancomycin hydrochloride, and resonance s_4 is no longer split by coupling to a_4 (9Hz in aglucovancomycin hydrochloride).

If a conformational change was involved upon binding , then monitoring the longitudinal relaxation times of free vancomycin, table 6.1, and comparing this data with that of vancomycin complexed to Ac-D-ala-D-ala, table 6.2, one ought to be able to identify those portions of the antibiotic proximal to peptide. Unfortunately, the difficulties encountered from overlapping resonances, exchange broadening upon complexation and the somewhat random changes observed in T_1 prevented meaningful analysis of the changes observed.

Table 6.1 Vancomycin longitudinal relaxation times (s).

Resonance	T_1	Resonance	T_1
t	1.11	z	0.54
v	0.99	f	0.52
k/n	0.96	bb	0.50
a	0.95	x	0.50
s_1	0.92	a_2	0.49
s_2	0.92	a_3	0.49
c	0.90	a_5	0.47
l	0.88	a_6	0.47
b	0.86	hh	0.44
d	0.82	ii/jj	0.44
g	0.80	a_1	0.40
s_5	0.80	gg	0.38
s_4	0.71	s_6	0.38
S_3	0.67	h/j	0.32
i	0.65	ff	0.29
a_4	0.61	o	0.25
m	0.61	aa/ee	0.22
y	0.54		

Data recorded in dmso-d_6 at 45°C (270MHz)

Table 6.2 Vancomycin/Ac-D-ala-D-ala (1:1)
Longitudinal Relaxation Times (s)

Resonance	T_1	Resonance	T_1
s_1	1.55	ala_1NH/ala_2NH	0.63
s_2	1.55	bb	0.63
t	1.28	z	0.62
g	1.21	s_4	0.61
r	1.20	s_5	0.61
k/n	1.19	x	0.53
v	1.04	b	0.48
f	1.00	a_1	0.47
c	0.95	a_6	0.47
s_3	0.88	gg	0.43
l	0.88	ala_1Me/ala_2Me	0.43
ala-Ac-Me	0.84	a	0.40
d	0.77	o	0.39
i	0.75	ii/jj	0.37
a_2	0.64	ff	0.33
y	0.63		

Data recorded in dmso-d_6 at 45°C (270MHz).

In addition Convert and co-workers[66] recognised that important Coulombic interactions known to exist[64] between the peptide carboxylate group and the protonated N-methyl group of the vancomycin N-methylleucine side chain could not be accounted for by this model. They therefore proposed the minor modification entailing rotation of the flexible leucine side chain from its position as indicated by the x-ray data of CDP-I to one in which the distance between the groups in question was approximately halved (figure 5.3).

In the related antibiotic ristocetin A the aglycone structure[51] is similar to vancomycin except that the iso-asparagine and N-methylleucine residues are replaced by a biphenyl ether unit. However, the amide bonds are retained in the same relative positions to those found in vancomycin and it also has a primary amino group in a similar position to that of the N-methyl function of vancomycin. It therefore seemed reasonable that one would expect the respective binding sites of these two antibiotics to be

similar. The binding site of ristocetin A[67] was found to involve a favourable interaction between the peptide carboxylate and the primary amino function mentioned above. In addition, hydrogen bonds were proposed between four of the six secondary amide NH protons of the antibiotic and the peptide. A further hydrogen bond was invoked from the peptide C-terminal NH proton to the antibiotic. This last hydrogen bond and two of the four from the antibiotic had previously been proposed in the analogous binding site of vancomycin. The remaining two hydrogen bonds involved NH protons proximal to ring 3 of ristocetin A thus forming a pocket of NH protons around the peptide carboxylate anion. The analogous two NH protons of vancomycin being on the 'rear face' or the 'side' of the molecule (according to the structure derived from the x-ray data of CDP-I) could not conceivably be involved in the binding site unless a major conformational change had occurred.

The binding of ristocetin A with Ac-D-ala-D-ala is well defined because in dmso-d_6 at temperatures below 40°C, most of the resonances are in slow exchange, on the nmr timescale, with their free components which allowed direct observation of the bound state. In particular, the resonances of the secondary amide bonds were assigned for both bound and free components; those protons which shifted markedly downfield upon complexation were clearly involved in hydrogen bond formation. In contrast, vancomycin is in intermediate exchange with Ac-D-ala-D-ala, even at 19°C (just above the freezing point of dmso-d_6), which means that an averaged view of the bound and free components is obtained. In order to simplify interpretation of the information contained in the spectrum of vancomycin complexed to peptide it was decided to seek experimental conditions where slow exchange prevailed.

It was known from the work of Nieto and Perkins that the complex of vancomycin with the tripeptide Ac_2-L-lys-D-ala-D-ala had an association constant approximately two orders of magnitude greater than that with the dipeptide Ac-D-ala-D-ala which had been used in all of the high-field nmr studies so far performed in dmso-d_6. It was therefore considered worthwhile to perform experiments using Ac_2-L-lys-D-ala-D-ala, the synthesis of which is outlined below.

6.1.1 SYNTHESIS OF AC_2-L-LYSYL-D-ALANYL-D-ALANINE

In general, polypeptides are constructed by reaction of the N-terminus of an amino acid with the free carboxylate of the next amino acid in the sequence (with suitable protection of the carboxylate and amino groups respectively). The strategy for the synthesis of Ac_2-L-lys-D-ala-D-ala is shown in figure 6.1.

(1) **Protection of D-ala-NH_2** : The most commonly used protecting groups for amino functionalities are t-butyloxycarbonyl (t-BOC) or carbobenzoxy (CBZ); the former was used in this case. The traditional reagent used in this reaction is t-butyloxycarbonylazidoformate[68] but in view of its explosive tendencies at 70°-80°C it was decided to use the more stable reagent t-butyloxycarbonyl-oxyimino-2-phenylacetonitrile (t-BOC-ON)[69]. The free amino acid D-alanine was reacted with t-BOC-ON (scheme 6.1), and the resulting t-BOC-D-ala was separated from the oxime by extraction with a water/ethyl acetate mixture. Acidification, further extraction with ethyl acetate, followed by crystallisation from ethyl acetate/n-hexane produced a crystalline product which was recrystallised in good yields.

(2) **Protection of D-ala-COOH** : The benzyl ester is the preferred protecting group for carboxylates and can be prepared by incubating the amino acid in benzyl alcohol and polyphosphoric acid[70] at 90°C for several hours. Extraction with ether, adjustment of the aqueous phase to pH10 with base, further extraction with ether followed by treatment with dry hydrogen chloride gas results in precipitation of the benzyl ester hydrochloride, usually as a crystalline solid. However, with D-alanine an oil was obtained, the proton nmr spectrum of which showed minor splitting (2Hz) of each line of the methyl doublet indicating that racemization had probably occurred. It was therefore decided to prepare the p-toluene sulphonic acid salt of the benzyl ester[71] since crystalline products result with most amino acids. The benzene sulphonic acid serves as a catalyst, in lieu of hydrogen chloride, for the direct esterification of amino acids in benzyl alcohol. The use of p-toluene sulphonic acid renders the

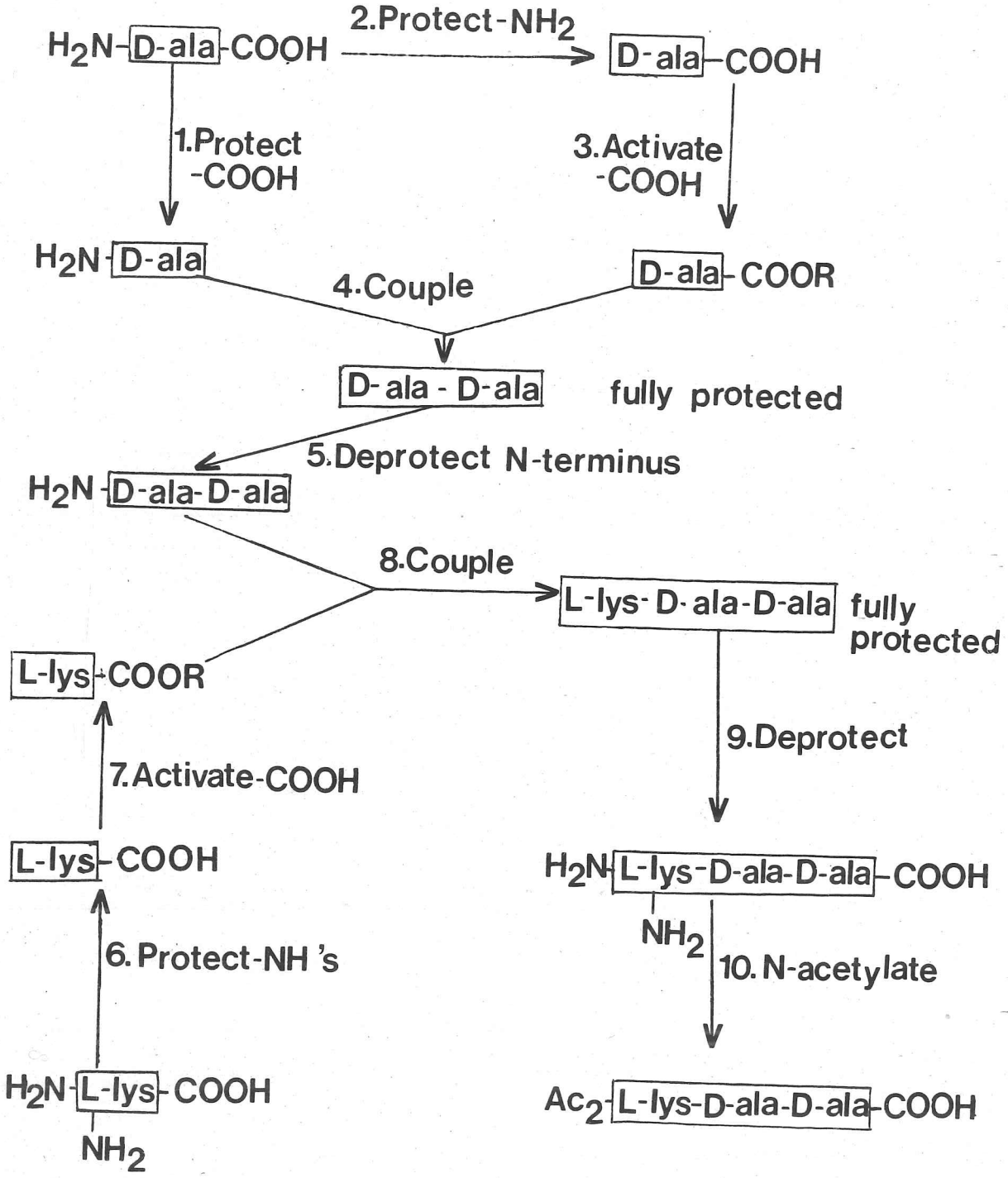

FIGURE 6·1 Strategy for the preparation of Ac_2-L-lys-D-ala-D-ala

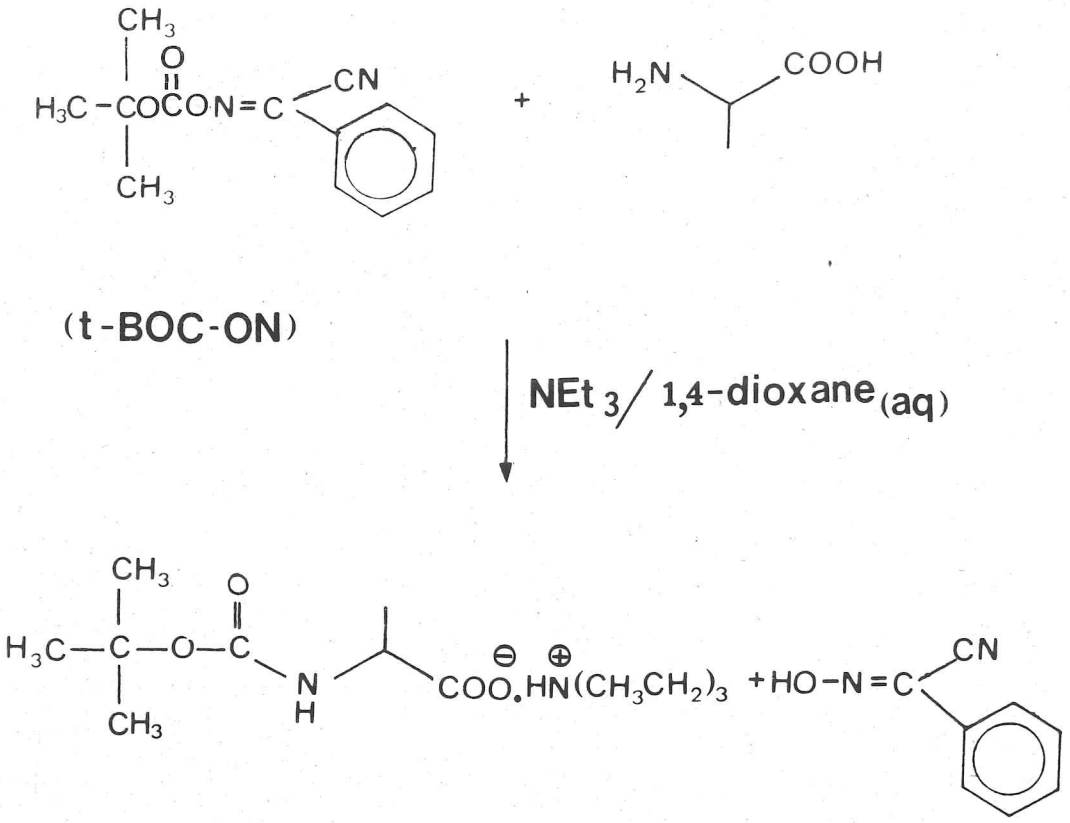

SCHEME 6·1

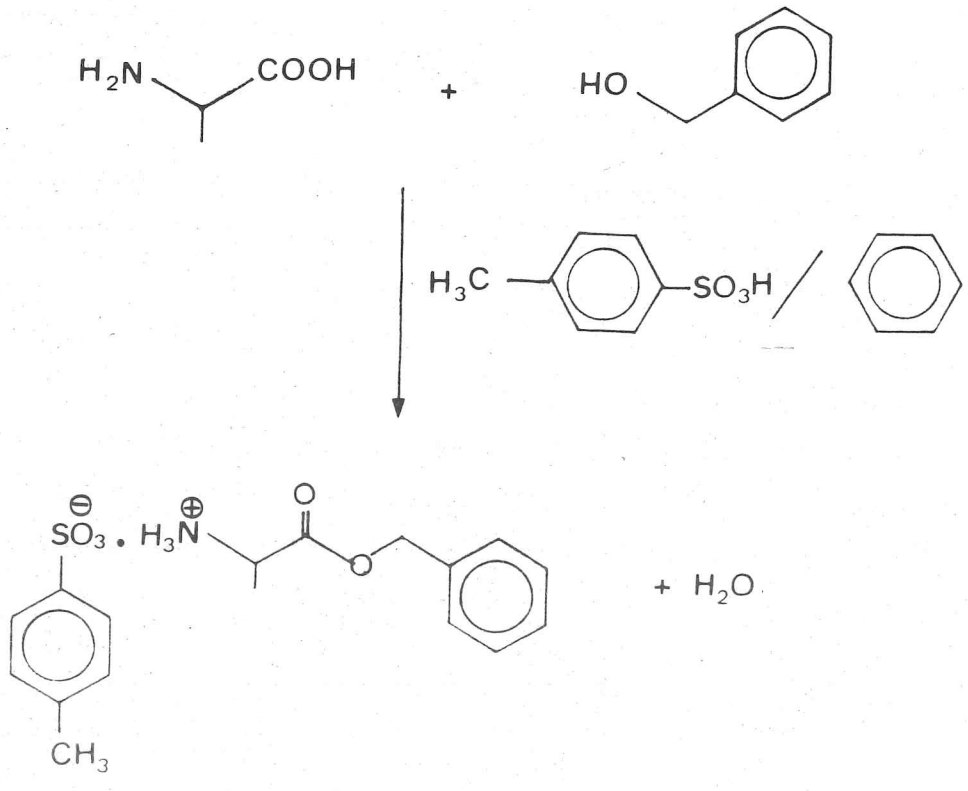

SCHEME 6·2

amino acid soluble in excess benzyl alcohol as its benzene sulphonic acid salt. Water formed during the esterification process is removed by azeotropic distillation. The need for both large excesses of benzyl alcohol and high temperatures to remove the water of reaction, in order to achieve a favourable equilibrium, is thereby avoided. In addition, since the temperature of the reaction mixture never exceeds 80°C the danger of racemization of optically active amino acids and the occurrence of appreciable decomposition of the product is avoided.

Azeotropic distillation of D-alanine in benzene with molar equivalents of p-toluene sulphonic acid and benzyl alcohol, was performed using a Dean-Stark tube (scheme 6.2). Upon completion of the reaction, dry diethyl ether was added to the cold reaction mixture; crystallisation occurred upon chilling in ice. Recrystallisation from methanol/diethyl ether gave a good yield of D-ala benzyl ester p-toluene sulphonic acid salt. The free base was released by dissolving the salt in base, extracting into diethyl ether, and adding petroleum ether (boiling range 40° to 60°C) to crystallise in reasonable yields.

(3) **Protection of L-lys-$(NH_2)_2$** : In the final tripeptide L-lysine will be di-N-acetylated; it therefore seemed reasonable to protect the amino groups by acetylation from the beginning. However, reaction of L-lysine hydrochloride with aqueous acetic anhydride under basic conditions produced a mixture which was non-extractable with organic solvents, being soluble only in aqueous solution. In view of this shortcoming it was considered simpler to use the t-BOC group which had already been successfully used to protect the amino group of D-alanine; acetylation could be performed on the completed tripeptide. Although the same procedure was employed as that which was successful with D-alanine (except two-molar equivalents of the t-BOC-ON reagent were necessary for the dibasic lysine) it was not possible to isolate pure di-t-BOC-L-lysine. In order to avoid further delay in the synthesis of the target tripeptide it was decided to purchase L-lysine which was di-N-protected with the carbobenzoxy group.

(4) **Activation of L-lys-COOH** : In order to facilitate the coupling of N-protected lysine to C-protected alanine it was desirable to activate the carboxylate group of the former by ester formation. The di-CBZ-L-lysine was reacted with N-hydroxysuccinimide[72] in the presence of dicyclohexylcarbodiimide (scheme 6.3). The resultant urea was removed by filtration to give a clear solution which upon rotary-evaporation gave an oil. The succinimide ester was readily crystallised in good yield by the addition of diethyl ether and methanol. Further purification was unnecessary.

(5) **Protection of D-ala-D-ala-COOH** : In order to reduce the number of steps in the synthesis it was decided to use the readily available dipeptide D-ala-D-ala as one of the starting materials. The carboxylate group was protected utilising the p-toluene sulphonic acid salt of the benzyl ester in much the same manner as that used successfully with the single amino acid D-alanine [1].

(6) **Coupling of L-lys to D-ala** : Trial coupling of di-CBZ-L-lys succinimide ester to D-ala benzyl ester was effected by combining a solution of the former in 1,2-dimethoxyethane with a solution of the latter in aqueous sodium hydrogen carbonate (scheme 6.4). Immediate precipitation of the dipeptide resulted, with good yields and purity.

(7) **Coupling of L-lys to D-ala-D-ala** : The free base of D-ala-D-ala benzyl ester proved difficult to isolate using the procedure outlined above in (2) for D-alanine. The reaction was therefore performed using the p-toluene sulphonic acid salt of the benzyl ester which was readily available. A solution of the activated lysine moiety in 1,2-dimethoxyethane was added to a weakly basic solution of the C-protected D-ala-D-ala residue. Immediate precipitation of a crystalline solid ensued which upon examination by nmr spectroscopy proved to be the required protected tripeptide. The regenerated N-hydroxysuccinimide and p-toluene sulphonic acid remained in solution.

---

[1] See (2) above.

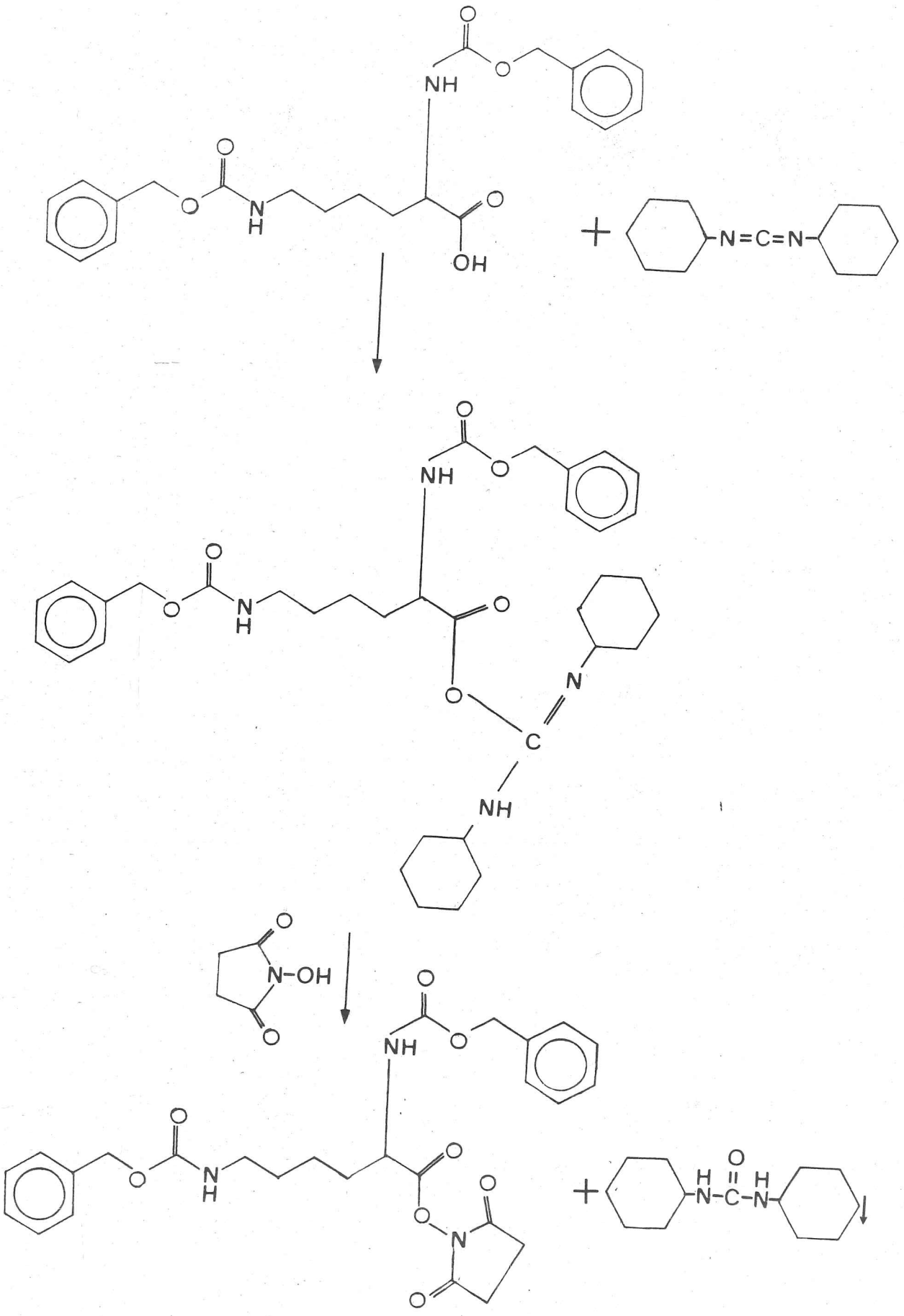

(N,N′-di-CBZ-L-lys succinimide ester)

SCHEME 6·3

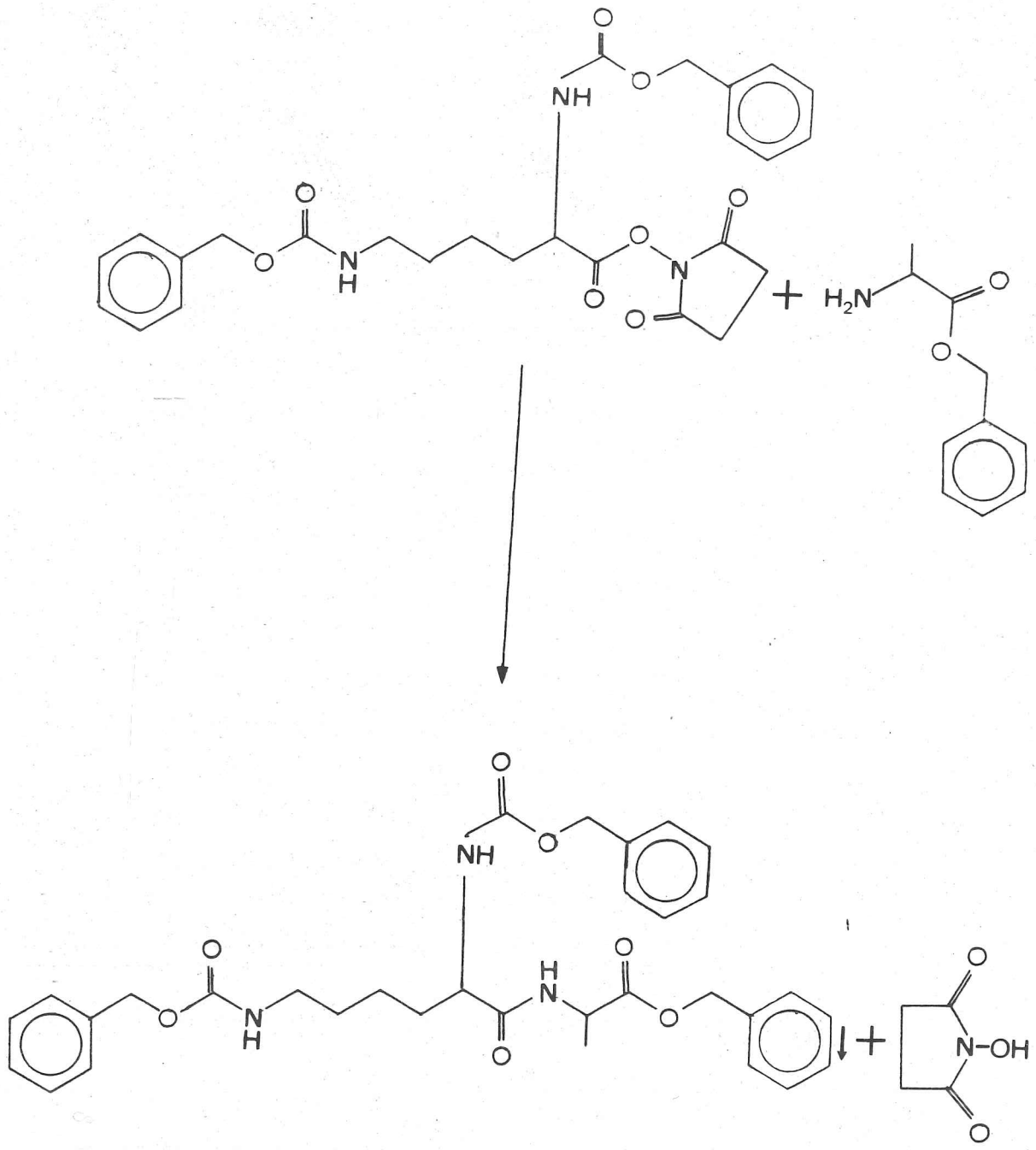

SCHEME 6·4

(8) **Deprotection of L-lys-D-ala-D-ala** : The benzyl ester and the two benzyloxycarbonyl protecting groups were readily removed by hydrogenation in the presence of 10%Pd/C catalyst. Reaction was allowed to proceed for several hours to ensure that hydrogenation was complete. The reaction mixture was then filtered to remove the catalyst and rotary-evaporated at 70°C to yield the free tripeptide as an oil which was not purified further.

(9) **Acetylation of L-lys-D-ala-D-ala** : The oily residue of the free tripeptide from the hydrogenation was dissolved in a minimum of water to which was added an excess of acetic anhydride. The reaction mixture was stirred for two hours, the solvents were then removed by rotary-evaporation at 70°C to give an oil. Purification of this oil of Ac_2-L-lys-D-ala-D-ala proved to be something of a problem. Ion-exchange was performed to remove trace amounts of mono-acetylated tripeptide. Dissolving the Ac_2-tripeptide oil in ethanol and inducing crystallisation by the addition of diethyl ether to reduce the solubility was the most successful method. Reduced yields were obtained because of the difficulty in harvesting the crystals which were very soluble in ethanol; an excess of diethyl ether was necessary throughout.

6.1.2 VANCOMYCIN/AC-D-ALA-D-ALA BINDING STUDIES

The proton nmr spectrum at 100MHz of vancomycin complexed to Ac_2-L-lys-D-ala-D-ala in dmso-d_6 at 19°C still exhibited intermediate exchange characteristics. In view of the fact that the rate of chemical exchange is dependent upon the shift difference in Hz between the bound component and free component resonances a spectrum at 270MHz was also taken. Unfortunately intermediate exchange conditions still prevailed and an alternative approach was therefore necessary. The problem of obtaining slow exchange was finally overcome by using dmso-d_6 solutions containing ~30% carbon tetrachloride, the mixed solvent system being employed to decrease the unimolecular rate constant for dissociation of the complex by reducing the freezing point (to less than 0°C) and in addition by inhibiting the breaking of hydrogen bonds present in the complex because of the increased lipophilic nature of the solvent.

(8) **Deprotection of L-lys-D-ala-D-ala** : The benzyl ester and the two benzyloxycarbonyl protecting groups were readily removed by hydrogenation in the presence of 10%Pd/C catalyst. Reaction was allowed to proceed for several hours to ensure that hydrogenation was complete. The reaction mixture was then filtered to remove the catalyst and rotary-evaporated at 70°C to yield the free tripeptide as an oil which was not purified further.

(9) **Acetylation of L-lys-D-ala-D-ala** : The oily residue of the free tripeptide from the hydrogenation was dissolved in a minimum of water to which was added an excess of acetic anhydride. The reaction mixture was stirred for two hours, the solvents were then removed by rotary-evaporation at 70°C to give an oil. Purification of this oil of Ac_2-L-lys-D-ala-D-ala proved to be something of a problem. Ion-exchange was performed to remove trace amounts of mono-acetylated tripeptide. Dissolving the Ac_2-tripeptide oil in ethanol and inducing crystallisation by the addition of diethyl ether to reduce the solubility was the most successful method. Reduced yields were obtained because of the difficulty in harvesting the crystals which were very soluble in ethanol; an excess of diethyl ether was necessary throughout.

6.1.2 VANCOMYCIN/AC-D-ALA-D-ALA BINDING STUDIES

The proton nmr spectrum at 100MHz of vancomycin complexed to Ac_2-L-lys-D-ala-D-ala in dmso-d_6 at 19°C still exhibited intermediate exchange characteristics. In view of the fact that the rate of chemical exchange is dependent upon the shift difference in Hz between the bound component and free component resonances a spectrum at 270MHz was also taken. Unfortunately intermediate exchange conditions still prevailed and an alternative approach was therefore necessary. The problem of obtaining slow exchange was finally overcome by using dmso-d_6 solutions containing ~30% carbon tetrachloride, the mixed solvent system being employed to decrease the unimolecular rate constant for dissociation of the complex by reducing the freezing point (to less than 0°C) and in addition by inhibiting the breaking of hydrogen bonds present in the complex because of the increased lipophilic nature of the solvent.

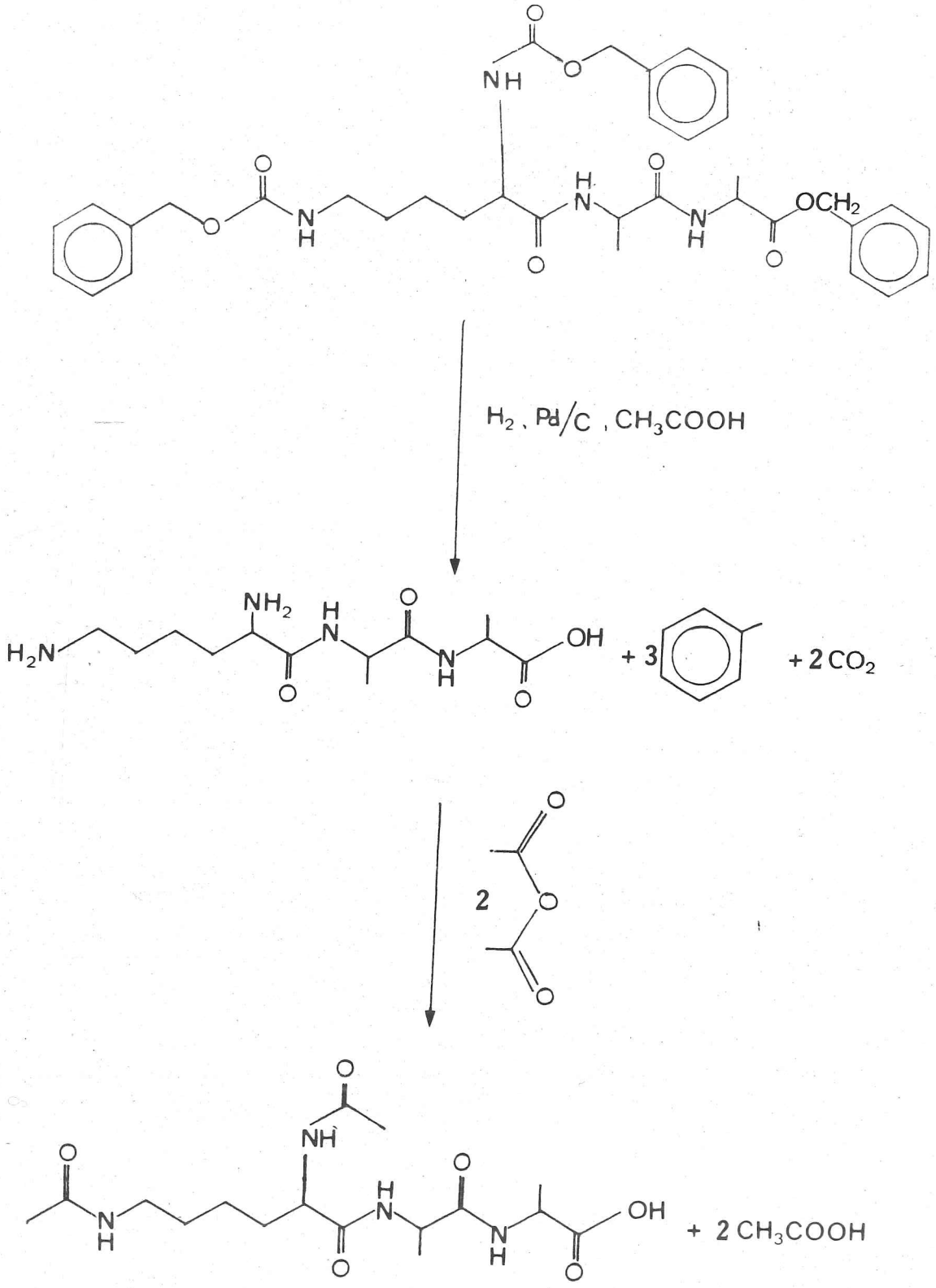

(N,N′-Ac_2-L-lys-D-ala-D-ala)

Deprotection & acetylation of lys-ala-ala

SCHEME 6·5

Upon cooling a solution of vancomycin and Ac-D-ala-D-ala (~1:1) in the above solvent mixture to -1°C the complex goes into slow exchange with its free components at 270MHz. By means of variable temperature and spin decoupling studies it has been possible to assign the vast majority of the proton resonances both in the free state and in the complex for aglucovancomycin and vancomycin. From figure 6.2 it can be clearly seen that, with the exception of exchangeable protons, none of the resonances of aglucovancomycin have a shift greater than 0.1ppm in the temperature range 10°-90°C. However, since no marked shifts were observed (figure 6.3) after the addition of one molar equivalent of Ac-D-ala-D-ala it would appear that complex formation does not occur in dmso-d_6 solution at the natural pH of aglucovancomycin (pH~2.5). The addition of sufficient base (sodium methoxide in dmso-d_6 solution) to deprotonate the carboxylate groups and the N-methyl group produced large shifts of many resonances (figures 6.4 and 6.5). In addition, notable shifts upon the addition of peptide are shown in table 6.3 relative to the chemical shifts in the same solution at 75°C.

Table 6.3 Aglucovancomycin/Ac-D-ala-D-ala (~1:1)
Shifts Upon Binding (ppm)

Resonance	Shift	Resonance	Shift
ala_1Me	-0.66	s_4	+0.28
ala_1NH	+0.61	hh	+0.25
cc	+0.59	s_5	+0.21
a_2	+0.56	s_3	+0.21
j	-0.47	ii/jj	-0.20
ala_2NH	+0.44	h	-0.19
a_3	+0.33	t	-0.19
a_1	+0.33	a	-0.19
b	-0.31	f	+0.17
ala_2CH	+0.29	ala_2Me	-0.17

Data recorded in dmso-d_6/30%CCl_4 solution containing NaOMe at 0°C, shifts relative to resonance positions in the same solution at 75°C (270MHz).
Lowfield shifts are positive.

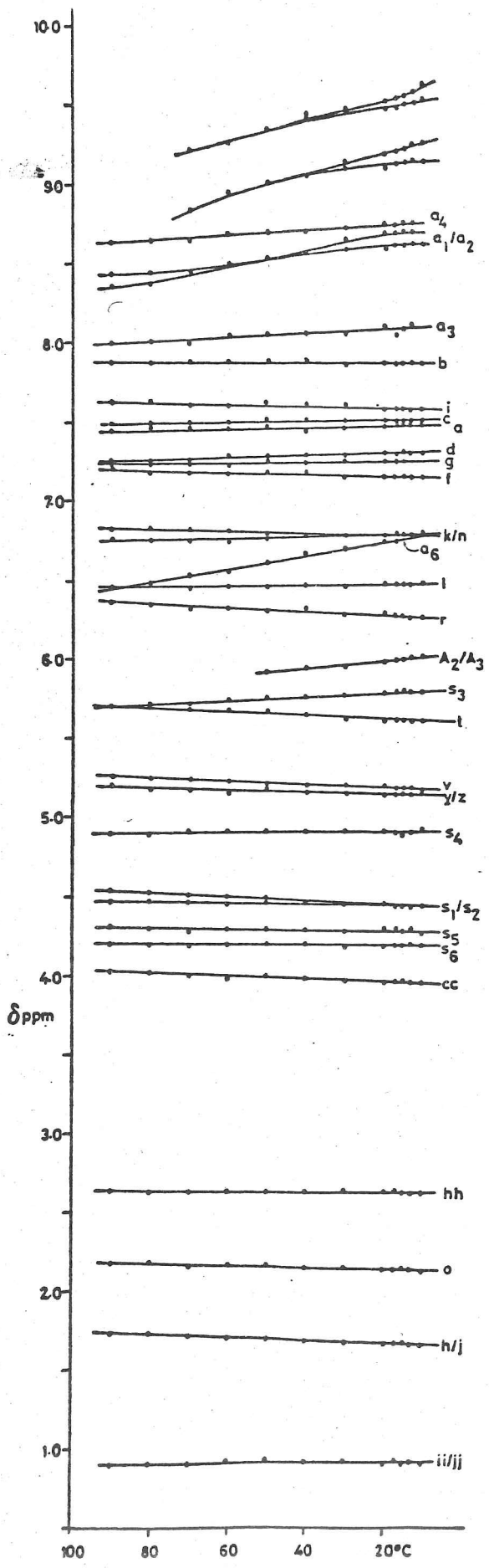

FIGURE 6·2 Temperature dependence of aglucovancomycin (above 30°C dmso-d_6, 30°C & below dmso-d_6/30% CCl_4, 270MHz)

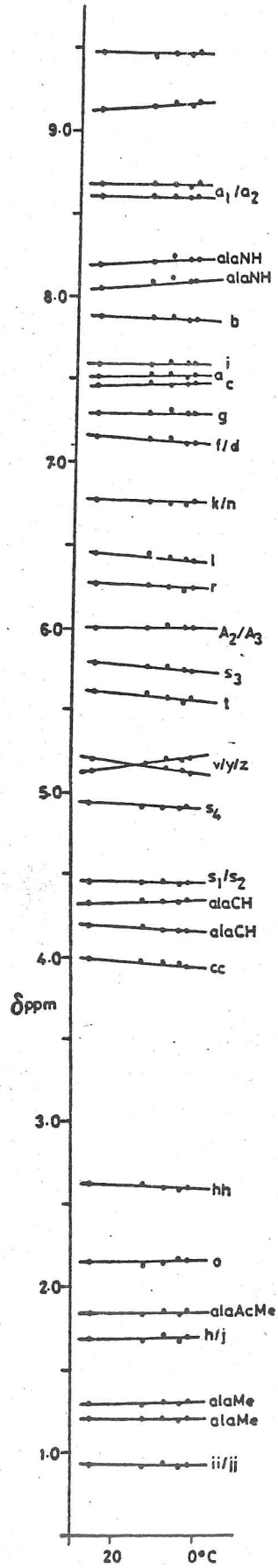

FIGURE 6.3 Temperature dependence of aglucovancomycin /Ac-D-ala-D- ala (III) (above 30°C dmso - d_6, 30°C & below dmso-d_6/ 30% CCl_4, 270 MHz)

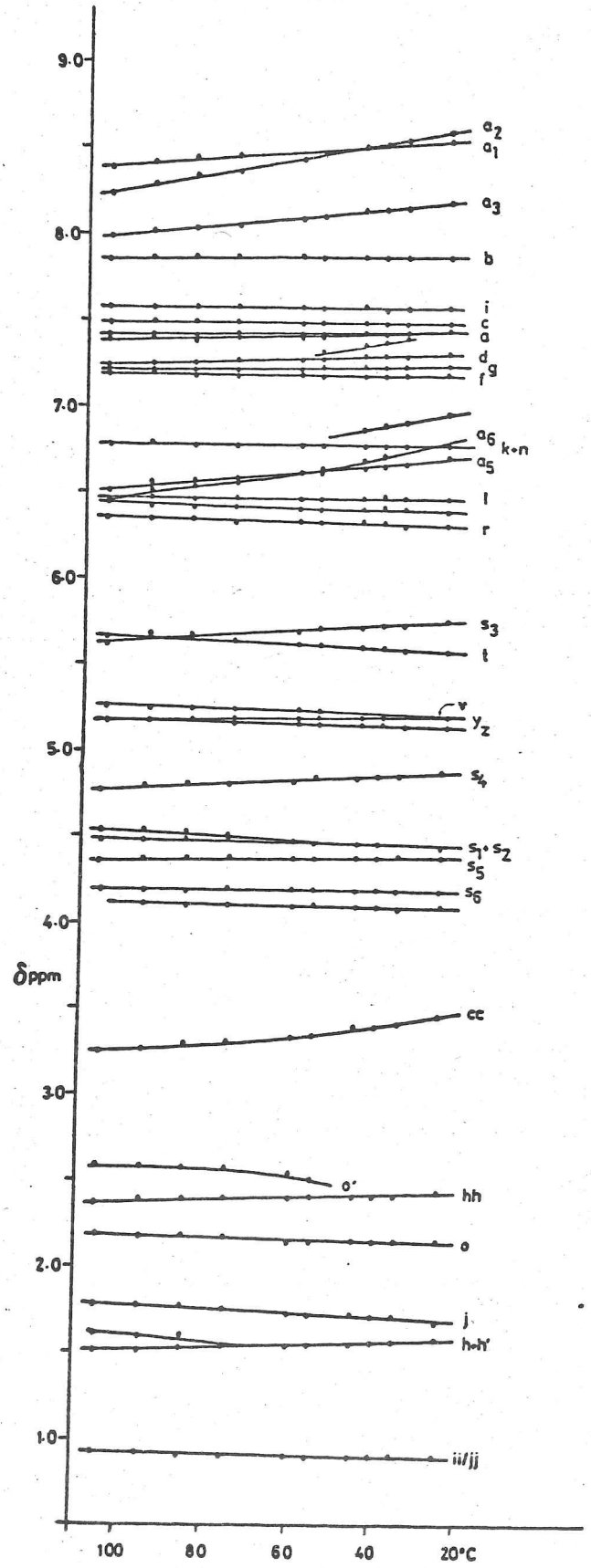

FIGURE 6·4 Temperature dependence of aglucovancomycin (dmso-d_6 + NaOMe, 270MHz)

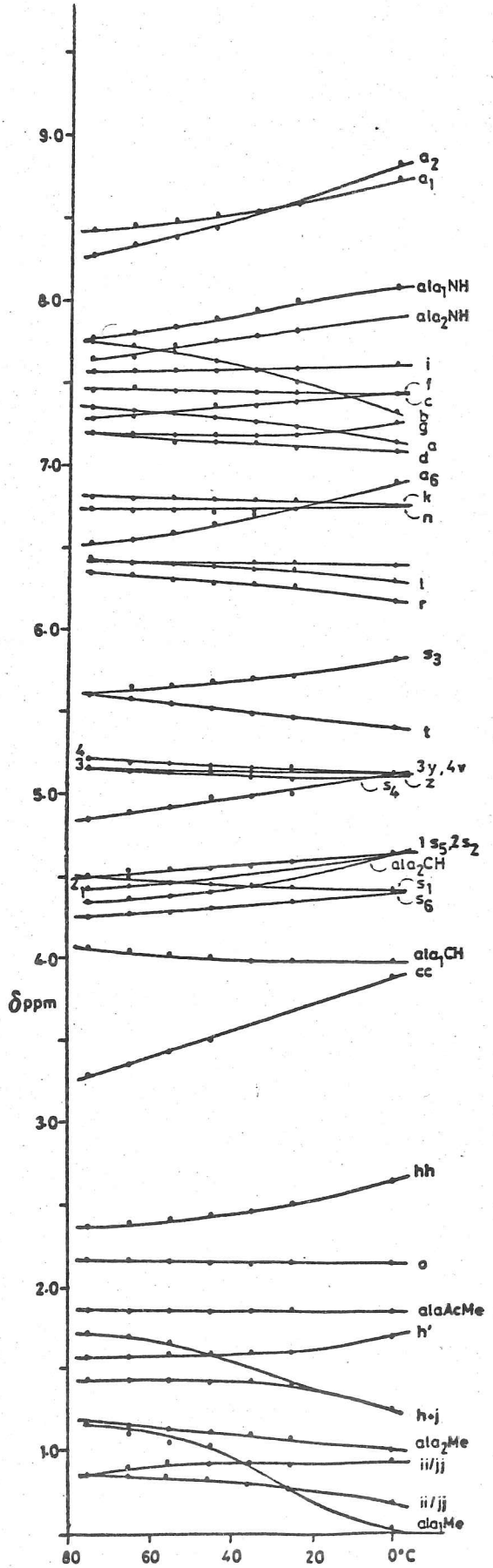

FIGURE 6.5 Temperature dependence of aglucovancomycin/Ac-D-ala-D-ala (1:1) (above 30°C dmso-d_6, below 30°C dmso-d_6/30%CCl_4)

The most striking features in the spectrum are two resonances, one at each extreme of the spectrum, in analogous positions to those found in the ristocetin A/Ac-D-ala-D-ala slow exchange complex. The high field resonance at 0.51ppm was readily assigned from the temperature variation studies as being the ala_1Me which is situated over the face of an aromatic ring and hence is greatly ring-shielded. The low-field resonance, however, was not as readily identified since it sharpened from the base-line noise at its bound resonance frequency (11.72ppm) and was therefore not followed with temperature variation. The resonance was found to be exchangeable upon the addition of deuterium oxide (D_2O) and it was speculated that it could be the analogous secondary amide proton to that of ristocetin A, which was also found at a remarkably low-field position (11.83ppm). Of the remaining shifted resonances several (cc, j, hh and h) can be ascribed to deprotonation of the N-methyl function of the N-methylleucine residue. The downfield shifts of cc and hh must be due to a conformational change since deprotonation would normally produce upfield shifts. However, downfield shifts of both of these resonances are observed over the same temperature range in the absence of peptide although to a lesser extent. It is therefore unlikely that salt-bridge formation occurs with aglucovancomycin, especially not at pH8. The other resonances are presumably shifted because a change has occurred in their environment, either involving a direct effect with the peptide (or antibiotic, as the case may be) or from an induced conformational change upon binding. In view of the fact that the full binding site is not involved in the aglucovancomycin complex (as evidenced by the fact that complex formation only occurs under conditions of pH where a zwitterionic salt bridge, known to exist in the vancomycin complex, cannot be formed) the studies were continued using vancomycin.

A temperature variation study of the vancomycin resonances is presented in figure 6.6. On comparing the most shifted resonances (table 6.4) with those of aglucovancomycin (table 6.3) a marked similarity is noted both in the resonances affected and in the magnitude of the shift.

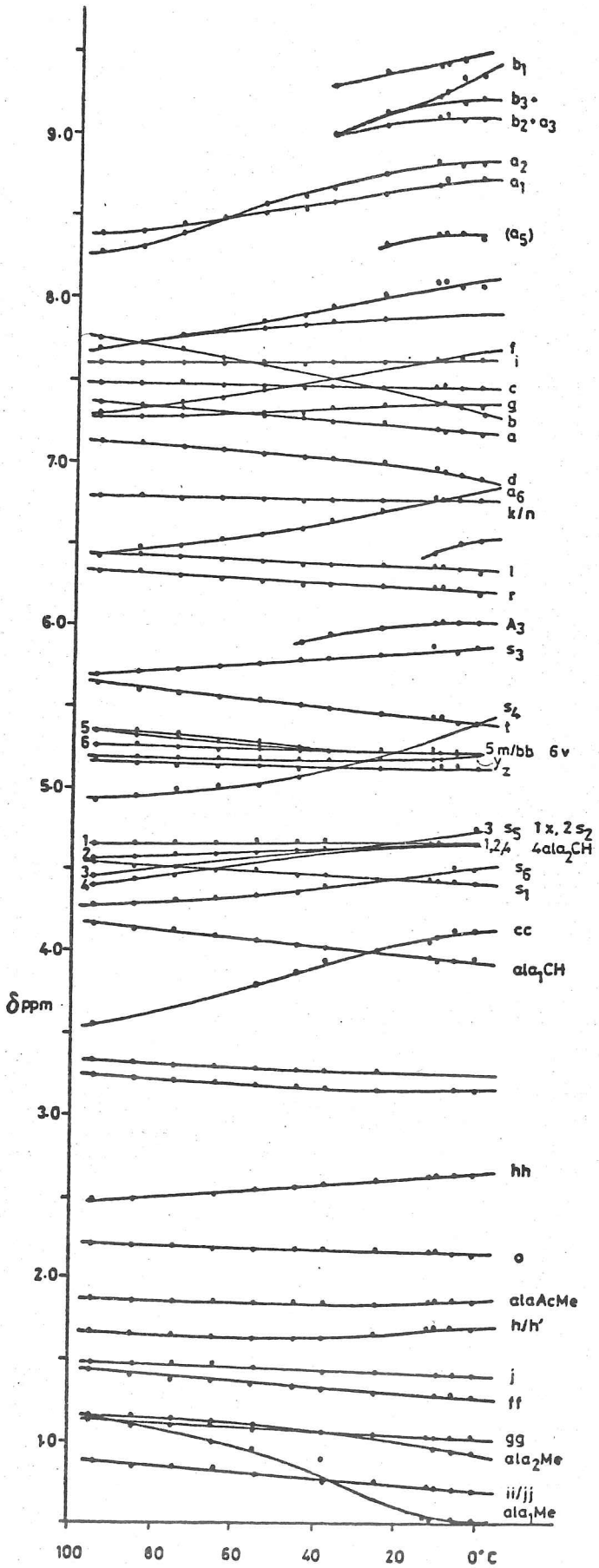

FIGURE 6.6 Temperature dependence of vancomycin/Ac-D-ala-D-ala(1:1) (above 30°C dmso-d_6, below 30°C dmso-d_6/30%CCl_4, 270MHz

Table 6.4 Vancomycin/Ac-D-ala-D-ala (1:1)
Shifts Upon Binding (ppm)

Resonance	Shift	Resonance	Shift
ala_1Me	-0.66	ala_2Me	-0.25
cc	+0.57	ala_2CH	+0.24
a_2	+0.54	t	-0.23
s_4	+0.48	ala_2NH	+0.23
b	-0.45	d	-0.22
ala_1NH	+0.40	ala_1CH	-0.22
a_6	+0.36	s_6	+0.21
f	+0.35	ii/jj	-0.20
a_1	+0.34	a	-0.19
r	-0.33	ff	-0.17
s_5	+0.27	hh	+0.15

Data recorded in dmso-d_6/30%CCl_4 solution at 1°C, shifts relative to resonance positions in the same solution at 95°C (270MHz). Positive shifts are downfield.

One interesting feature that perhaps is not evident from the data as presented is that the amide protons a_3, a_4 and a_5 were broadened by chemical exchange to such an extent that it was not possible to identify their bound positions at this stage. Double irradiation of the low field (11.73ppm) exchangeable resonance produced only a slight change in the shape of the peak at 5.41ppm, a shoulder becoming more prominent. However, irradiation of this shoulder produced ~60% increase in the peak height of the resonance at 11.73ppm, thus confirming spin-coupling between these two resonances. From the temperature variation studies the resonance at 5.41ppm was identified as the α-CH proton s_4, thus identifying the peak at 11.73ppm as being the secondary amide NH proton a_4. The spin-coupling between these two protons in free vancomycin is zero hence spin-decoupling has no effect; a conformational change would therefore be necessary in order to observe an effect upon spin-decoupling of these protons in the complex. The large downfield shift for a_4 of 3.73ppm must be due to hydrogen bond formation upon complexation, the analogous proton in the ristocetin A complex undergoes a similarly large downfield shift of 4.67ppm.

A CPK model of vancomycin incorporating a modified binding site[73] was built, based on the above data and being guided by reference to the ristocetin A binding site. The proton a_4 can only be brought from the side of the molecule (as in the x-ray model) into the proximity of the carboxylate anion of the peptide, and hence a hydrogen bonding position, by means of a conformational change involving the β-hydroxy-chlorotyrosine unit of which it is a part, the iso-asparagine unit and the N-methylleucine residue. The proposed changes are described below and can best be appreciated by reference to figures 6.7 and 6.8.

(1) The αCH-CO bond of the N-terminal N-methylleucine unit is rotated through ~180°; from a position where the $\alpha C - H_{cc}$ bond of this residue is nearly eclipsed with the $N - H_{a4}$ bond of the neighbouring β-hydroxy-chlorotyrosine unit (figure 6.7) to one where this $\alpha C - H_{cc}$ bond is approximately eclipsed with the carbonyl bond of the N-methylleucine (figure 6.8).

(2) The $-CH_y(OH)-CH_{s4}NH-$ bond of the 'right-hand' β-hydroxy-chlorotyrosine unit is rotated as indicated in (6.1) until the conformation (6.2) is attained. This change brings the amide proton a_4 of the β-hydroxy-chlorotyrosine unit very close to proton a of ring 3.

(3) The rigid CONH unit, connecting the carbonyl of the above β-hydroxy-chlorotyrosine unit to the amide proton a_5 of iso-asparagine, is rotated about the two bonds connecting it to its α-carbons. This rotation, viewed from the iso-asparagine methylene group, is in a clockwise direction through ~120°; during the rotation of the CONH unit, its amide proton a_5 traverses the face of the chlorine-bearing aromatic ring, its final position being on the same face as the chlorine atom.

(4) The iso-asparagine methylene group is rotated, viewed in the $-CH_2 \rightarrow CO-$ direction, anticlockwise by ~90°. As a consequence the methylene group, which is initially disposed relative to the carbonyl as in (6.3), is finally oriented as in (6.4).

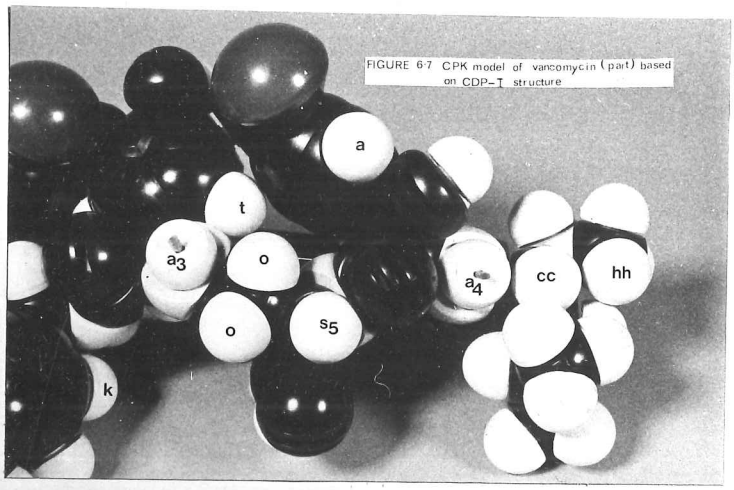

FIGURE 6·7 CPK model of vancomycin (part) based on CDP-I structure

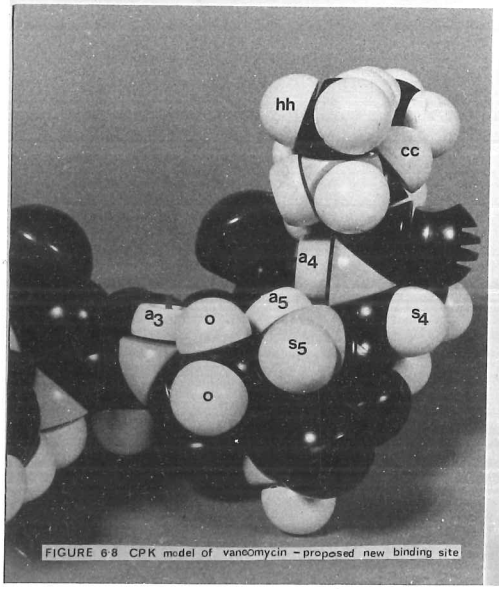

FIGURE 6·8 CPK model of vancomycin – proposed new binding site

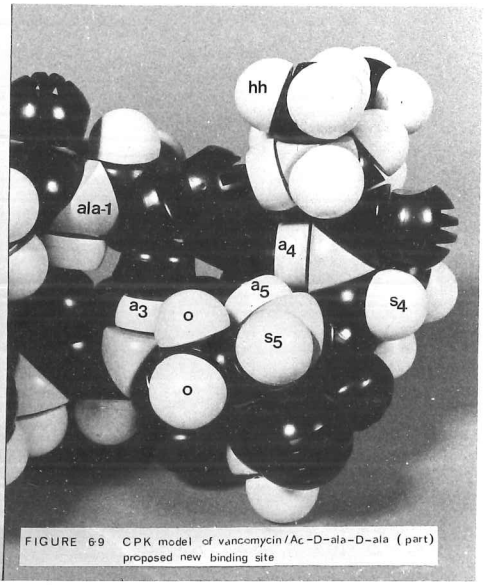

FIGURE 6·9 CPK model of vancomycin/Ac-D-ala-D-ala (part) proposed new binding site

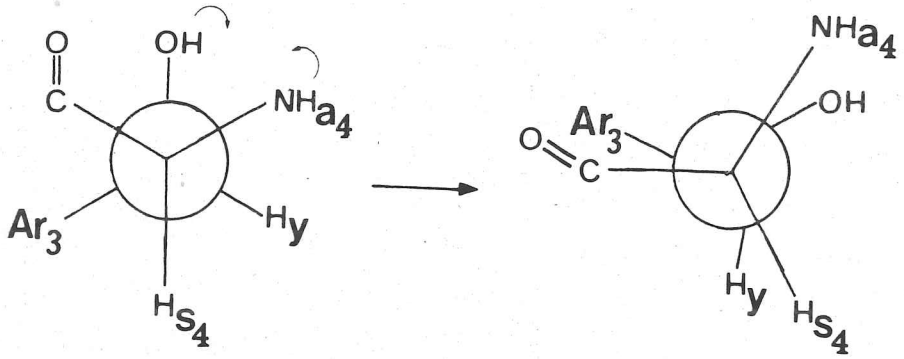

(6·1) (6·2)

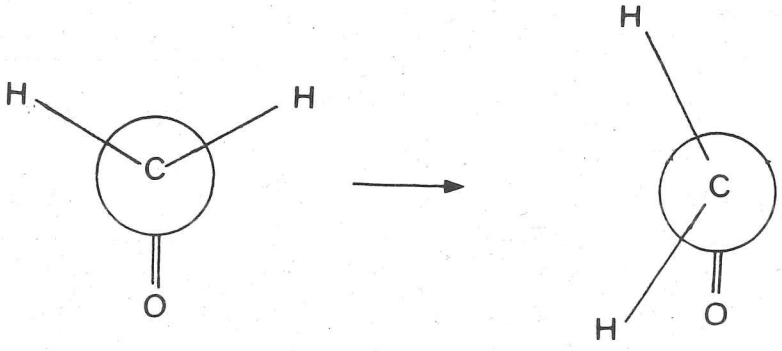

(6·3) (6·4)

The proximity of the peptide carboxylate anion to the cationic N-methyl group, and the amide protons a_4, a_5 and a_3 is shown in figure 6.9. Further evidence in support of these modifications to form a carboxylate anion receptor pocket is now presented. Experiments with peptide analogues were performed using excusively 400MHz proton nmr in the slow exchange regime unless otherwise stated. A typical spectrum and expansions of vancomycin alone and complexed to Ac-D-ala-D-ala at $0^{o}C$ are shown in figures 6.10-6.14. The bound and free positions of the dipeptide protons were confirmed by double irradiation and transfer of saturation studies on vancomycin in the presence of excess peptide. The full assignment of the vancomycin/Ac-D-ala-D-ala spectrum is listed in table 6.5.

FIGURE 6·10 Vancomycin dmso-d_6 / 30% CCl_4 , 5°C , 400MHz

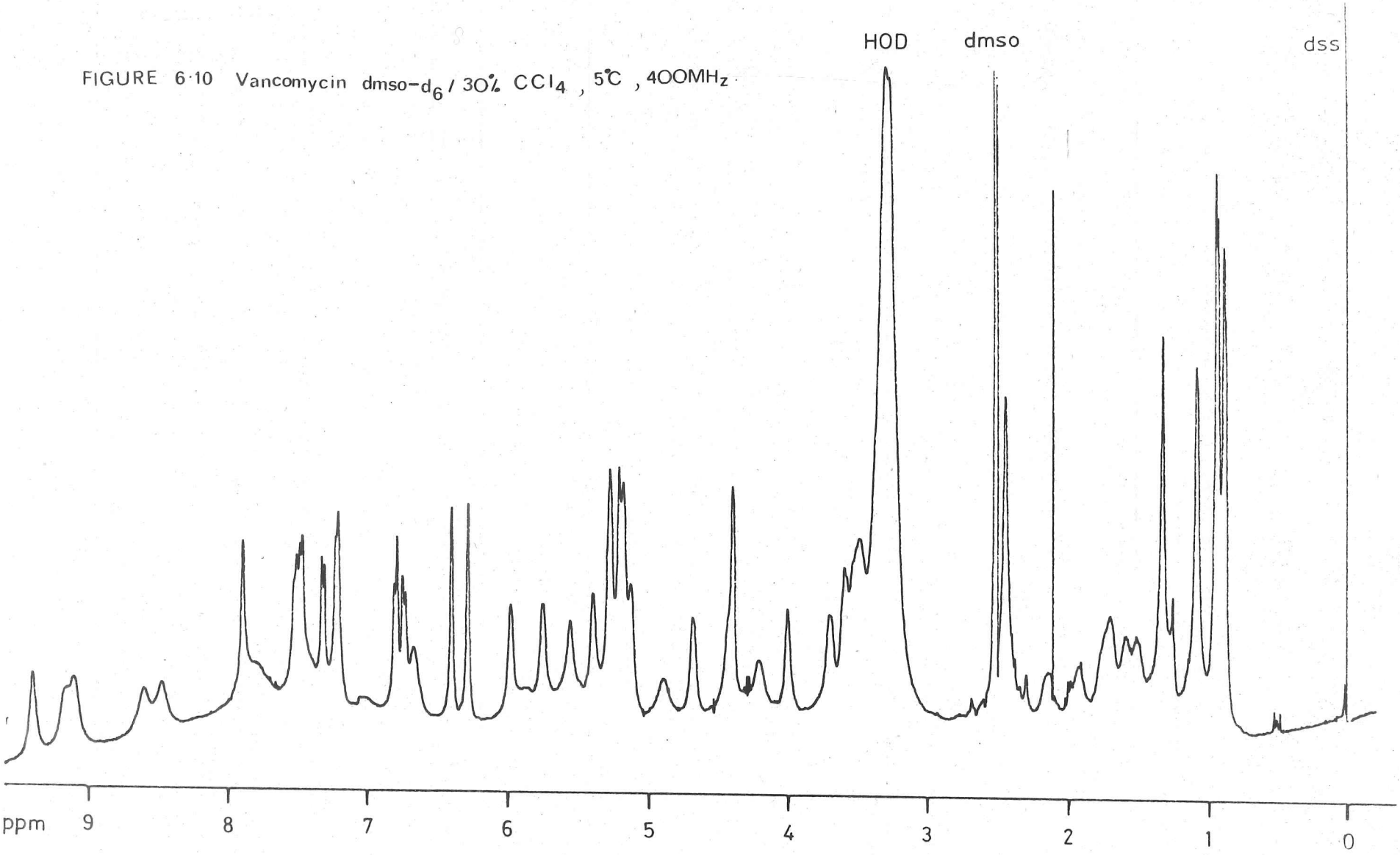

FIGURE 6·11 Vancomycin/Ac-D-ala-D-ala (1:2) dmso-d_6 / 30% CCl_4 , 0°C , 400 MH_z.

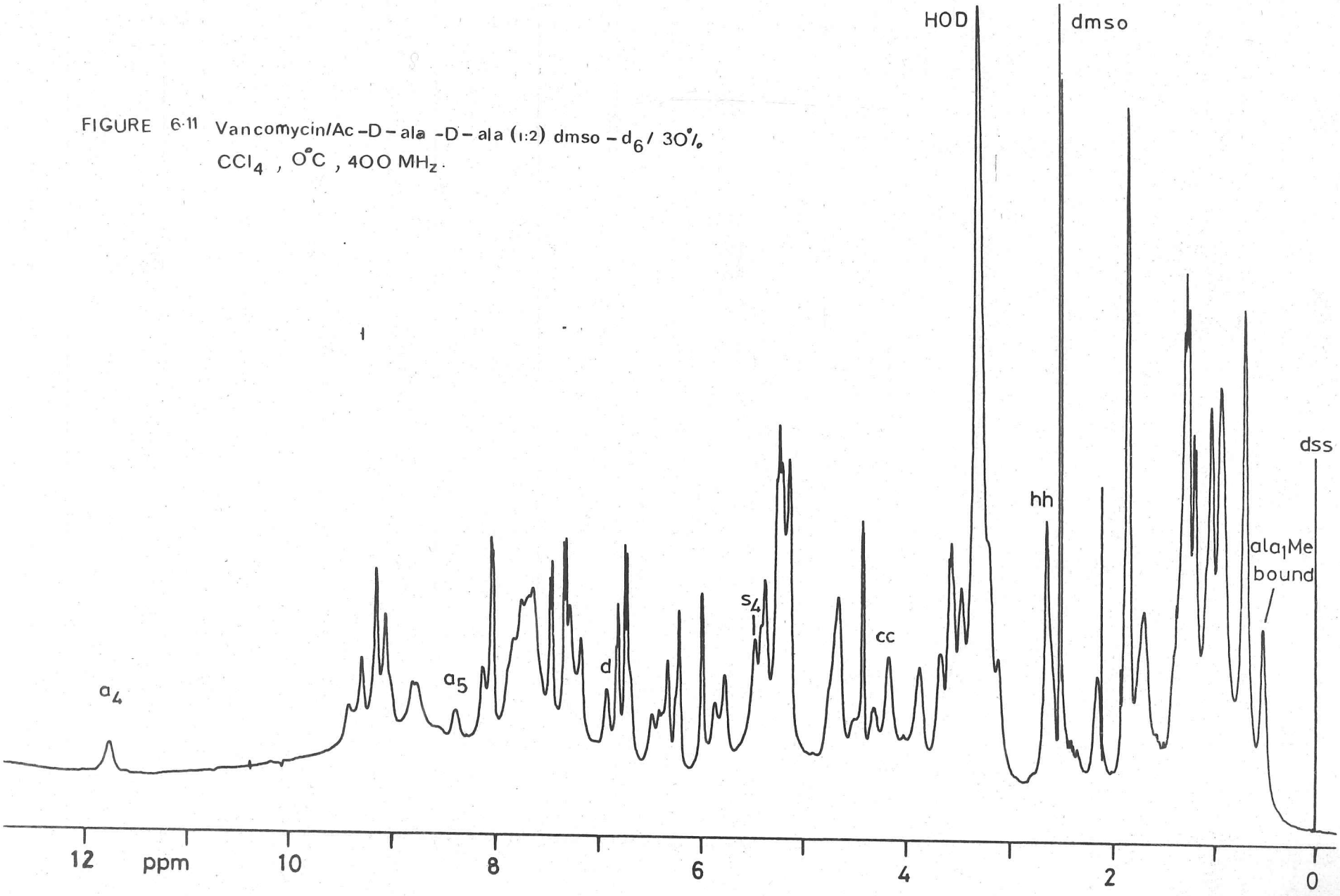

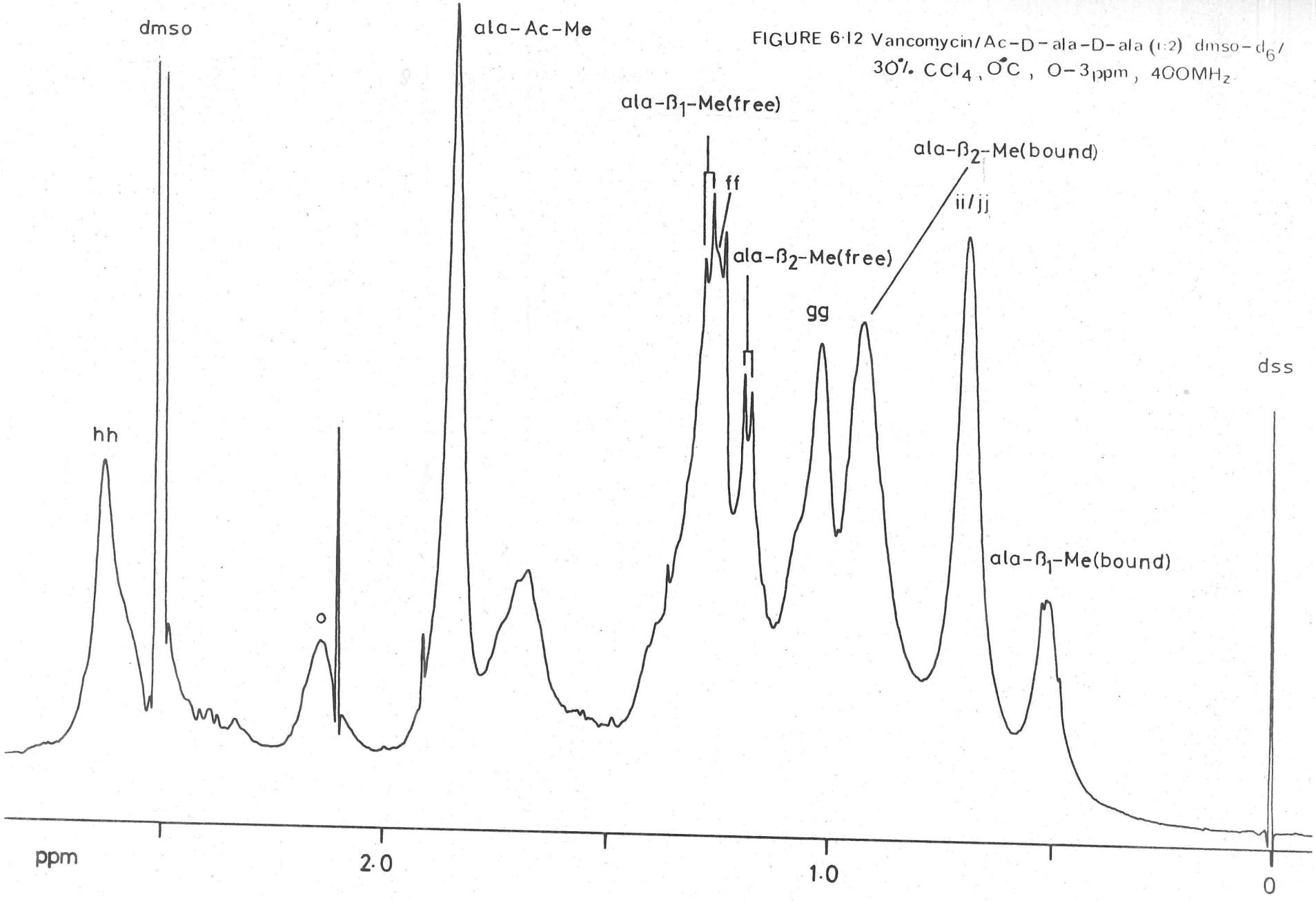

FIGURE 6·12 Vancomycin/Ac-D-ala-D-ala (1:2) dmso-d_6/ 30% CCl_4, 0°C, 0–3ppm, 400MHz

FIGURE 6·13 Vancomycin / Ac-D-ala-D-ala(1:2) dmso-d_6 / 30% CCl_4, 0°C, 4-6 ppm, 400MHz

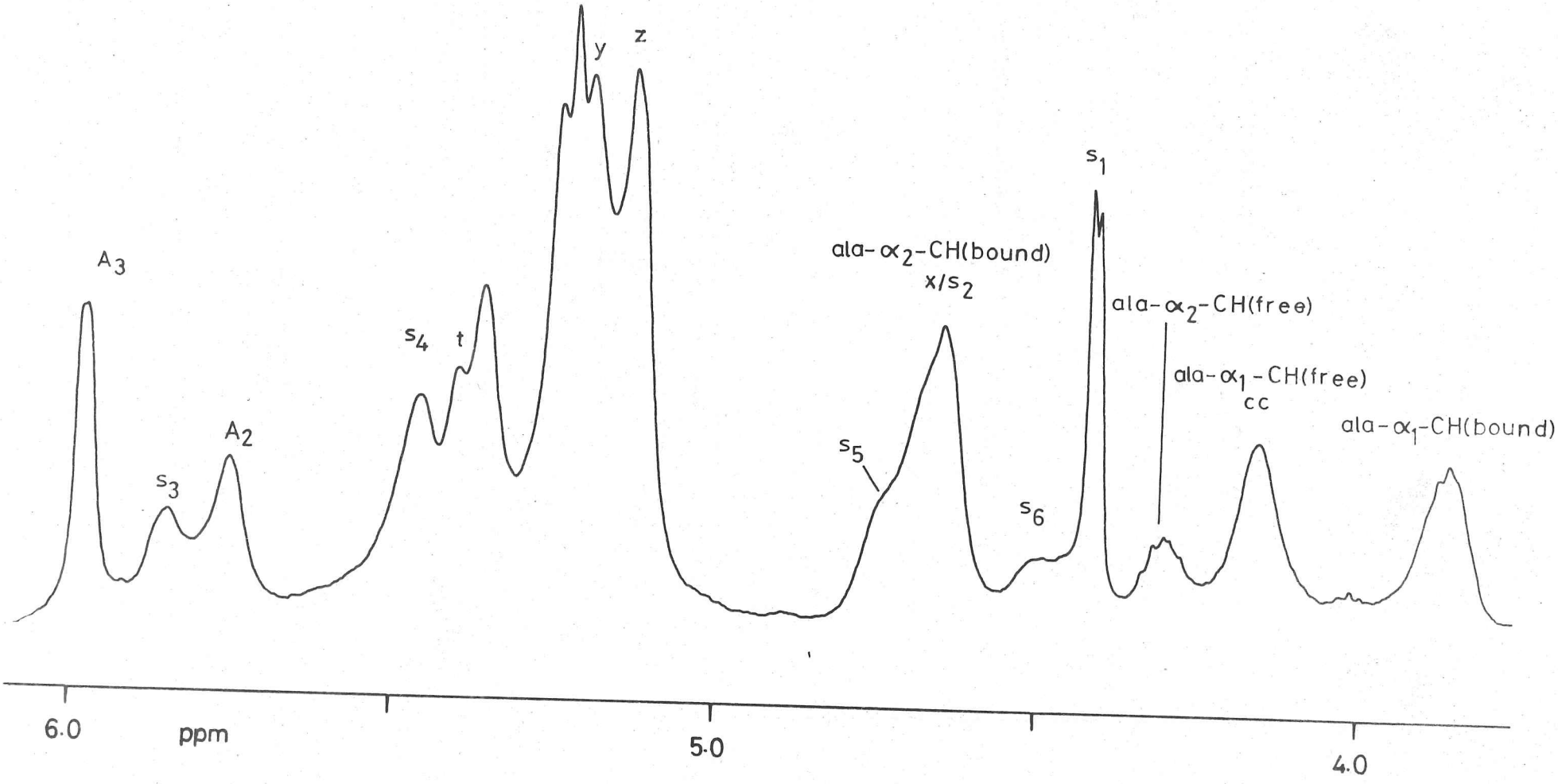

FIGURE 6·14 Vancomycin/Ac-D-ala-D-ala(1:2), dmso-d_6/30% CCl_4, 0°C, 6-9·5 ppm, 400 MHz

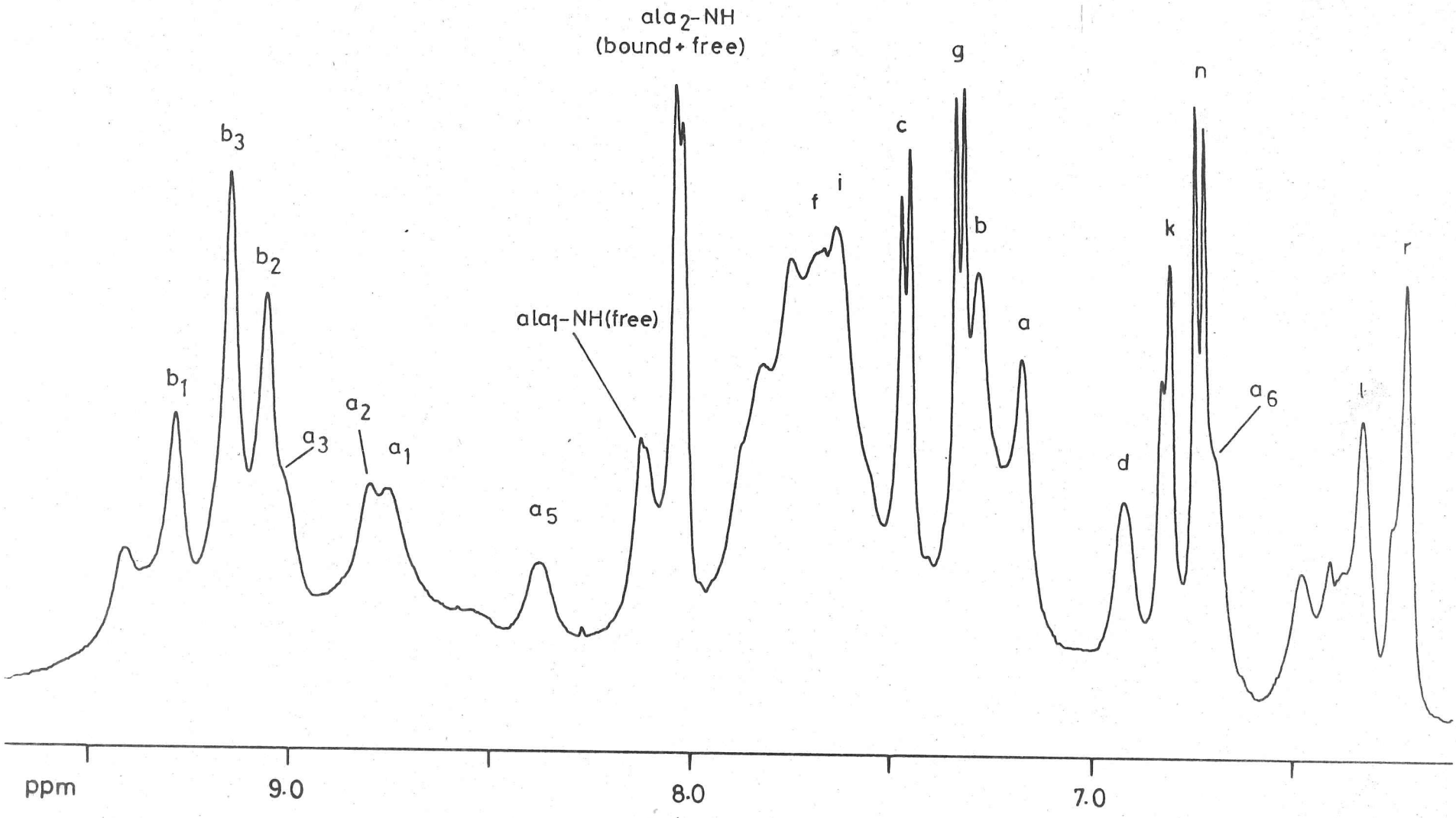

Table 6.5 Vancomycin/Ac-D-ala-D-ala (1:2) Assignment

δppm	Assignment	δppm	Assignment
0.51	ala_1Me_b	5.40	t
0.69	ii/jj	5.47	s_4
0.93	ala_2Me_b	5.76	A_2
1.02	gg	5.86	s_3
1.18	ala_2Me_f	5.98	A_3
1.26	ff	6.20	r
1.28	ala_1Me_f	6.31	l
1.38	j	6.69	a_6
1.69	h/h	6.73	n
1.85	ala-Ac-Me	6.81	k
2.14	o	6.92	d
2.60	o	7.17	a
2.65	hh	7.28	b
3.14-3.66	sugar protons	7.32	g
3.86	ala_1CH_b	7.46	c
4.16	cc/ala_1CH_f	7.63	i
4.30	ala_2CH_f	7.75	f
4.41	s_1	8.02	ala_2NH_{b+f}
4.50	s_6	8.10	ala_1NH_f
4.61	s_2/x	8.37	a_5
4.68	ala_2CH_b	8.75	a_1
4.74	s_5	8.79	a_2
5.13	z	9.00	a_3
5.19	y	9.05	b_2
5.22	v/m/bb	9.15	b_3
5.24		9.28	b_1
5.36	A_1(?)	11.75	a_4

Data collected in dmso-d_6/30%CCl_4 at 0°C (400MHz),
Subscript b=bound, f=free.

The spectrum of the slow-exchanging complex was complicated by the appearance of several exchangeable resonances, due to amino and sugar hydroxyl protons, in the 5.36-9.41 region. Justification for the assignment of resonances not identified from the variable temperature studies will be given in the following text.

The nuclear Overhauser effect proved invaluable in the identification of the ristocetin A binding site; it has proved similarly useful in this study of vancomycin (negative effects only were observed). The standard Bruker gated nOe pulse sequence [2] was used throughout. The nOe's present in vancomycin under the experimental conditions used for the binding studies are shown in table 6.6, and are found to be identical in many cases to those found in vancomycin in dmso-d_6 at 70°C[37]. It therefore appears unlikely that a major change in conformation has occurred upon the addition of 30% carbon tetrachloride to the solution of vancomycin in dmso-d_6.

Table 6.6 Vancomycin nOe's (all negative)

Resonance Irradiated	nOe (%)
s_6	a(25), b(20), f(25), z(20)
s_4	y(30), a(20)
s_3	a_2(50), t(18), v(20), k(9)
y	a(14), s_4(10)
t	d(6), s_3(15), v(7), gg(18), ii/jj(17)
d	i(25), a_3(10)
g	c(40), v(8)
a_6	c(15), z(15), A_3(10)
a_4	y(20), bb(10), ff(12)
a_2/a_3	s_3(40), s_2(15), v(15), s_6(10), k(10), d(7)
a_1	s_6(17), f(20), s_2(30), b(8), z(14)

Data collected in dmso-d_6/30%CCl_4 solution at 5°C (400MHz).

In certain cases the initial build up of the nOe was studied by varying the length of the irradiating pulse, thus obtaining data relating directly to protons in the immediate vicinity of the irradiated peak. As the length of the pulse is increased so spin diffusion throughout the molecule, especially through exchangeable nuclei, has a greater effect thus limiting the usefulness of the 'nOe' information. The main difficulties encountered in nOe experiments came from spin diffusion. Although this is not unexpected for a molecule the size of vancomycin, the

---

[2] See Bruker Software Manual

problem was greatly amplified if the sample had not been completely desiccated (over phosphorous pentoxide/sodium hydroxide), as evidenced by a large water peak (HOD) at around 3.3ppm.

The nOe time dependence of the amide proton a_4, in the vancomycin/Ac-D-ala-D-ala complex, is shown in figure 6.15 (a typical nOe difference spectrum, from which the data is derived, is shown in figure 6.16). The protons to which the nOe builds up most rapidy, and must therefore be closest to the irradiated proton a_4, are i, a_5, cc and m/bb. The effect observed to the latter pair of sugar anomeric protons is probably due to spin diffusion, as evidenced by the slower initial nOe build up and the fact that the curve continues to rise beyond the theoretical maximum nOe level of 100% with no sign of curtailment within the bounds of the experiment. On the basis of this data and the binding site proposed above the exchangeable but unidentified resonance (the only such resonance in this region of the spectrum) at 8.37ppm was tentatively assigned as the amide proton a_5. The apparently anomalous but large nOe to i can be explained only if the aromatic ring 3, to which it is bonded, is rotated through 180° to bring it to the 'front face' of the molecule. This postulate would also account for the nOe observed[37], in both directions in aglucovancomycin and vancomycin, between protons a and y, which are seemingly on opposite faces of the molecule. The most plausible explanation to account for this (the ring is too hindered to rotate freely) is that during the preparation of the crystals of CDP-I, used in the x-ray analysis, a retro-claisen type of rearrangement (scheme 6.6) occurred in which the αCH—βCH bond of the ring 3 β-hydroxy-chlorotyrosine unit was cleaved. This would allow reconnection of this bond with the chlorine atom either on the front face, as in CDP-I, or on the rear face, as in vancomycin.

A similar nOe time dependence study was performed for the amide proton a_5 (figures 6.17 and 6.18). Again considering the initial nOe build up, and despite considerable spin diffusion with the longer pulse durations it can be clearly seen that the nearest protons are a_4, a_3, i, o and s_5. This confirms that the resonance at 8.37ppm is indeed the amide proton a_5, and is also substantial evidence in support of the proposed modifications to the vancomycin binding site. Further nOe's are presented

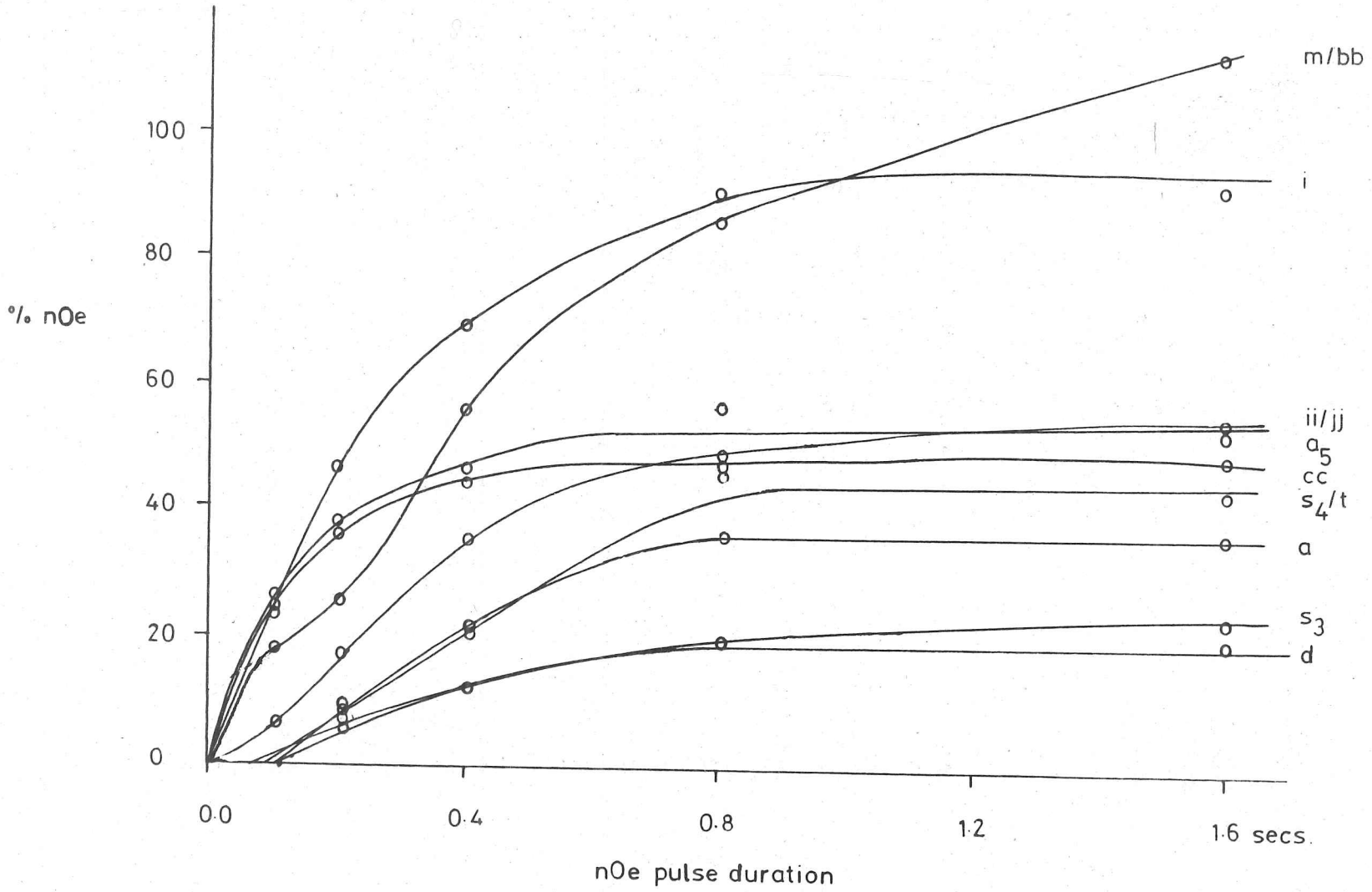

FIGURE 6·15 Proton a_4 nOe time dependence, 1°C

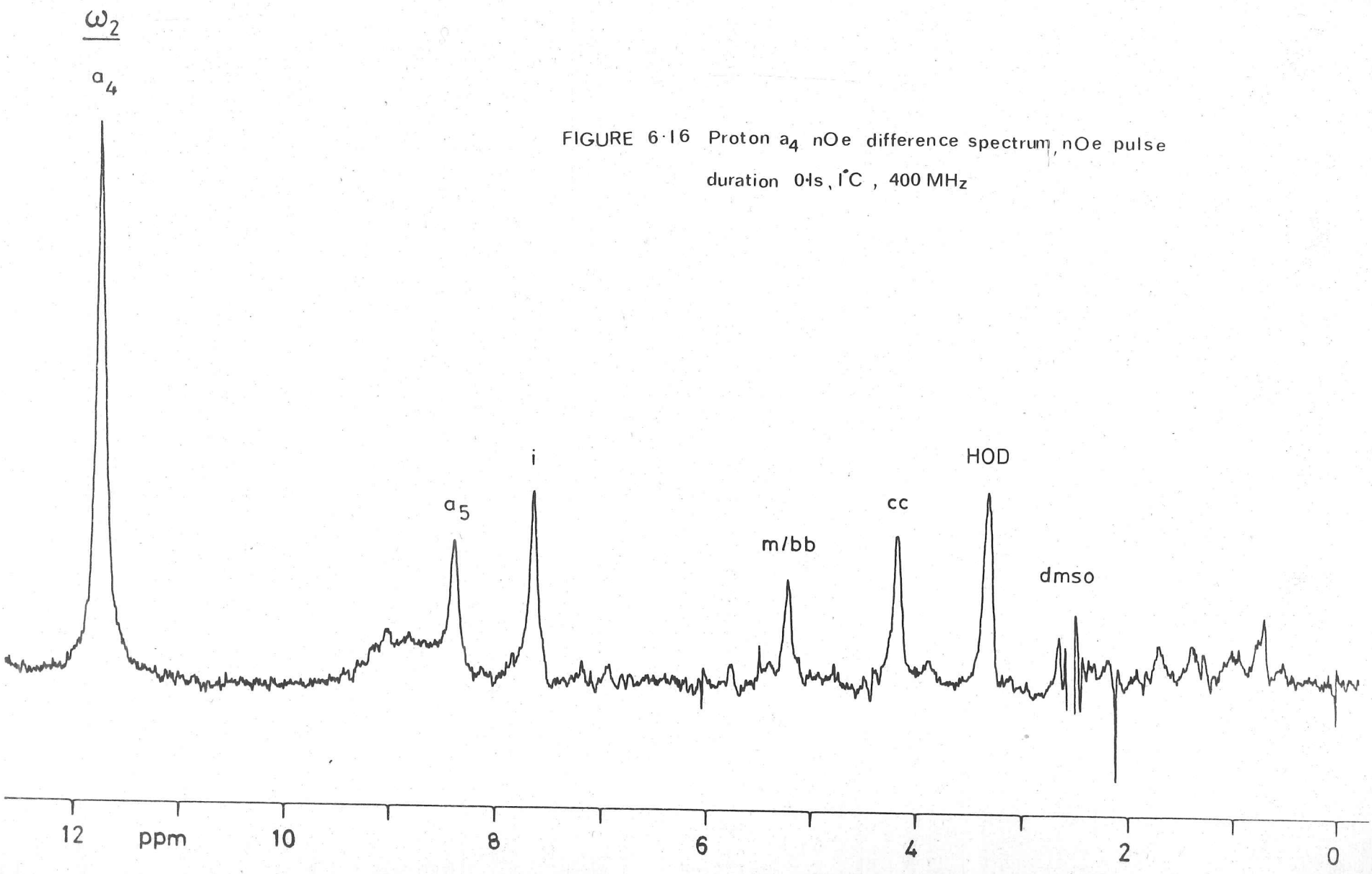

FIGURE 6·16 Proton a_4 nOe difference spectrum, nOe pulse duration 0·1s, 1°C, 400 MHz

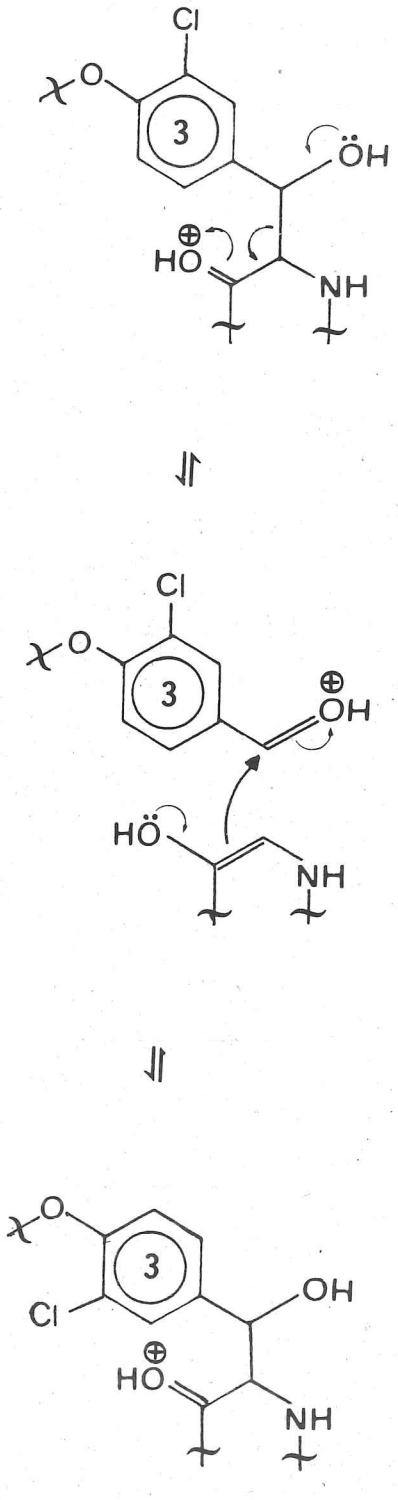

SCHEME 6·6

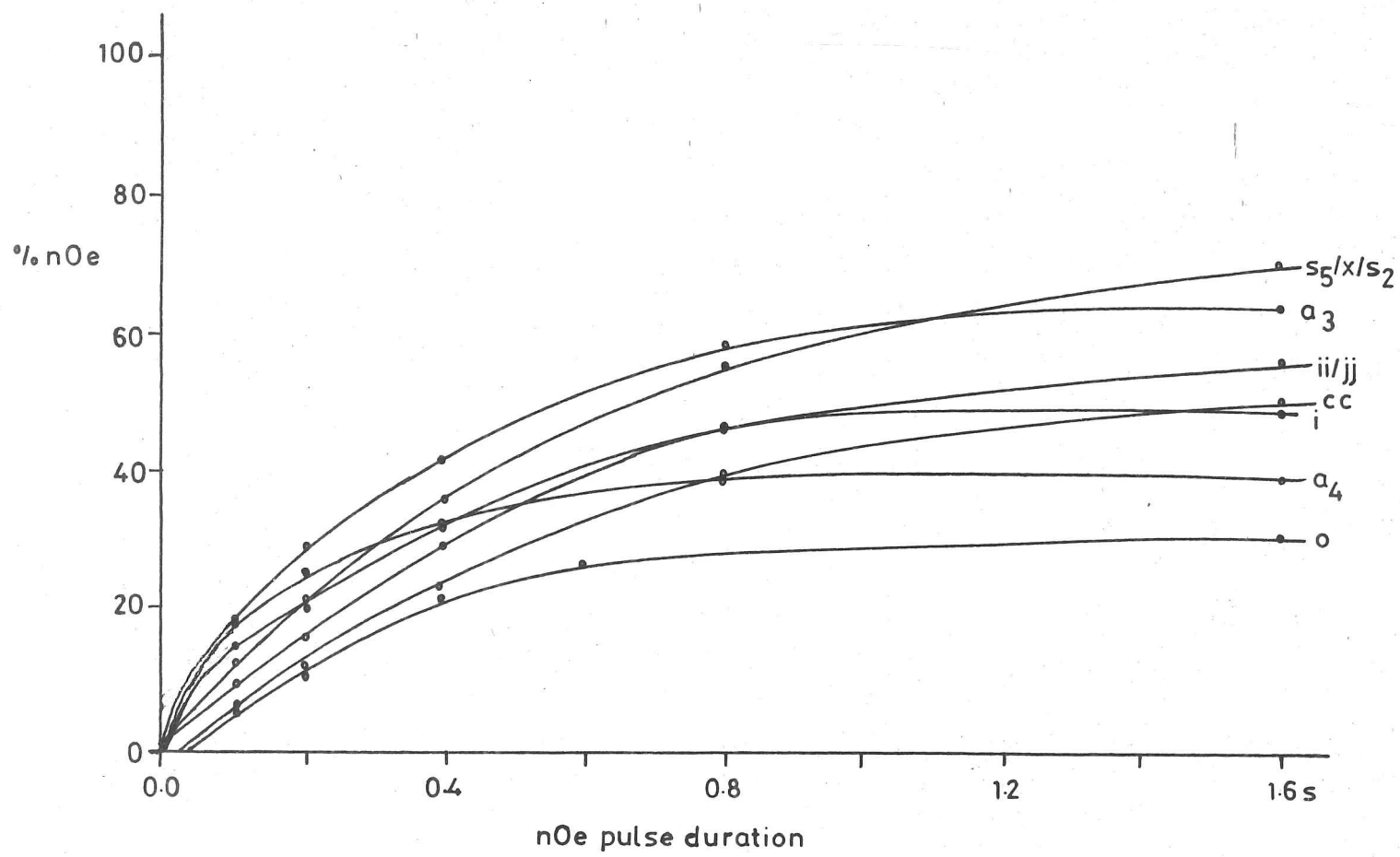

FIGURE 6.17 Proton a_5 nOe time dependence, 12°C

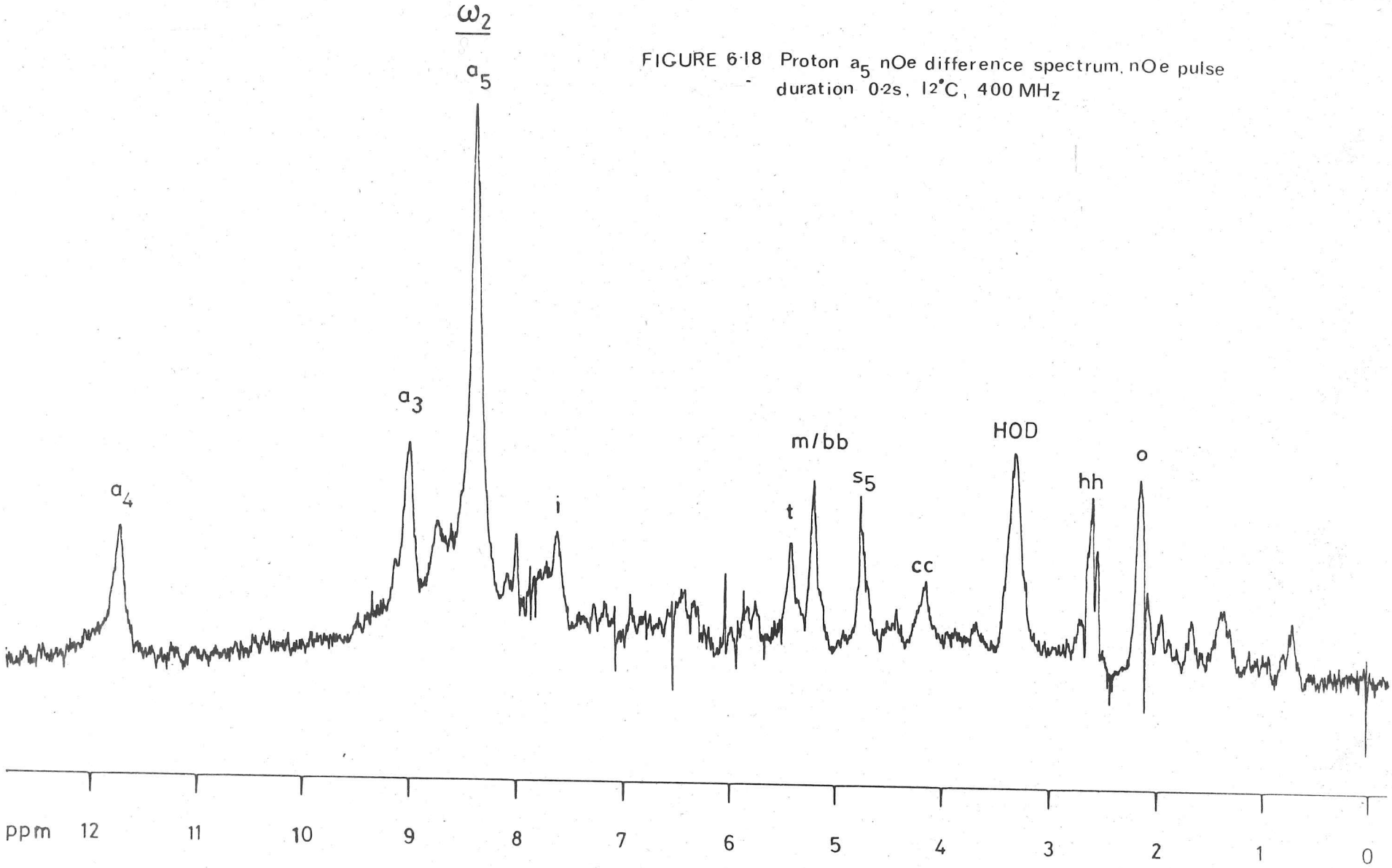

FIGURE 6·18 Proton a_5 nOe difference spectrum, nOe pulse duration 0·2s, 12°C, 400 MHz

in table 6.7.

Table 6.7 Vancomycin/Ac-D-ala-D-ala (~1:2) nOe's and TOS*

Resonance Irradiated	nOe/TOS (%)
ala_1Me_b	ala_1Me_f(30), d(7), ala_1CH_b(7)
ala_2Me_b	ala_2Me_f(10), f(7)
ala-Ac-Me_b	ala_2NH_b(15)
ala_1CH_f	ala_1CH_b(30)
ala_2CH_f	ala_2CH_b(40)
ala_2NH_b	ala-Ac-Me_b(20)
ii/jj	j(15), ala_2Me_b(25)
gg	ff(8), x(10)
ff	gg(10)
h	j(40)
s_1	z(10)
s_2	b(12)
s_3	t(10), a_2(30)
x	c(10)
s_5	o(15)
s_6	s_2(30), z(10), f(10)
a_1	f(8)
a_2	s_3(15)
a_3	t(8)
o	s_5(20)
z	A_3(10)
d	i(25)
a	y(50)
b	z(10)
g	c(30)
c	g(50), a_6(15)
i	d(7), a_4(7)
r	s_1(7), b_1(10)
l	b_2(30), b_1(7)
b_1	r(30), l(20)
b_2	l(20), b_3(20)
b_3	b_2(30), n(30)
A_2	y(20)
A_3	z(25), a_6(20), c(30)

* Transfer of saturation (TOS) indicated by effects between bound (b) and free (f) components.

Data collected in dmso-d_6/30%CCl_4 solution at 5°C (400MHz). All nOe's were negative.

The position of the amide proton a_3 was confirmed by the observation of an nOe to the somewhat isolated aromatic proton t, to which few nOe's were observed. Other important effects observed were between the bound ala_1Me and the aromatic proton d (also reported in the study of the analogous ristocetin A complex) and a large effect between proton a and proton y. The remaining nOe's provide confirmation of many spectral assignments that have already been mentioned.

Re-interpretation of the data presented by Convert and co-workers[66] further supports the proposed carboxylate anion receptor pocket. They noted a marked change in the chemical shifts of the iso-asparagine methylene protons upon complex formation; in addition a large perturbation ($>$+25Hz) of the iso-asparagine amide proton a_5 was reported. Both of these effects have also been noted in this study, although of increased magnitude. In view of the downfield shift of the amide proton a_3 upon complex formation (due to hydrogen bonding), it was concluded that the perturbation of a_5 could not be due to hydrogen bond formation since the x-ray structure shows a_3 and a_5 to be on opposite faces of the molecule. Further, seemingly anomalous shifts of protons d and i (also considered from the x-ray study to be on the rear face) were observed. In the light of the proposed conformational change and the structural modification involving rotation of ring 3 by 180°, it can be seen that the data are consistent with the hydrogen bonding of both a_3 and a_5 (in addition to a_4) to the carboxylate anion; the protons d and i now being on the front face are proximal to the peptide binding site which would account for their observed shifts (the large shift observed for proton a is still reasonable in view of the fact that it is adjacent to the portion of the molecule undergoing the most major changes in conformation); and the methylene protons of the iso-asparagine residue do move considerably relative to a_3 in accord with their change in chemical shift.

6.1.3 VANCOMYCIN/AC_2-L-LYS-D-ALA-D-ALA BINDING STUDIES

The dipeptide Ac-D-ala-D-ala, although providing information on the conformation of the right-hand portion of vancomycin upon binding [3]

---

[3] See Section 6.1.2

still leaves unidentified possible interactions which may occur between the antibiotic and the bacterial cell wall. The data of Nieto and Perkins[63] indicates that the vancomycin carboxylate anion is involved in binding, as deduced from the association constant increase of 100 for the Ac_2-L-lys-D-ala-D-ala complex compared with the Ac-D-ala-D-ala complex. Interaction with the carboxylate group is presumed since ristocetin A, which has a methyl ester in the position of the vancomycin carboxylate group, has an association constant increase of just 10 for the similar peptide complexes. From studies of CPK models it can be seen that the lys-α-NH could interact with the carboxylate anion which would enable the flexible sidechain lys-ε-amino group to interact with the sugar moieties. Convert and co-workers[66] noted a large shift for the vancomycin amino sugar methyl group ff with Ac_2-L-lys-D-ala-D-ala compared with Ac-D-ala-D-ala.

Preliminary experiments only have so far been performed producing disappointingly few results relating to the interactions of Ac_2-L-lys, the third amino acid residue, with the antibiotic. This has mainly been due to considerable spin diffusion which has made spectral interpretation somewhat complicated, but additionally the appearance of seemingly anomalous resonances has hampered the full assignment of the spectrum. It has previously been noted that during experiments the decomosition of the Ac_2-L-lys-D-ala-D-ala produces extra peptide signals. The partial assignment of the spectrum of vancomycin complexed to Ac_2-L-lys-D-ala-D-ala is shown in table 6.8. The assignments have been based on the previous study with Ac-D-ala-D-ala [4] and nOe and transfer of saturation data, which is presented in table 6.9.

---

[4] See table 6.5

Table 6.8 Vancomycin/Ac_2-L-lys-D-ala-D-ala (~1:2) Assignment

δppm	Assignment	δppm	Assignment
0.52	ala_1Me_b	5.18	v/y
0.68	ii/jj	5.22-5.24	m/bb
0.93	ala_2Me_b	5.41	t
1.03	gg	5.50	s_4
1.22	ala_2Me_f	5.74	A_2
1.27	ff/ala_1Me_f/lysγCH_{2f}	5.82	s_3
1.38	lysδCH_{2f}	5.97	A_3
1.44	j	6.25	r
1.55	lysβCH_{2f}	6.36	l
1.78	lysε$AcMe_f$	6.63	a_6
1.84	lysε$AcMe_b$/lysα$AcMe_f$	6.68	n
2.00	lysα$AcMe_b$	6.76	k
2.16	o	6.91	d
2.57	hh	7.03	b
3.00	lysεCH_{2f}	7.15	a
3.09	sugar proton	7.28	g
3.18	lysεCH_{2b}	7.43	c
3.28-3.63	sugar protons	7.65	i/ala_2NH_f
3.88	ala_1CH_b	7.76	f
3.98	ala_1CH_f	7.84	lysεNH_b
4.17	cc(?)	7.96	lysεNH_f
4.21	lysαCH_f	8.06	lysαNH_f
4.36	ala_2CH_f	8.13	lysαNH_b
4.41	s_1/lysαCH_b	8.18	ala_1NH_f
4.63	ala_2CH_b	8.37	a_5
4.67	x/s_2	8.75	a_2
4.71	s_5	9.03	a_3
4.96	s_6	9.48	a_1
5.13	z	11.62	a_4

Data recorded in dmso-d_6/30%CCl_4 at 10°C (400MHz).
All nOe's are negative. Subscript b=bound, f=free.

Table 6.9 Vancomycin/Ac_2-L-lys-D-ala-D-ala (~1:2) nOe's and TOS*

Resonance Irradiated	nOe/TOS (%)
ala_1Me_b	ala_1Me_f(20), ala_1CH_b(12), gg(8), d(7)
ala_2Me_b	ii/jj(30), ala_2Me_f(15), gg(12), x/s_2(7), f(7)
gg	ala_2Me_b(15), ala_2Me_f(20), ala_2CH_b(10), ff/ala_1Me_f/lysγCH_{2f}(15)
ala_2Me_f	ala_2Me_b(12)
lysδCH_{2f}	lysεCH_{2f}(10)
lysβCH_{2f}	ff/ala_1Me_f/lysγCH_{2f}(20), ala_2Me_f(15)
lysαAcMe_b	lysαAcMe_f/lysεAcMe_b(30)
o	s_5(15), lysαAcMe_b(15), ii/jj(10)
lysεCH_{2f}	lysδCH_{2f}(10), lysεNH_f(5)
lysεCH_{2b}	lysεCH_{2f}(15), ff/ala_1Me_f/lysγCH_{2f}(8), z(8)
ala_1CH_b	ff/ala_1Me_f/ala_2Me_f/lysγCH_{2f}(16), ala_1CH_f(20), ala_1Me_b(15)
ala_1CH_f	ala_1CH_b(30), v/y/m/bb(10)
lysαCH_f	lysαCH_b/s_1(25), ala_2CH_b(10), v/y(10), ala_2Me_f(10), $x/s_2/s_5$(12)
ala_2CH_f	ala_2CH_b(35), lysδCH_{2f}(9), ff/ala_2Me_f/ala_1Me_f/lysγCH_{2f}(12)
s_1/lysαCH_b	lysδCH_{2f}(20), ala_2Me_f(15), lysαCH_f(15), ala_2CH_b(15), s_5(14), v/y/m/bb(15), lysαNH_b(15)
$ala_2CH_b/x/s_2$	ff/ala_1Me_f/lysγCH_{2f}(18), gg(14), ala_2CH_f(17)
$s_5/x/s_2/ala_2CH_b$	ala_2CH_f/s_1/lysαCH_b(20), f(12), v/y(15), ff/ala_1Me_f/lysγCH_{2f}(12)
s_6	v/y/z(60), $ala_2CH_b/x/s_2/s_5$(25), f(10), s_1/lysαCH_b(12), b(8), lysαAcMe_b(7)
v/y/z/m/bb	a(12)
t	v/y(40), $s_5/s_2/x/ala_2CH_b$(15), ff/ala_1Me_f/lysγCH_{2f}(10)
A_2	v/y(60), ala_2Me_f(20)
s_3	v/y(50), a_2(20)
r	l(30), v/y/m/bb(12)

Table 6.9 Continued

Resonance Irradiated	nOe/TOS (%)
n/a_6	k(40), v/y/m/bb(12), c(10)
k	n/a_6(40), v/y(10)
d	z/v/y/m/bb(25), i/ala_2NH_f(12), ala_1Me_b(15), ala_2CH_b/x/s_2/s_5(12) ff/ala_1Me_f/lysγCH_{2f}(10)
b	z/v/y/m/bb(30), ala_2CH_b/x/s_2/s_5(20), ala_1Me_f/ff/ala_2Me_f/lysγCH_{2f}(10), ala_2CH_f/s_1/lysαCH_b(10), s_6(10)
a	z/y/v/m/bb(40), g(15)
g	c(25), z/v/y/m/bb(22), a(9)
c	g(35), ala_2Me_f(13), a_6(12) z/v/y/m/bb(30)
i/f	z/v/y/m/bb(17), d(15)
f/i/lysεNH_b	ala_2CH_b/x/s_2/s_5(25), z/v/y/m/bb(25), ala_1Me_f/ala_2Me_f/ff/lysγCH_{2f}(12), ala_2Me_b(12)
lysεNH_b	lysεNH_f(18), ala_2CH_b/s_2/s_5/x(17), z/v/y/m/bb(16)
lysεNH_f	v/y/z/m/bb(25), lys$\varepsilon AcMe_b$/lys$\alpha AcMe_f$(15), ala_1Me_f/ff/ala_2Me_f/lysγCH_{2f}(10) lysεNH_b(25), lysεCH_{2f}(20)
lysαNH_b/ala_1NH_f	v/y/m/bb(15), lys$\alpha AcMe_f$/lys$\varepsilon AcMe_b$(10), ala_2Me_f/ala_1Me_f/ff/lysγCH_{2f}(15), s_1/lysαCH_b(12), ala_2CH_b/s_2/s_5/x(11)
ala_1NH_f/lysαNH_b	lysδCH_{2f}(14), s_1/lysαCH_b(14), v/y/m/bb(12), ala_2Me_f(13)
a_5	s_5(15), v/y/m/bb(30), a_3(14), a_4(8), ii/jj(9)
a_2	s_3(30), v/y(30), ala_2CH_b/s_2/s_5/x(12), k(8)
a_3	v/y/m/bb(30), ala_2CH_b/x/s_2/s_5(30), t(20), a_5(5)
a_1	f(30), ala_2CH_b(10), z/y/v/m/bb(35), ala_2Me_f(15)
a_4	a_5(30), i(20), a_3(8), z/v/y/m/bb(30), ala_2Me_f(20)

Data recorded in dmso-d_6/30%CCl_4 at 10°C (400MHz).
*Transfer of saturation (TOS) indicated by effects between bound (b) and free (f) components.

Compared to the vancomycin complex with Ac-D-ala-D-ala three resonances were found to be significantly (>0.1ppm) affected by the addition of a third residue to the bacterial cell wall analogue. They were s_6 (despite spin diffusion confirmatory nOe's to z, s_2, f and b can reasonably be identified) which was deshielded by 0.46ppm; b was shielded by 0.25ppm (confirmatory nOe's to z, s_6 and s_2); a_1 was deshielded by 0.73ppm (confirmatory nOe's to f, z and ala_2CH_b). From CPK model building studies the deshielding of a_1 and s_6 is due to the proximity of the lysylαAc-CO or a conformational change of the antibiotic carboxyl group induced upon the addition of tripeptide, or is perhaps a combination of the two effects. The shielding of aromatic proton b would occur if the aliphatic lysyl sidechain was oriented towards the sugar moieties.

Despite the effects of spin diffusion a similar pattern of nOe's was observed for the right-hand portion of the antibiotic. Notably the nOe previously observed with Ac-D-ala-D-ala from the ala_1Me group to the vancomycin proton d was also observed, and in both directions, with tripeptide. Transfer of saturation identified many of the peptide resonances except for three of the four bound lysyl methylene group protons which remained unidentified and may account for some of the effects observed in the methyl region.

Possible effects with the lysyl residue involved the lysεCH_{2b} (z and ff), lysαCH_b (ala_2CH_b and b), lys$\alpha AcMe_b$ (s_6) and lysεNH_b (z/m/bb). Since all of the perturbed nuclei were on or around the triaryl unit of vancomycin with no effects observed to nuclei on the biphenyl unit the obvious conclusion is that the lysyl sidechain is oriented towards z or the sugars, or is flexible and can occupy one of several positions in this region of the antibiotic. The lysNH protons were not significantly shifted upon binding, hydrogen bonding is therefore not confirmed to either of them although it probably occurs from the α-NH to the carboxyl of vancomycin, as evidenced by the deshielding of a_1 noted above.

6.1.4 CRYSTALLISATION STUDIES

The most conclusive manner in which to identify a binding site is by an x-ray study of the complex. Since the vancomycin derivative CDP-I could be readily prepared in a crystalline form it was feasible that if a bacterial cell wall analogue was present in solution, then under the same conditions crystals of CDP-I bound to the analogue may be obtained.

Crystals of CDP-I were obtained by heating (80°C, 2 days) aqueous solutions (pH3.4 or 4.2) of vancomycin. Dark brown, irregular shaped crystals were produced at both pH's, although superior crystals were obtained at pH4.2. An equimolar (50mM) solution of vancomycin and Ac-D-ala-D-ala was prepared. It was found to be more acid (pH2.4) than a solution of vancomycin alone and a precipitate formed above pH3. Incubation for 16 hours at 80°C produced a gel only. A similar result was obtained with a 20mM solution. This result is perhaps not surprising in the light of the contention[74] that CDP-I does not bind to bacterial cell wall analogues.

Further studies were performed which involved diffusing a volatile precipitant onto the surface of the sample thereby slowly reducing the solubility of the components at the interface. Experiments were performed on vancomycin alone, an x-ray analysis of which could confirm the proposed rotation of ring 3, and with one equivalent of Ac-D-ala-D-ala present in solution with the antibiotic. Unfortunately none of the systems produced crystalline residues [5].

6.1.5 EPILOGUE

So far no evidence has been considered with respect to whether vancomycin in solution, and in the absence of bacterial cell wall analogues, adopts to any extent one particular conformation in preference to any other. Vancomycin alone in dmso-d_6 solution does appear to adopt the conformer found in the crystal; no evidence has been found to support the existence of the alternative conformation [6] formed upon

---

[5] See Chapter 8 for experimental details

[6] Proposed in Section 6.1.2

complexation. Data in support of this last statement can be found by comparing the data in figure 6.15 [7] with those presented in table 6.6 [8] . In the latter case only do protons y and a_4 experience an nOe to and from one another and in addition proton s_4 exhibits an nOe to proton a_5[37]. These effects would only be observed if the conformation of vancomycin in solution was similar to that deduced from the crystal study.

The proposed carboxylate anion receptor pocket (figure 6.8) bears a remarkable resemblance to that found in ristocetin A[67]. However, the receptor pocket of ristocetin A for the carboxylate anion is conformationally rigid whereas that for vancomycin is formed on demand from a conformationally mobile part of the molecule. Thus, in the dissociation of the vancomycin/Ac-D-ala-D-ala complex, numerous additional rotors will become available. This extra loss of order which can occur upon dissociation of the complex may well account for, at least in part, the smaller free energy of activation (ΔG=55KJ.mole^{-1}, T_c=16°C, $\delta\nu$=308Hz) for dissociation relative to the value (ΔG=75KJ.mole^{-1}) found for the ristocetin A/Ac-D-ala-D-ala complex.

6.2 RISTOCETIN A - CRYSTALLISATION STUDIES

The structure of ristocetin A, based on chemical and nmr studies, has recently been proposed[51]. Although the data appears unequivocal, confirmation by an x-ray crystal study is desirable.

At first glance through the literature this task does not seem too daunting since one of the early papers on ristocetin[74] describes the routine preparation of ristocetin crystals from an aqueous ethanolic solution. The experiments involved dissolving ristocetin (commercially available as the hydrogen sulphate) in four parts of water, eight parts of 95% ethanol solution was then added and the solution warmed.

---

[7] The nOe's of a_4 in the complex
[8] The nOe's of free vancomycin

Crystallisation proceeded over a period of several days. A photograph of the crystals and x-ray diffraction data was presented. Repeating this experiment was an obvious starting point for the present studies, but although it was attempted several times no success was enjoyed and other techniques and solvent systems were therefore evaluated.

Crystallisations are generally effected by dissolving the sample (a few milligrams) in a suitable solvent and then reducing its solubility by the addition of a second solvent, almost to the point at which precipitation would occur. Crystals often form if this process progresses slowly enough. Small molecules (for example some of the protected amino acids described in Section 6.1.1) often crystallise by simply shaking in such two solvent systems. However, for a molecule as complex as ristocetin more refined techniques are required. The two methods which have been most extensively used in these studies are vapour diffusion, in which a volatile precipitant diffuses onto the surface of the sample solution thereby reducing the solubility until crystallisation (or precipitation) occurs; and the layering method, in which the precipitant is carefully layered on top of the sample solution. The latter method was found to be more vigorous than the former, often producing precipitation when crystals were obtained in the analogous vapour diffusion experiment. Many solvent systems were evaluated and several of them produced crystalline residues, although only a water/75% acetone system was found to produce crystals of suitable quality for x-ray analysis. This system was also used to increase the purity of the antibiotic which then produced a larger number of single crystals in preference to multiple crystals. The crystals, although of exceptional quality, were found to be unstable upon x-ray bombardment for more than 3-4 hours, which was insufficient for the collection of a full data set.

Ristocetin A is supplied as the hydrogen sulphate salt, since this does not produce crystals suitable for analysis it was suggested[75] that conversion to another salt, for example the iodide, may generate crystals of a different form which might be more stable towards x-rays. The iodide salt was prepared by reaction of an aqueous solution of ristocetin A with an aqueous solution of barium iodide, the supernatant of ristocetin A iodide salt was separated from the precipitate of barium sulphate by

Crystallisation proceeded over a period of several days. A photograph of the crystals and x-ray diffraction data was presented. Repeating this experiment was an obvious starting point for the present studies, but although it was attempted several times no success was enjoyed and other techniques and solvent systems were therefore evaluated.

Crystallisations are generally effected by dissolving the sample (a few milligrams) in a suitable solvent and then reducing its solubility by the addition of a second solvent, almost to the point at which precipitation would occur. Crystals often form if this process progresses slowly enough. Small molecules (for example some of the protected amino acids described in Section 6.1.1) often crystallise by simply shaking in such two solvent systems. However, for a molecule as complex as ristocetin more refined techniques are required. The two methods which have been most extensively used in these studies are vapour diffusion, in which a volatile precipitant diffuses onto the surface of the sample solution thereby reducing the solubility until crystallisation (or precipitation) occurs; and the layering method, in which the precipitant is carefully layered on top of the sample solution. The latter method was found to be more vigorous than the former, often producing precipitation when crystals were obtained in the analogous vapour diffusion experiment. Many solvent systems were evaluated and several of them produced crystalline residues, although only a water/75% acetone system was found to produce crystals of suitable quality for x-ray analysis. This system was also used to increase the purity of the antibiotic which then produced a larger number of single crystals in preference to multiple crystals. The crystals, although of exceptional quality, were found to be unstable upon x-ray bombardment for more than 3-4 hours, which was insufficient for the collection of a full data set.

Ristocetin A is supplied as the hydrogen sulphate salt, since this does not produce crystals suitable for analysis it was suggested[75] that conversion to another salt, for example the iodide, may generate crystals of a different form which might be more stable towards x-rays. The iodide salt was prepared by reaction of an aqueous solution of ristocetin A with an aqueous solution of barium iodide, the supernatant of ristocetin A iodide salt was separated from the precipitate of barium sulphate by

centrifugation. Freeze drying was used to concentrate and dry the sample. Several solvent systems were tried but none produced a crystalline product.

The technique of salting-out, which has been successfully employed for oligopeptides and proteins, was also tried but produced crystals of a needle-like form which were not suitable for x-ray analysis.

The derivative Ψ-aglycone of ristocetin was also used for crystallisation studies since, if successful, it would greatly simplify interpretation of the data both because the molecular weight was significantly reduced and because the mobile tetrasaccharide unit (which may obscure details of the aglycone moiety) had been removed. Crystalline residues were not obtained from any of the solvent systems tried.

Confirmation of the binding site of ristocetin A was sought using both Ac-D-ala-D-ala and Ac_2-L-lys-D-ala-D-ala. Crystals of both comlexes with ristocetin A were obtained from the water/75% acetone system although only the dipeptide formed a stable complex. The crystals of ristocetin A and Ac-D-ala-D-ala were cubic in nature, having a unit cell of $\sim$140,000$\mathring{A}^3$ and was comprised of trimer sub-units, of which there were 24 per unit cell. Unfortunately there are no methods currently available which could be used to analyse such a crystal to the desired resolution.

6.3 TRIOSTIN A

It has previously been reported[53] that in deuteriochloroform triostin A exists in two symmetrical conformations separated by an energy barrier of 92KJ.mole^{-1}. One conformer is favoured in polar solvents, the other in non-polar solvents. The postulated difference between them, apart from minor movements about the cyclic peptide backbone, is the chirality of the disulphide cross-bridge. This conclusion was based on nmr chemical shifts, coupling constants, temperature and solvent shifts, and lanthanide induced shifts (LIS)[54]. Direct evidence, largely dependent upon nOe's, is

now presented which more precisely describes the conformers.

The 400MHz ^{1}H nmr spectrum in deuteriochloroform (figures 6.19-6.22) was assigned using double irradiation techniques, with reference to the assignments previously made at 270MHz[53]. The existence of significant proportions of each conformer produced complex spectra, from the overlap of resonances and transfer of saturation upon the execution of nOe experiments. Both positive and negative nOe's were observed in deuteriochloroform solution at 30°C and all were below 2% in magnitude. It therefore seemed that these conditions were on the threshold for changing the sign of the nOe (the position of minimum nOe). An increase in temperature would have been expected to produce larger and more positive enhancements whereas a decrease in temperature would have favoured negative effects. However, the small temperature variations that one could reasonably achieve with the nmr machine were insufficient to significantly influence the equilibrium existing between the two conformers. It was desirable to manipulate the equilibrium such that one conformer was greatly favoured over the other in order that spectral simplification could be accomplished.

Solutions containing solely triostin-p could readily be obtained by adding 25% dmso-d_6 to a solution in deuteriochloroform, however the n-conformer was more of a problem. In addition to polarity and solubiltiy problems a solvent was required which would produce larger nOe's, preferably negative, than those observed in deuteriochloroform at 30°C. In order to attain this last objective increasing the solvent viscosity or decreasing the temperature would be necessary. In view of the added consideration of changing the equilibrium of the conformers in favour of triostin-n the former was most desirable. The recent work of Williamson and Williams[76] has shown that the oil Voltalef 10S has great application for the manipulation of the nOe. It is very viscous (1550cp at 25°C) compared to other common solvents such as chloroform (0.54cp) and dmso-d_6 (1.98cp) and since it is a polymer of chloro-trifluoroethylene it has no protons to interfere in the spectrum. It is not in itself a good solvent but it is miscible with most organic solvents thus enabling solutions of many reasonably non-polar molecules to be obtained.

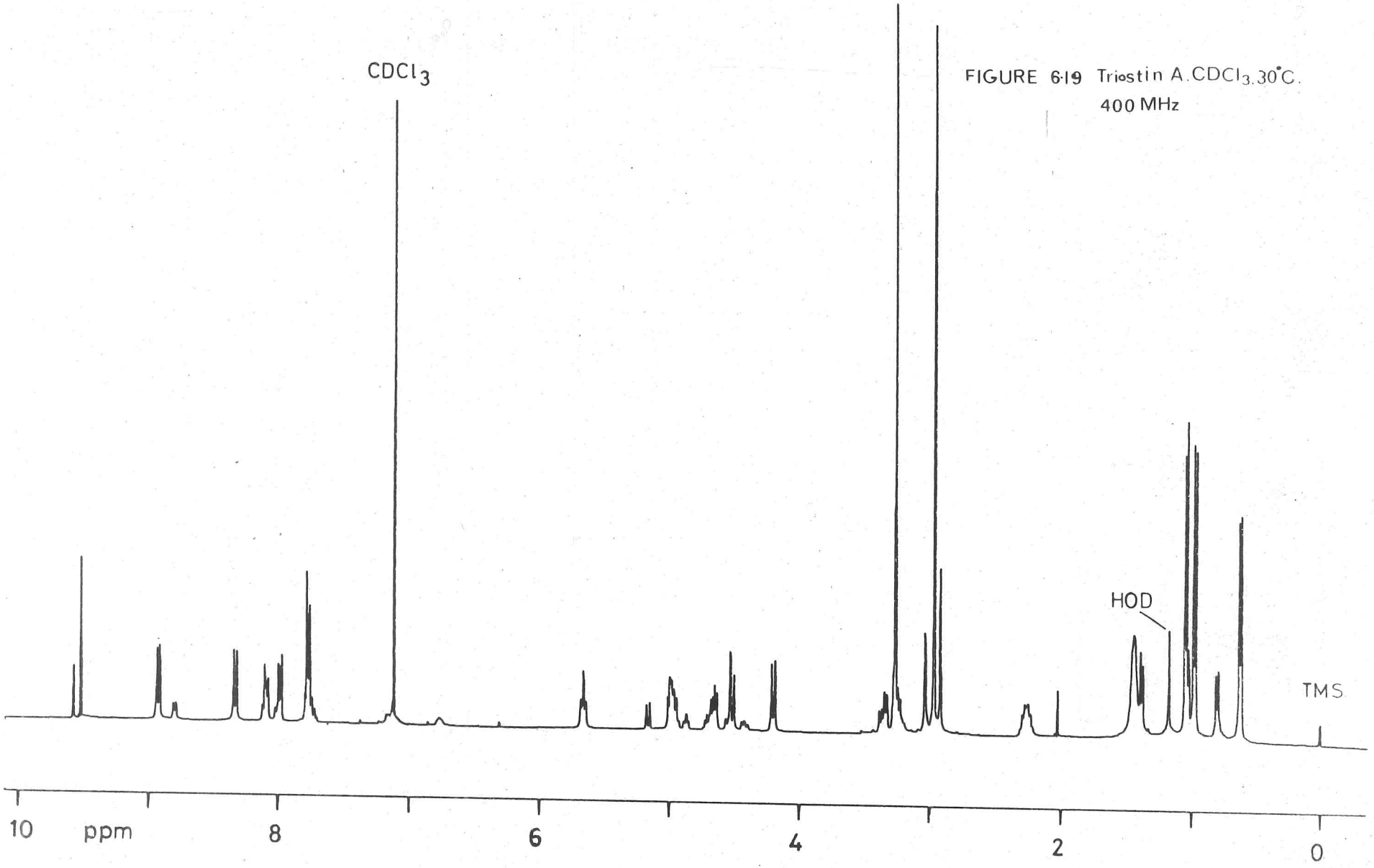

FIGURE 6.19 Triostin A. $CDCl_3$, 30°C. 400 MHz

FIGURE 6·20 Triostin A, $CDCl_3$, 30°C, 0·5 –3·5 ppm . 400 MH_z

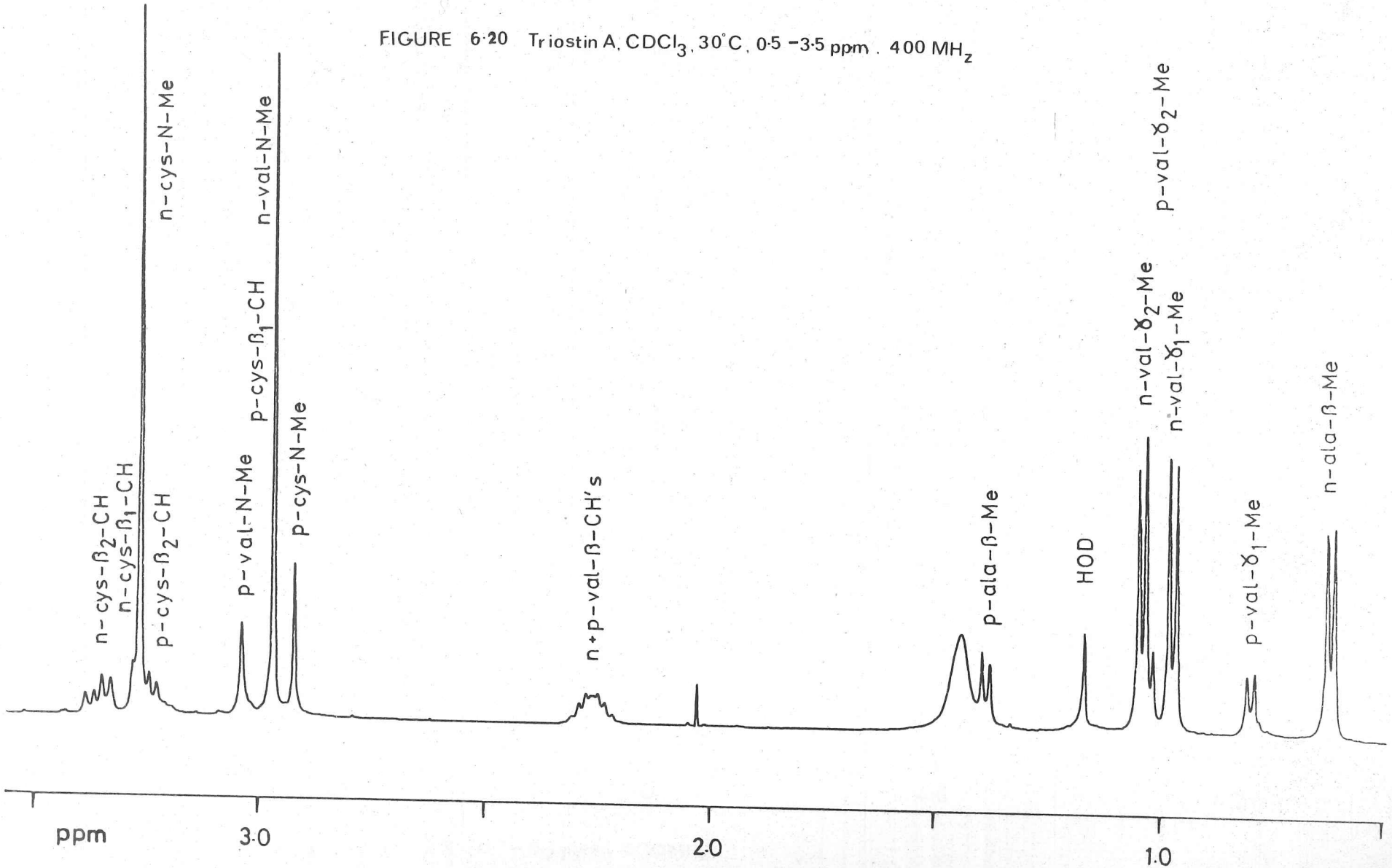

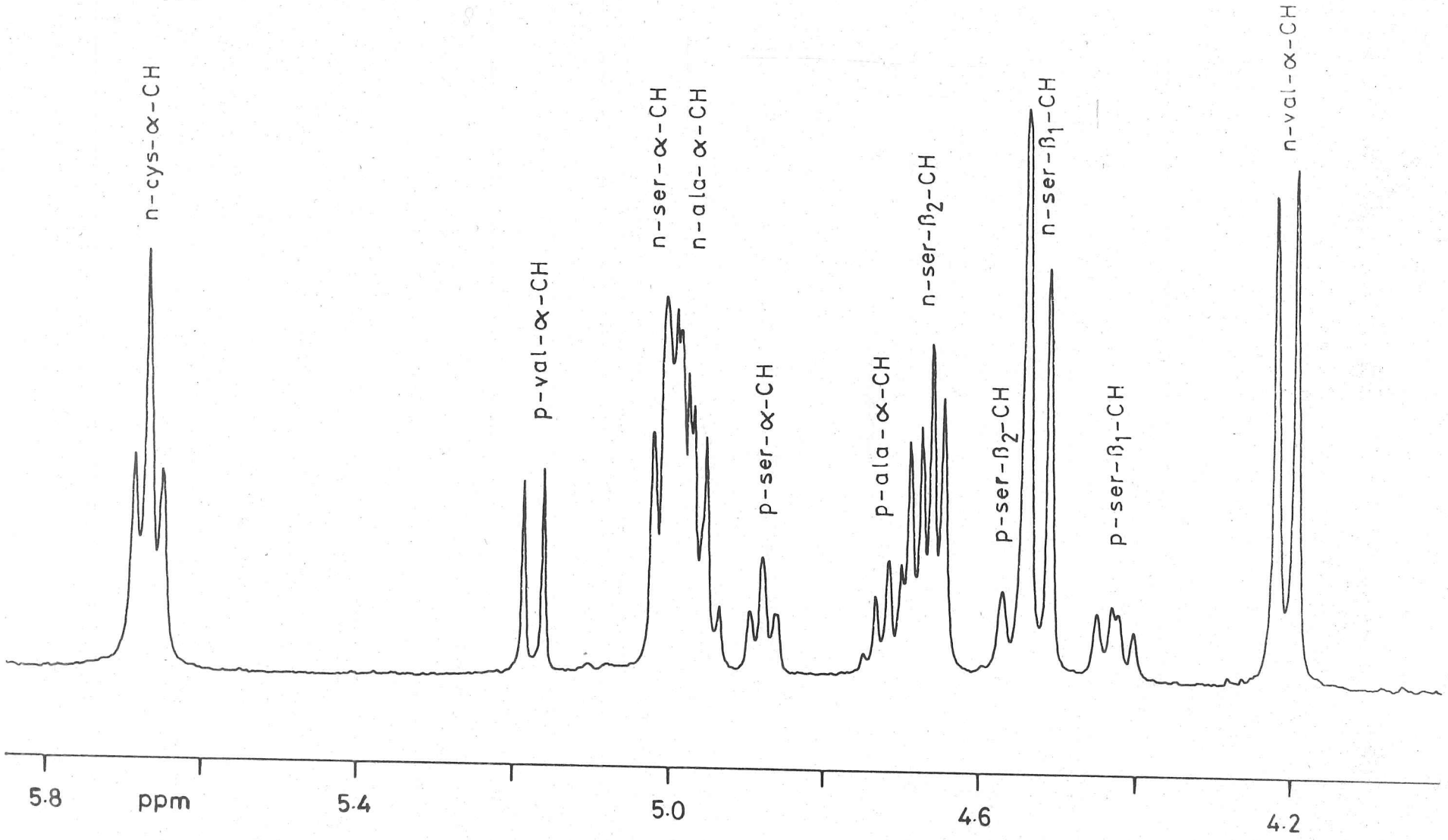

FIGURE 6·21 Triostin A, $CDCl_3$, 30°C, 4·2 – 5·8 ppm, 400MHz

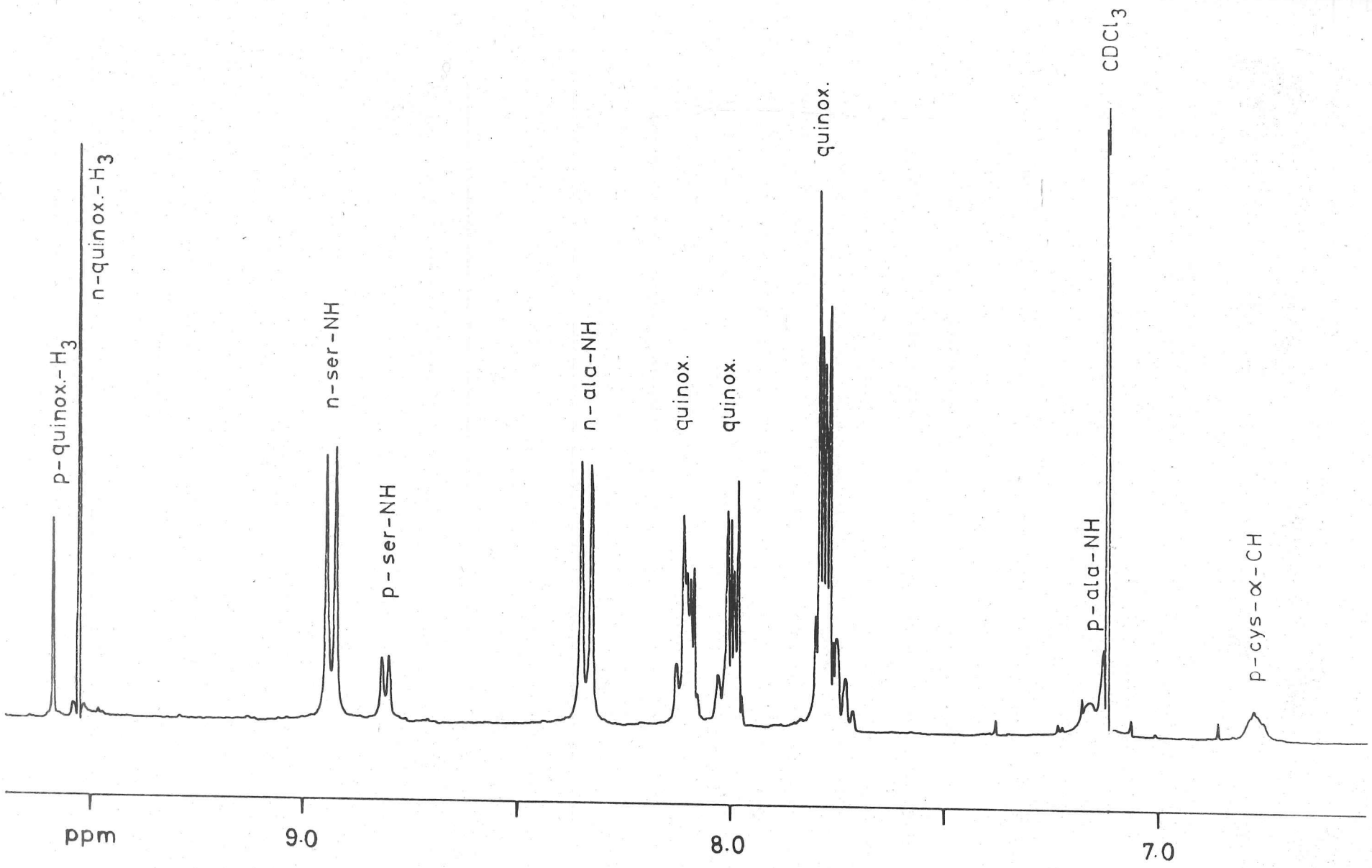

FIGURE 6·22 Triostin A , $CDCl_3$, 30°C , 6·5 – 9·5ppm , 400MHz

Triostin A was dissolved in deuteriochloroform and Voltalef 10S was then added; a 1:1 solution was the highest oil concentration possible without precipitation of the antibiotic. Unfortunately at 30°C the equilibrium was only slightly moved in favour of triostin-n (~2:1), but an nOe series produced some very interesting results. Irradiation of the n-cys-α-CH produced a 16% negative effect to the n-val-α-CH and essentially little else (figure 6.23), this was supported by an 18% negative effect in the reverse direction (figure 6.24). In order to check whether this enhancement was unique to triostin-n the p-cys-α-CH resonance was irradiated; a 19% negative nOe was observed to one of the N-methyl groups only (figure 6.25). The previous studies [9] have shown that echinomycin and triostin-p have similar conformations. The cys-α-CH and the val-N-Me are known to be on the upper, quinoxaline-ring bearing face of the antibiotic disc whereas the cys-N-Me is on the lower face. From examination of a CPK model of triostin-p it can be readily appreciated that the cys-α-CH and val-N-Me are potentially close enough to touch one another whereas no sizeable interaction is feasible with the cys-N-Me. The enhanced N-Me was therefore assigned to the valine residue. A 12% nOe from the p-cys-N-Me to p-ala-CH further supports this model. In addition a 7% nOe from the p-cys-N-Me to p-val-β-CH indicates that the bulky valine side-chain is oriented towards the lower face, away from the binding site. A 5% nOe from the p-cys-β_2-CH to p-cys-N-Me, with no effect observed between the p-cys-α-CH and the p-cys-β-CH protons, suggests that the p-cys methylenes are on the lower face. From CPK model building the disulphide bond can readily move from the lower to the upper face with little distortion to the rest of the molecule and so cannot be assigned to either face with certainty, indeed it may be that in solution it freely interconverts between the two. The observed nOe's are presented in tables 6.7 and 6.8.

---

[9] See Section 2.3

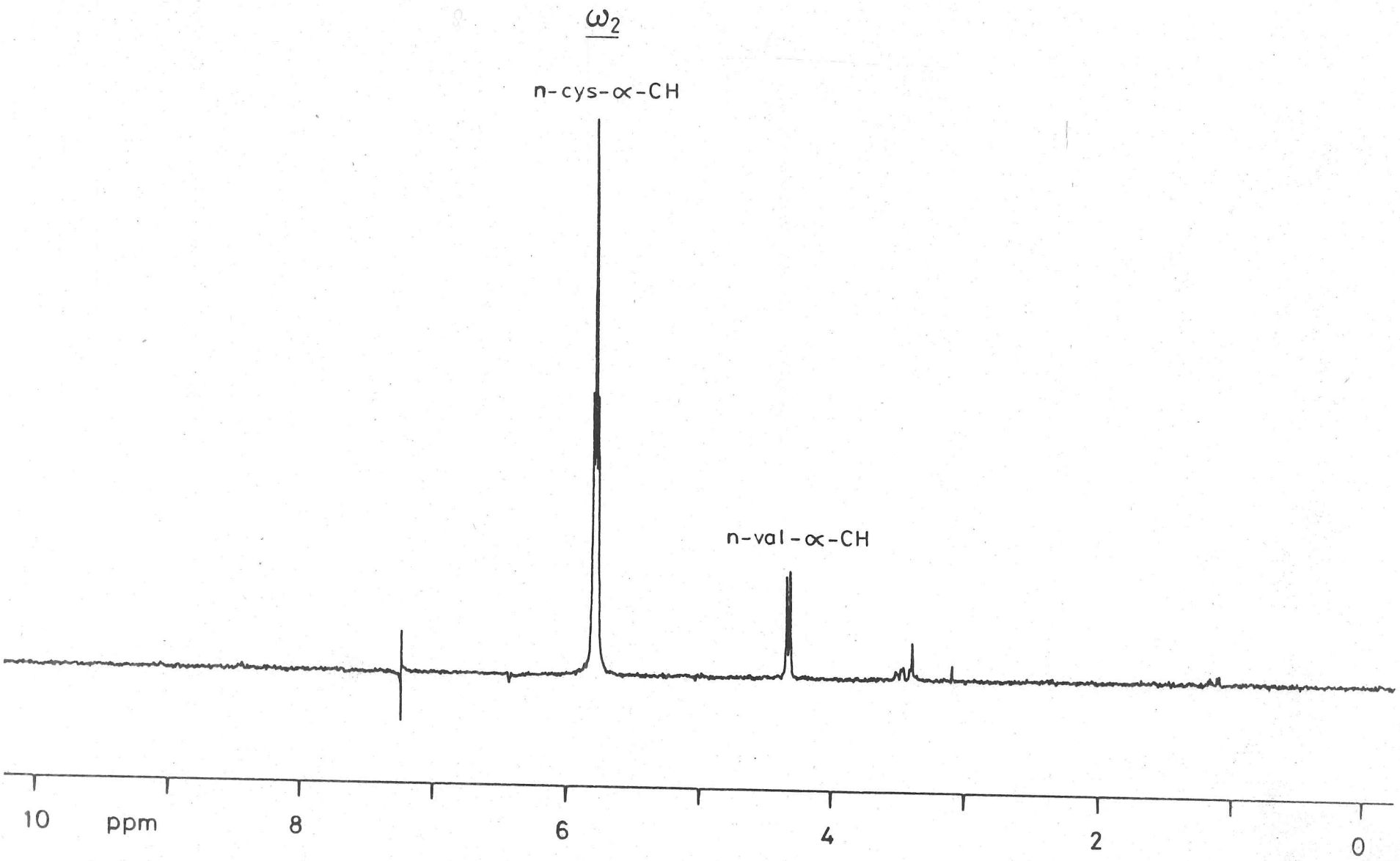

FIGURE 6·23 n-cys-α-CH nOe difference spectrum, 30°C, 400 MHz.

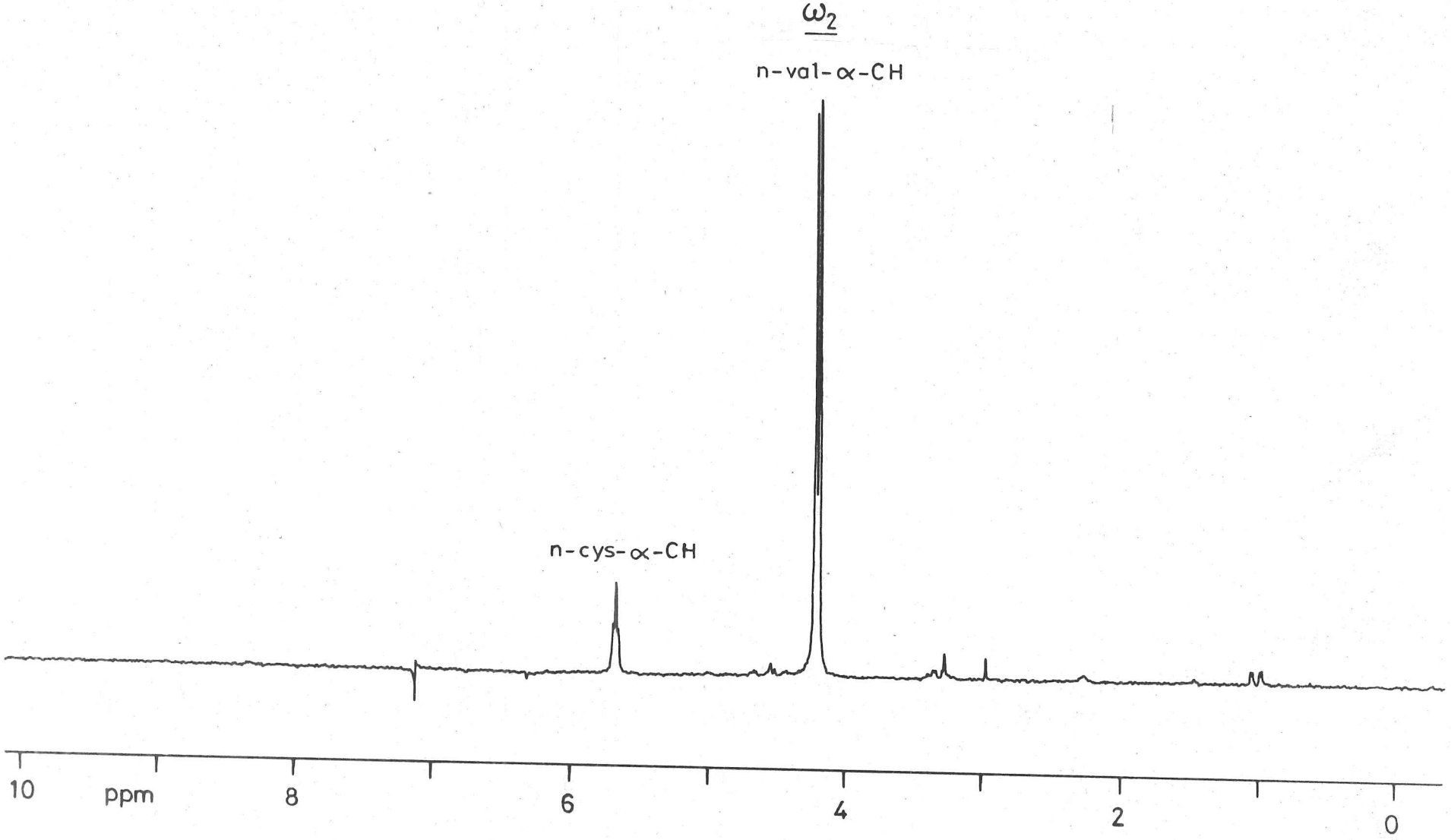

FIGURE 6·24 n-val-α-CH nOe difference spectrum, 30°C, 400MHz

FIGURE 6·25 p-cys-∝-CH nOe difference spectrum, 30°C , 400MHz

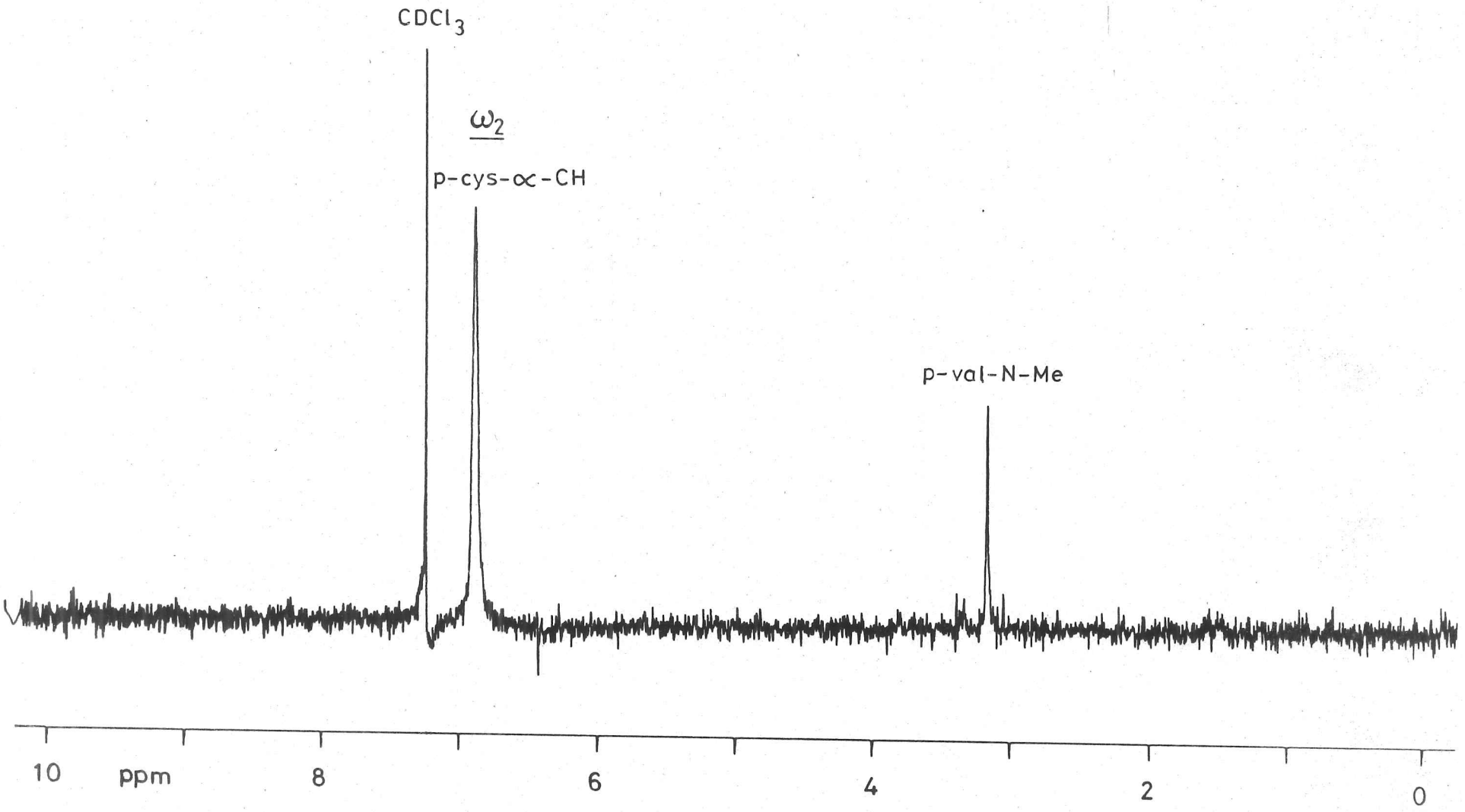

Table 6.10 Triostin-n nOe's (all negative)

Resonance Irradiated	nOe (%)
cys- α CH	val- α CH(16), cys- β_2CH(2), cys- β_1CH(2), cys-N-Me(3)
cys-N-Me/cys- β_1CH	cys- β_2CH(40), ala-CH(4), cys- α CH(3) val- α CH(3), val-N-Me(3)
cys- β_2CH	val- α CH(4), cys- α CH(4), val-N-Me(2)
val- α CH	cys- α CH(18), val- γ Me's(3), val- β CH(3), cys- β_1CH(4), cys-N-Me(3), ser- β_1CH(2)
val- β CH	val-N-Me(5), val- γ Me's(4), val- α CH(1)
val-N-Me	val- β CH(10), val- γ_1Me(4), cys-N-Me(5)
val- γ Me'S	val- β CH(6), ala-Me(4), val- α CH(3), val-N-Me(3)
ala-Me	ala-NH(6), ser- α CH/ala-CH(7), val- γ Me's(3), ser-NH(3), cys-N-Me(1)
ala-NH	ser-NH(7), ser- α CH/ala-CH(7), ala-Me(5), cys-N-Me(3), ser- β_2CH(3)
ala-CH/ser- α CH	cys-N-Me(8), ser- β_1CH(3),ser- β_2CH(2), ala-Me(2), ala-NH(2), ser-NH(2)
ser- β_1CH	ser- β_2CH(29), val- α CH(5), ser- α CH(5), ala-NH(3), cys-N-Me(2)
ser- β_2CH	ser- β_1CH(40), ser- α CH/ala-CH(10), ala-NH(5), ser-NH(4), cys-N-Me(2)

Data recorded in $CDCl_3$/Voltalef 10S (1:1) at 30°C (400MHz).

Table 6.11 Triostin-p nOe's (all negative)

Resonance Irradiated	nOe's (%)
cys-α CH	val-N-Me(19)
cys-β_2CH	val-N-Me/cys-β_1CH(8), cys-N-Me(5)
cys-N-Me	ala-CH(12), val-β CH(7), ala-Me(7)
val-α CH	val-γ_2Me(5)
val-β CH	val-γ_2Me(4), val-N-Me(2)
val-γ_2Me	val-β CH(6), val-γ_1Me(4), val-α CH(3)
val-γ_1Me	val-β CH(3), val-α CH(2)
ala-Me	ala-CH(2), val-N-Me(1)
ala-CH	cys-N-Me(7), ala-Me(3)
ala-NH	ser-α CH(5), val-N-Me(2), ala-Me(3)
ser-α CH	ser-β_2CH(15), ser-β_1CH(7), val-α CH(3)
ser-β_1CH	ser-β_2CH(50), ser-α CH(12)
ser-β_2CH	ser-β_1CH(15), ser-α CH(4)
ser-NH	ser-α CH(4)

Data recorded in $CDCl_3$/Voltalef 10S (~1:1) at 30°C (400MHz)

The data was by no means unambiguous as far as the interpretation was concerned; considerable problems were encountered from transfer of saturation and overlapping resonances, as in neat deuteriochloroform solution. However, the effects observed between the n-cys-α-CH and the n-val-α-CH were so large, relative to any other nOe involving either of these protons, that they obviously provide the main dipolar relaxation mechanism for each other. In order for this to be realised they would need to be very close in space and without any other proton in the immediate vicinity.

The cys-α-CH is rigidly held at the intersection of the cross-bridge with the peptide backbone and therefore cannot be significantly moved. The p-val-α-CH must therefore be moved towards the cys-α-CH. Rotation of the cys-val amide bond is necessary and can involve moving the N-Methyl group inwards towards the centre of the disc, or outwards. Both options necessarily involve the trans configuration being modified either partially or completely towards the cis amide bond. The val-α-CH and cys-α-CH can be moved together by moving the N-Me group inwards such that Φ is reduced from 180° to ~130°, further movement is not possible

because of steric crowding. However, the anticipated nOe between the n-val-N-Me and the n-ala-NH , which have been moved very close together, is not observed, and the arrangement is also somewhat strained. In addition the lanthanide induced shifts cannot be reconciled with the structure attained.

The more likely change involves rotation of the val-α-CH inwards towards the cys-α-CH. The val-N-Me is necessarily moved to cis with respect to the cys-CO to allow the close approach of the two α-CH protons. The cys-β-CH protons are moved close to the cys-α-CH and the val-α-CH protons since the only nOe's involving the cys-β-CH's are with these two α-CH protons. These few changes also have the effect of moving peptide residues on opposite sides of the ring together, above the disc. Notably the two alanine residues are now opposite one another, the NH of one being proximal to the carbonyl of the other. It is therefore apparent that hydrogen bonding of the ala-NH, previously proposed to be with the quinoxaline carbonyl, is actually across the ring to the other ala residue's carbonyl function. Hydrogen bonding across the ring is known to occur in tandem[26], but is between the ala-CO and the val-NH. Obviously N-methylation of the valine residue prevents an analogous interaction in triostin-n. Further minor changes of conformation may be involved but no other major changes. It is noticeable that the molecule is converted from an open conformation to a globular arrangement, which would also account for the larger number of nOe's observed in triostin-n compared to triostin-p.

In order to obtain further nOe's, and increase the effects already observed, spectra were recorded in $CDCl_3$/Voltalef 10S at $-10^{o}C$ (table 6.12). This also had the effect of moving the equilibrium in favour of the n-conformer ($\sim$10:1).

Table 6.12 Triostin-n nOe's (all negative)

Resonance Irradiated	nOe (%)
cys-α CH	val-α CH(73), cys-β_2CH(43), val-N-Me(7), cys-β_1CH/cys-N-Me(41), val-γ Me's(12)
cys-β_1CH/cys-N-Me	cys-β_2CH(67), cys-α CH(21), val-α CH(19), val-N-Me(11)
val-α CH	cys-α CH(55), cys-β_1CH/cys-N-Me(29), cys-β_2CH(20), val-γ Me's(19), val-β CH(15), val-N-Me(11)
val-β CH	val-N-Me(43), val-γ Me's(40), val-α CH(5), cys-N-Me(4)
val-γ_1Me	val-γ_2Me(17), val-N-Me(14), val-β CH(10), cys-N-Me(7), val-α CH(5)
val-γ_2Me	val-γ_1Me(15), val-β CH(9), val-N-Me(4), cys-N-Me(4), val-α CH(4)
val-N-Me	val-βCH(8), cys-N-Me(3)
ala-CH	cys-N-Me(49), ala-Me(20), ala-NH(9)
ala-Me	ala-CH(13), ala-NH(9), cys-N-Me(8), ser-NH(5)
ala-NH	ala-CH/ser-αCH(29), ser-NH(27), ala-Me(20),cys-N-Me(10)
ser-α CH	ser-β_1CH(24), ser-β_2CH(20), cys-N-Me(13), ala-NH(11), ser-NH(10)
ser-β_1CH	ser-β_2CH(100), ser-α CH(62), ala-NH(23), ser-NH(18), cys-N-Me(9), val-N-Me(5)

Data recorded in $CDCl_3$/Voltalef 10S (~1:1) at -10°C (400MHz)

A large increase in spin-diffusion was evident from the fact that several cumulative nOe's from individual protons exceeded 100%, the theoretical maximum nOe from any single nucleus. The previously proposed model was supported by an overall pattern of nOe's which was very similar to that in the same solvent system at 30°C, although the magnitude of the observed effects was greater. The effects between cys-α-CH and the val-α-CH were greatly increased and were the largest nOe's observed between non-geminally coupled protons. The difference spectrum after irradiation of the n-val-β-CH proton (figure 6.26) shows similarly large increases in the nOe's to the n-val-N-Me and to the n-val-γ-methyls, confirming their assignment. The lack of any significant nOe to the n-val-α-CH proton

FIGURE 6·26 n-val-β-CH nOe difference spectrum, −10°C, 400MHz

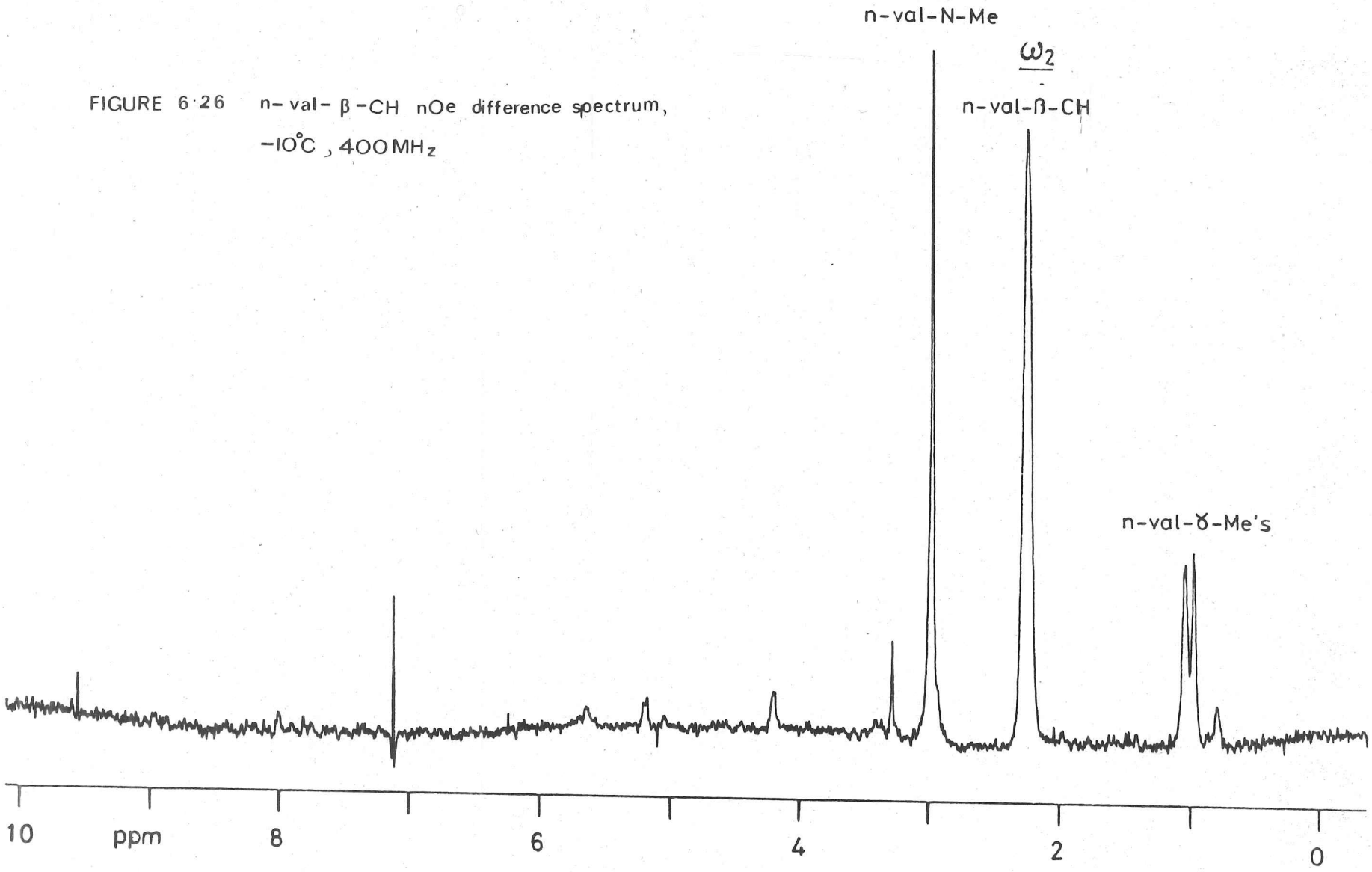

indicates that the n-val- β-CH is effectively masked from it by the n-val-N-Me and the n-val- γ-Methyl groups. No new nOe's were observed that were of diagnostic significance.

The triostin-p nOe's, previously recorded in the presence of triostin-n, were ratified by recording spectra in dmso-d_6 solution (table 6.13).

Table 6.13 Triostin-p nOe's (negative unless otherwise stated)

Resonance Irradiated	nOe (%)
cys- α CH	val-N-Me(21), cys- β_2CH(5), cys- β_1CH(4), cys-N-Me(1)
cys- β_2CH	cys- β_1CH(30), cys- α CH(8), cys-N-Me(8), ala-Me(8), val- γ Me's(12)
cys-N-Me	ala-CH/ser- β_2CH(12), val- γ Me's(10), ala-Me(8), cys- β_2CH(4), cys- α CH(1)
val- α CH	val- γ Me's(5), ser- α CH(5), val- β CH(2), ala-NH(2), ala-Me(2)
val- β CH	val- γ Me's(1)
val- γ Me's	val- α CH(2), cys-N-Me(2)
val-N-Me	cys- α CH(20), val- γ Me's(8), ala-Me(6), val- β CH(6), ser-NH(2)
ala-Me	ala-CH(10), ala-NH(8), cys-N-Me(6), val- γ Me's(2)
ala-NH	ala-Me(5), val- γ Me's(3), ala-CH(1), ser-NH(1), cys-N-Me(1)
ala-CH/ser- β_2CH	ser- β_1CH(15), cys-N-Me(8), ser- α CH(7), ala-Me(2), ala-NH(1)
ser- β_1CH	ser- β_2CH/ala-CH(28), val- γ Me's(11), ser- α CH(10), cys-N-Me(5), ala-Me(3)
ser- α CH	ser-NH(3), ser- β_1CH(3), val- α CH(3), ser- β_2CH/ala-CH(3)
ser-NH	val- γ Me's(20), ser- β_2CH/ala-CH(6), ala-Me(13), ala-NH(6), ser- α CH(5), Q-H_3(+4), cys-N-Me(3), ser- β_1CH(1)

Data recorded in dmso-d_6 at 19°C (400MHz)

The spectrum of triostin-p was assigned by double irradiation techniques and with reference to the assignments previously made in

deuteriochloroform (figure 6.27). The difference spectrum obtained after double irradiation of the cys-β_2-CH proton (figure 6.28) identified the cys-β_1-CH proton in a position 0.67ppm highfield of its position in deuteriochloroform. Similarly, the ala-NH shifts 1.09ppm downfield in dmso-d_6 solution. Both of these effects are obviously due to the effects of solvation and may be due solely to hydrogen bonding of solvent to the ala-NH, which apart from deshielding the amide proton could also shield the cys-β_1-CH. The assignment of triostin in various solvents is presented in table 6.14.

Again the overall pattern of the nOe's of triostin-p in dmso-d_6 closely resembled that observed in deuteriochloroform solution. Spin diffusion was evident from the apparent nOe's between distant protons, for example between the cys-N-Me and the ser-NH. An enhancement between the cys-α-CH and the cys-methylene protons, not previously observed, indicates that these protons are proximal. In addition the nOe's between the cys-β_2-CH and the cys-N-Me, and the absence of any other effects involving the cys-methylene protons would indicate a cross-bridge orientation as in (6.5).

FIGURE 6 27 Triostin-p, dmso-d_6, 19°C, 400 MHz

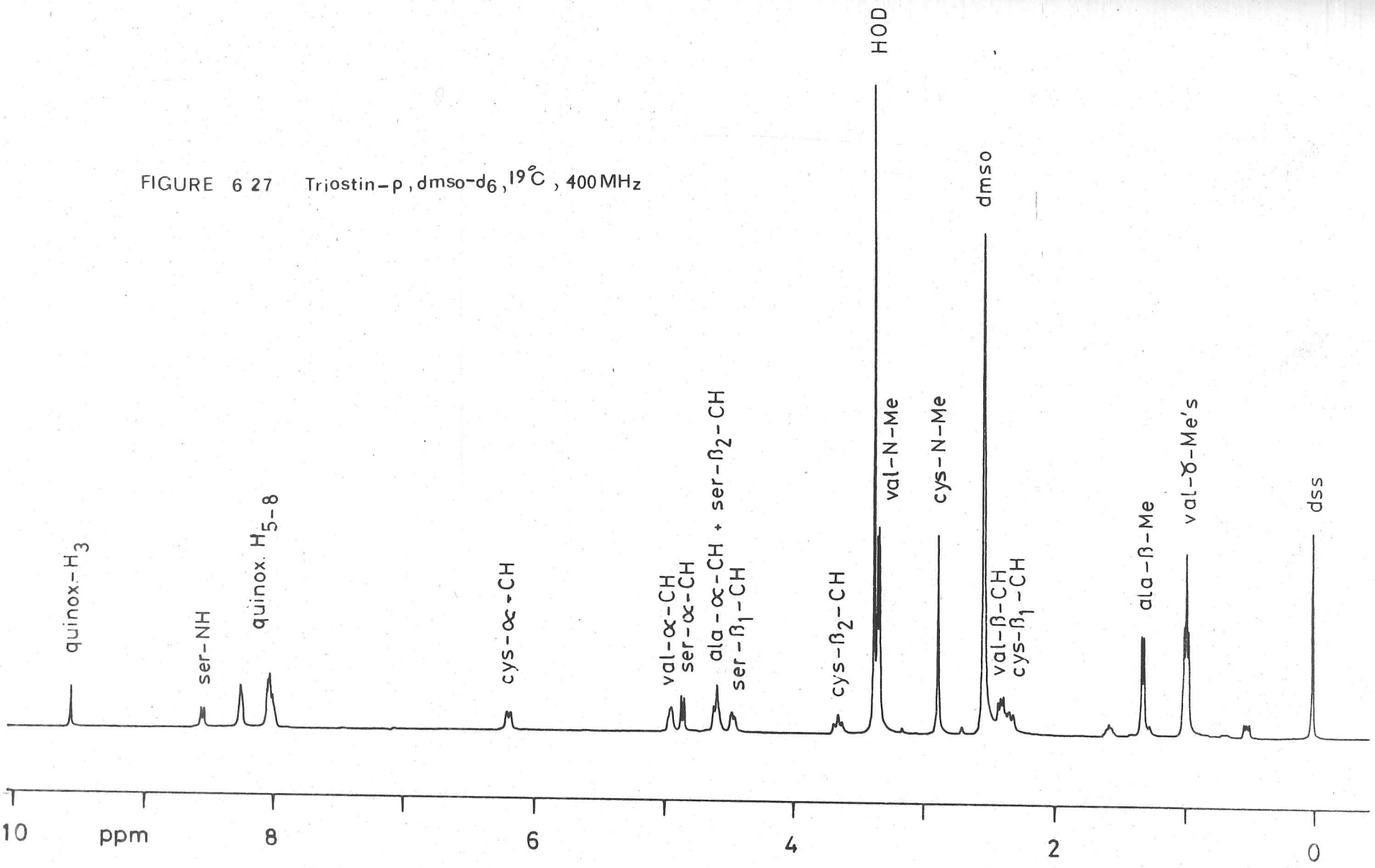

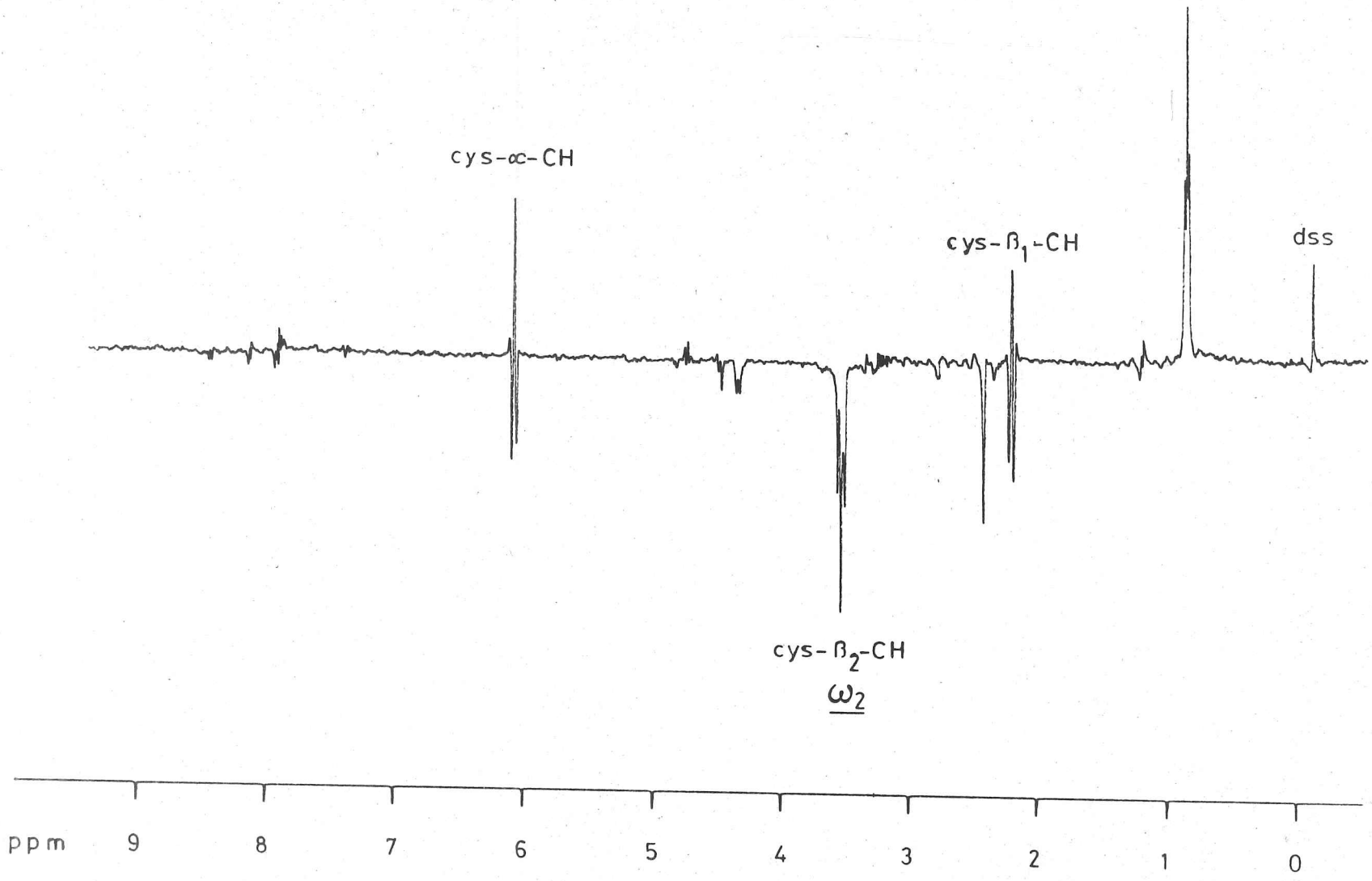

FIGURE 6·28 p-cys-β_2-CH decoupling difference spectrum, 19°C, 400 MHz

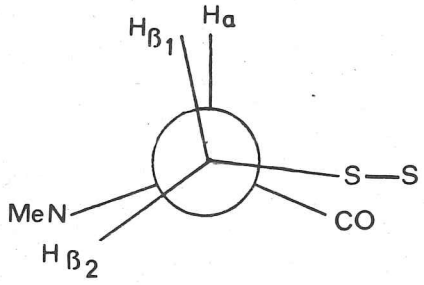

(6·5)

Table 6.14 Triostin A ^1H Chemical Shift (δ ppm) Correlations

Resonance	Conformer	$CDCl_3$	dmso-d_6	$CDCl_3$/Voltalef 10s
cys-α-CH	n	5.66		5.64
cys-α-CH	p	6.76	6.19	
cys-β_1-CH	n	3.26		3.27
cys-β_1-CH	p	2.99	2.32	
cys-β_2-CH	n	3.35		3.39
cys-β_2-CH	p	3.23	3.64	
cys-N-Me	n	3.25		3.27
cys-N-Me	p	2.92	2.88	
val-α-CH	n	4.20		4.19
val-α-CH	p	5.16	4.86	
val-β-CH	n	2.28		2.24
val-β-CH	p	2.27	2.39	
val-γ_1-Me	n	0.97		0.96
val-γ_1-Me	p	0.80	0.97	
val-γ_2-Me	n	1.06		1.04
val-γ_2-Me	p	1.02	0.99	
val-N-Me	n	2.97		2.97
val-N-Me	p	3.02	3.29	
ala-CH	n	4.97		4.97
ala-CH	p	4.71	4.59	
ala-Me	n	0.61		0.62
ala-Me	p	1.39	1.31	
ala-NH	n	8.32		8.38
ala-NH	p	7.15	8.24	
ser-α-CH	n	5.00		5.03
ser-α-CH	p	4.88	4.95	
ser-β_1-CH	n	4.52		4.54
ser-β_1-CH	p	4.42	4.45	
ser-β_2-CH	n	4.65		4.64
ser-β_2-CH	p	4.54	4.59	
ser-NH	n	8.91		8.98
ser-NH	p	8.79	8.54	
Quinox.-H_3	n	9.53		9.56
Quinox.-H_3	p	9.60	9.56	

The $CDCl_3$ data was recorded at 30°C,
the dmso-d_6 data at 19°C and the
$CDCl_3$/Voltalef 10S (~1:1) solution data at -10°C (400MHz).

7. CONCLUSIONS

The studies described in this dissertation have been conveniently divided into three sections according to antibiotic. It is pertinent to retain this distinction in this summary.

7.1 VANCOMYCIN

The binding of Ac-D-ala-D-ala to vancomycin has been studied in detail. The antibiotic undergoes a considerable conformational change around the right-hand (N-methylleucine, etc.) part of the molecule. Protons a_3-a_5-a_4 and the protonated N-methylleucine amino group form a carboxylate binding pocket which is very similar to that previously proposed for ristocetin A with the same dipeptide. The main achievement which enabled this detailed study to be performed was the attainment of slow exchange conditions by the use of mixed solvent systems in the nmr studies.

A simple procedure was developed for the preparation of the tripeptide Ac_2-L-lys-D-ala-D-ala involving reaction of the commercially available di-CBZ-L-lysine (activated as the succinimide ester) with the benzyl ester of the commercially available dipeptide D-alanyl-D-alanine. Hydrogenation and acetylation produced the required peptide. This peptide was then used for preliminary binding studies with vancomycin. The 400MHz spectrum of the complex was partially assigned and the protons a_1, s_6 and b identified as the only resonances which were significantly shifted ($\geq$0.1ppm) by the presence of the third peptide residue. The few nOe's involving bound lysyl protons indicated that the sidechain was oriented towards the triaryl unit of vancomycin. The large deshielding of a_1 can reasonably be accounted for by a hydrogen bond between the lysαNH and the vancomycin carboxylate, although the NH proton was not significantly

deshielded.

One interesting observation derived from the mode of action studies was the fact that nOe's involving protons d and i of vancomycin with protons on the front face of the molecule and more importantly between d and ala_1Me_b were contrary to the accepted structure of vancomycin. Rotation by 180^o of ring 3 of vancomycin must be involved and this would also account for the large, but previously unexplained, nOe between a and y.

7.2 RISTOCETIN A

Extensive crystallisation experiments were initiated with the aim of obtaining a confirmatory (or otherwise) x-ray analysis for the previous chemical and nmr studies of ristocetin A. Several systems were successful in producing crystalline residues but one in particular, water/75%acetone, was superior with regard to crystal quality. In addition the water/75% acetone system is the first method for the routine preparation of ristocetin A crystals. Unfortunately the crystals proved unstable under x-ray bombardment but hopefully the ristocetin A purified by this method will be more amenable to crystallisation with other systems (possibly one of those already tried [1] with commercial grade ristocetin A) which may produce a stable crystalline form. The first crystals of ristocetin A complexed to Ac-D-ala-D-ala were also obtained from the water/75% acetone system although in this case it was the enormous size of the unit cell ($\sim$140,000$\mathring{A}^3$) which prevented a crystal structure being obtained. Crystals of ristocetin A complexed to Ac_2L-lys-D-ala-D-ala were also obtained but these were unstable upon storage and were not analysed further. Attempted crystallisations of the ristocetin A Ψ-aglycone derivative were completely without success.

---

[1] See table 8.3

7.3 TRIOSTIN A

The two conformers of triostin A have been studied using ^{1}nmr. The previously proposed conformation of triostin-p (favoured in polar solvents) has been confirmed but the conformation of triostin-n (favoured in non-polar solvents) is shown to be considerably different to that of triostin-p or the previous proposal for triostin-n.

Triostin-p may be considered to be a flat disc, with the peptide backbone around the edge, cross-bridged by a disulphide bond. The two quinoxaline ring systems are on the same side , termed the upper face, along with the val-N-Me and ala-CO. The remaining cys-N-Me, cys-CO and ser-CO are on the lower face. The val-CO, involved in an ester linkage to the seryl residue is assumed to be in a trans orientation in the plane of the disc. The cross-bridge retains a large amount of flexibility and cannot be described by any one conformer.

The largest nOe's observed in triostin-n between non-geminally coupled nuclei involved the val-αCH and cys-αCH protons. In order to reconcile this and other observed effects with the conformation in solution of triostin-n a globular structure is proposed. With the aid of a CPK model it can be appreciated that the close approach of the two protons noted above can readily be accomplished by conversion of the val-cys amide bond from a trans to a cis configuration. In addition, the alanyl residues on opposite sides of the disc are proximal and hydrogen bonding between them is postulated.

Since the addition of 25% dmso to triostin in chloroform solution results in the complete conversion of triostin-n to triostin-p the conformation of the former is unimportant with respect to its antibiotic action and the intercalation with DNA, both of which only occur in aqueous solution. However, the conformation of triostin-n does provide evidence of the flexibility of the molecule in solution.

7.4 NMR SPECTROSCOPY

As a consequence of the antibiotic studies nmr methods were developed in order to modify chemical exchange phenomema and to manipulate the nOe. The attainment of slow exchange conditions for vancomycin/Ac-D-ala-D-ala was accomplished by the use of mixed solvent systems. This reduced the temperature at which experiments could be performed, and in addition increased the lipophilic nature of the solvent thereby decreasing solvent exchange with the sample molecules. The nOe was effectively manipulated (towards the negative regime) by the use of the viscous oil Voltalef 10S. Considerably enhanced effects were observed (2% positive nOe's were converted to up to 73% negative nOe's) and in addition the chemical equilibrium between the two conformers of triostin-A was affected by the increased viscosity and the increased lipophilic nature of the solvent. The techniques developed would also have application in similar studies of other antibiotics and could potentially yield structural information relating to the solution situation in an analogous manner to that provided in the solid state by the widely used x-ray crystallography methods.

8. EXPERIMENTAL

Samples of ristocetin A were kindly supplied by Lundbeck Company, Copenhagen, Denmark. Commercial samples of vancomycin hydrochloride (Eli Lilley Inc. USA) were purchased and used without further purification. Samples of triostin A were kindly supplied by Mr A.Cornish and Dr M.J.Waring, Department of Pharmacology, University of Cambridge Medical School, Cambridge. The oil Voltalef 10S was a kind gift from Pechiney Ugine Kuhlmann, Paris, France. The following compounds were purchased, D-alanine (BDH), L-lysine hydrochloride (BDH), D-alanyl-D-alanine (Bachem Inc. USA, and Uniscience of Cambridge), di-carbobenzoxy-L-lysine (Sigma Chemicals Ltd.), t-butyl-oxycarbonyloxyimino-2-phenylacetonitrile (Aldrich Ltd.), Sephadex G-25 (Pharmacia Fine Chemicals). All other compounds used were readily available standard laboratory reagents (generally of 'Analar' grade) which were used without purification, unless otherwise stated. Most solvents were dried and redistilled before use.

Analytical TLC was performed on Merck plates coated with silica GF_{254}, the results being visualised with a UV lamp (where applicable). The abbreviation BWA refers to the n-butanol/water/acetic acid (3:1:1) elution system which was used extensively. Various methods of visualisation were tested for use with the synthetic peptide studies including a simple iodine jar (a few crystals of iodine were placed in the bottom of a jar which was sealed after inclusion of the exposed plate) and the chlorine/starch/iodide method (the exposed plate was sprayed with chlorine gas and the reaction carried out for 40 minutes in a sealed bottle, the plate was then sprayed with starch (2%)/potassium iodide (2%) solution). Difficulties with visualisation were encountered with both of these methods and the standard protein stain, ninhydrin, was therefore employed[77]. The exposed plate was sprayed with concentrated hydrochloric acid (to hydrolyse the amide bonds) and left for 15 minutes, it was then covered with another glass plate (to prevent rapid evaporation of solvent) and heated at 100°C for 30 minutes, after which the glass cover was removed and heating was continued for a further 10 minutes. Visualisation was

effected by spraying the plate with ninhydrin (0.5% in n-butanol) and heating to 100°C, orange/brown spots developed by reaction with primary amino groups.

8.1 PREPARATIONS

8.1.1 AC-D-ALA-D-ALA

D-ala-D-ala (285mg) was dissolved in minimal water (2.5ml), distilled acetic anhydride (2ml) was added to this solution. Although immiscible at first a clear solution slowly formed with stirring for 30 minutes. Rotary-evaporation at 50°C was used to remove solvent and produce an oil which was redissolved in distilled water and freeze-dried. A gummy solid was formed with the distinctive smell of acetic acid, this impurity was confirmed by nmr. Removal of acetic acid was performed using rotary-evaporation at 70°C for 1 hour, redissolution of the residue in water and freeze-drying produced a white fluffy powder which had no visible impurities by nmr.

Yield: 350mg (98%)

^{1}H nmr (100MHz, dmso-d_6, 90°C) δ1.22 (d, ^{3}J7.3Hz, 3H, ala_2Me), 1.27 (d, ^{3}J7.5Hz, 3H, ala_1Me), 1.85 (s, 3H, acetyl-Me), 4.20 (m, ^{3}J7.3Hz, 1H, ala_1CH), 4.33 (m, ^{3}J7.3Hz, 1H, ala_2CH), 8.05 (d, ^{3}J7.3Hz, 1H, ala_2NH), 8.18 (d, ^{3}J7.3Hz, 1H, ala_1NH). The 400MHz spectrum is shown in figure 8.1.

8.1.2 N-HYDROXYSUCCINIMIDE

Succinic anhydride (100g) and hydroxylamine hydrochloride (70g) were slowly heated on an oil-bath, using a rotary-evaporator in order that volatile products could be conveniently trapped in liquid nitrogen. When the initial evolution of gases had ceased the temperature was raised to 125°C where fusion occurred with further evolution of gases. The temperature was slowly raised to 160°C where, upon cessation of the

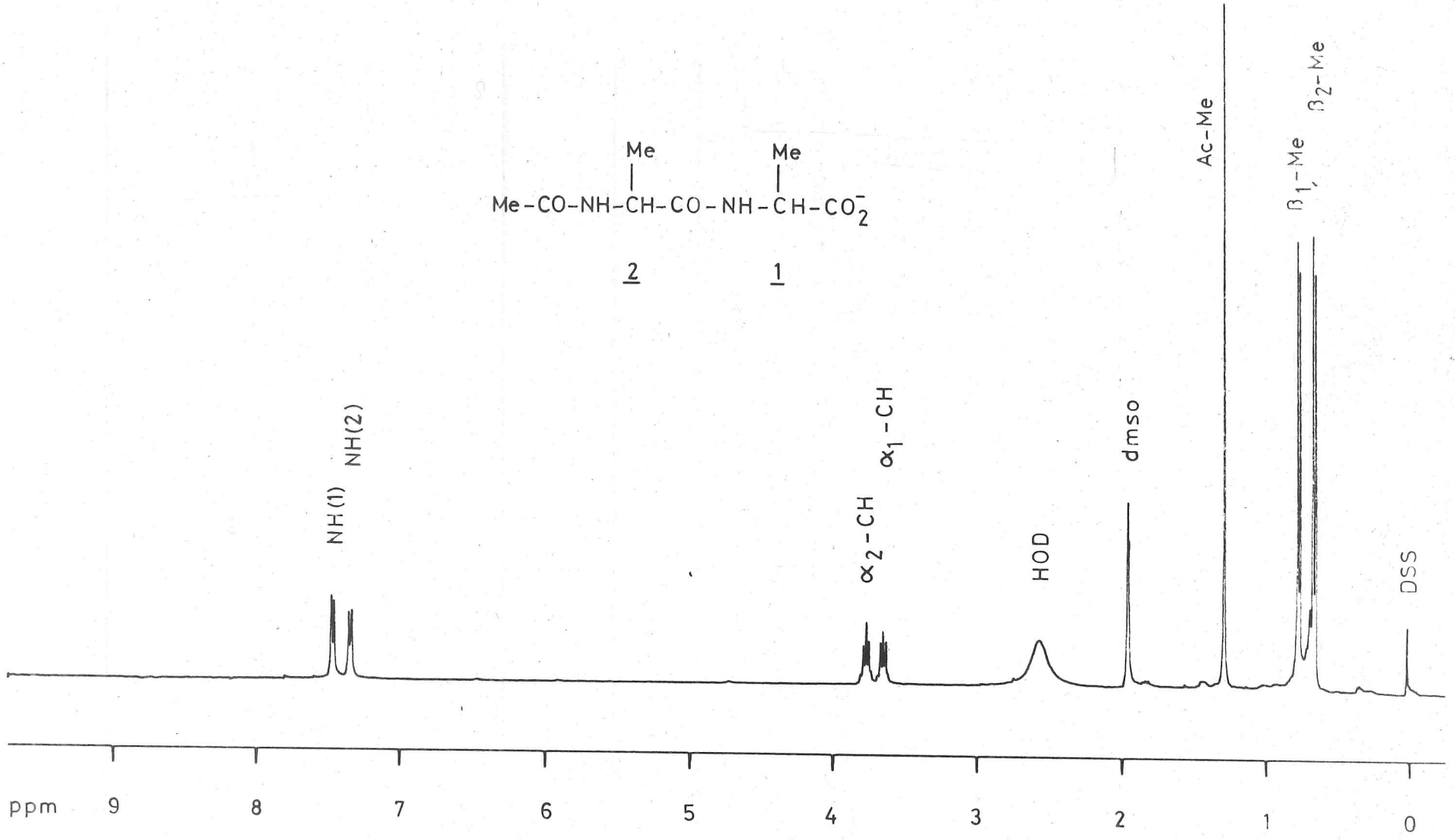

FIGURE 8·1 Ac–D–ala–D–ala dmso-d_6 / 30% CCl_4 , 12°C , 400 MHz

evolution of water, heating was discontinued. At 125°C the amber liquid was poured into diethyl ether (400ml) which was vigorously stirred. The solid residue which formed was heated to boiling with n-butanol (400ml) after decantation of the diethyl ether. Filtration and chilling of the filtrate caused the slow crystallisation of N-hydroxysuccinimide which was washed with n-butanol and diethyl ether. Recrystallisation from boiling ethyl acetate gave a white solid.

Yield: 0.24g (20%) Melting Point:98° ± 1°C

^{1}H nmr (dmso-d_6, 100MHz, 30°C) δ 2.62 (s, 4H, 2xCH_2); compare with succinic anhydride under the same conditions, δ 2.95 (s, 4H, 2xCH_2).

8.1.3 t-BUTYLOXYCARBONYL-D-ALANINE

This single-pot reaction of D-alanine (0.89g), t-butyloxycarbonyloxyimino-2-phenylacetonitrile (t-BOC-ON, 2.71g), triethylamine (2.10ml), water (6ml) and 1,4-dioxane (6ml), involved warming to 40°C and stirring for 3 hours. The t-BOC-D-alanine was isolated from the oxime by-product by diluting with water (15ml) followed by addition of ethyl acetate (20ml). The yellow aqueous layer, containing the protected amino acid, was separated and washed with further portions of ethyl acetate to produce a colourless liquid. Acidification to pH1 with dilute hydrochloric acid (3M) was followed by extraction into ethyl acetate. The volume of the ethyl acetate solution was reduced by rotary-evaporation before crystallisation was effected by the addition of n-hexane. Recrystallisation was also performed using ethyl acetate/n-hexane.

Yield: 0.83g (50%) Melting Point: 82° ± 0.5°C

^{1}H nmr (100MHz, dmso-d_6, 30°C) δ 1.23 (d, ^{3}J7.2Hz, 3H, alaMe), 1.40 (s, 9H, t-butyl), 3.83 (m, ^{3}J7.1Hz, 1H, alaCH), 7.80 (broad, 1H, alaNH).

8.1.4 D-ALANINE BENZYL ESTER - 1

Polyphosphoric acid (5g), prepared by dissolving phosphorous pentoxide (3.6g) in orthophosphoric acid (2ml), was stirred and warmed along with benzyl alcohol (25ml) until a homogeneous solution resulted. D-

alanine (1.1g) was added and the solution heated to 90°C, stirring was continued for 4 hours. The solution was acidified by pouring into water (200ml) containing concentrated hydrochloric acid (10ml). The aqueous phase of the amino acid benzyl ester hydrochloride was extracted with diethyl ether and the latter washed with dilute hydrochloric acid (2%). The aqueous extracts were combined and sodium hydrogen carbonate added to adjust to pH10. The free base was extracted into diethyl ether (3x100ml) and dried over anhydrous magnesium sulphate. Saturation of the ethereal solution with dry hydrogen chloride gas precipitated D-ala benzyl ester hydrochloride as a clear oil. Residual solvents were removed by rotary-evaporation. Purification by crystallisation was unsuccessful from methanol/diethyl ether or ethanol/n-hexane or ethanol/ethyl acetate. The nmr spectrum of the oil showed minor splitting (2Hz) of the alanine methyl doublet, probably due to racemization, which would explain the difficulties encountered in purification.

Yield: 2.14g (98%) oil.

8.1.5 D-ALANINE BENZYL ESTER p-TOLUENE SULPHONIC ACID SALT

This is essentially a one-pot reaction where D-alanine (0.56g), p-toluene sulphonic acid (1.21g), benzyl alcohol (2.5ml) and benzene (25ml) are refluxed overnight (15 hours). The use of a Dean-Stark tube proved efficient in removing the water of esterification as the azeotrope with benzene. The reaction mixture was cooled and dry diethyl ether (50ml) was added to induce crystallisation by reducing the product solubility; chilling in ice was found to be helpful in this respect. Recrystallisation was readily achieved from methanol/diethyl ether.

Yield: 1.93g (88%) Melting Point: $108^{\circ} \pm 0.5^{\circ}C$

^{1}H nmr (100MHz, dmso-d_6, 40°C) δ 1.44 (d, ^{3}J7.1Hz, 3H, alaMe), 2.31 (s, 3H, tosylMe), 4.20 (q, ^{3}J7.0Hz, 1H, alaCH), 5.27 (s, 2H, benzylCH_2), 7.12 (d, ^{3}J8.0Hz, 2H, tosyl), 7.42 (m, 5H, benzyl), 7.51 (d, ^{3}J8.2Hz, 2H, tosyl), 8.33 (broad, 1H, alaNH).

8.1.6 D-ALANINE BENZYL ESTER - 2

D-alanine benzyl ester p-toluene sulphonic acid salt (2.5g) was dissolved in chloroform (15ml), triethylamine (0.75ml) was then added to liberate the D-ala benzyl ester free base. The reaction proceeded for 30 minutes and then diethyl ether was added to precipitate the triethylamine/tosylate salt. The clear solution, obtained after filtration, was rotary-evaporated to dryness. The resulting gel started to crystallise and was aided by the addition of petroleum ether (boiling range 40°-60°C).

Yield: 0.52g (41%) Melting Point: 97° ±10°C

The ^{1}H nmr spectrum showed the crystalline product to be a mixture of the free base and the tosyl salt of D-ala benzyl ester in an approximate ratio of 1:2.

An alternative approach proved more successful. D-alanine benzyl ester p-toluene sulphonic acid salt (30mg) was dissolved in water (0.5ml) and sodium hydrogen carbonate added until pH9 was attained. The free base was extracted into diethyl ether and dried over magnesium sulphate. Removal of the solvents by rotary-evaporation produced an oil which crystallised upon the addition of petroleum ether (boiling range 40°-60°C).

Yield: 14mg

^{1}H nmr (100MHz, dmso-d_6, 30°C) δ 1.21 (d, ^{3}J7.0Hz, 3H, alaMe), 3.49 (q, ^{3}J7.0Hz, 1H, alaCH), 5.13 (s, 2H, benzylCH_2), 7.38 (m, 5H, benzyl).

8.1.7 D-ALANYL-D-ALANINE BENZYL ESTER - 1

Polyphosphoric acid (5g) [1] , was warmed with benzyl alcohol (2.5ml) until a homogeneous solution resulted. D-alanyl-D-alanine (0.2g) was added and the solution heated to 90°C, stirring was continued for 4 hours. The solution was further acidified by pouring into water (20ml)

---

[1] Preparation described above

containing concentrated hydrochloric acid (1ml). The aqueous phase, containing the hydrochloride of the amino acid benzyl ester, was extracted with diethyl ether and the latter washed with dilute hydrochloric acid (2%). The aqueous extracts were combined and sodium hydrogen carbonate added to pH10. The free base was extracted into diethyl ether (3x10ml) and dried over anhydrous magnesium sulphate. Saturation of the ethereal solution with dry hydrogen chloride gas produced a thick white oily precipitate. Solvents were removed by rotary-evaporation to yield a clear oil which was immiscible with water (and hence unlikely to be the expected hydrochloride salt). Attempted crystallisation from methanol/diethyl ether proved unsuccessful. It appeared from the nmr data that the spectrum of benzyl alcohol [2] was superimposed upon that of D-alanyl-D-alanine [3]

8.1.8 D-ALANYL-D-ALANINE BENZYL ESTER p-TOLUENE SULPHONIC ACID SALT

D-ala-D-ala benzyl ester p-toluene sulphonic acid salt was prepared in a similar manner to that successfully used for the single amino acid D-alanine. The dipeptide D-alanyl-D-alanine (0.4g), p-toluene sulphonic acid (0.49g), benzyl alcohol (1.5ml) and benzene (25ml) were refluxed for 16 hours with stirring. A Dean-Stark tube was used for the removal of the water of esterification as the azeotrope with benzene. The addition of diethyl ether to the cool reaction mixture and further chilling in an ice bath produced a white crystalline product which was recrystallised from methanol/diethyl ether.

Yield: 0.96g (91%) Melting Point: $162^{\circ} \pm 1^{\circ}C$

^{1}H nmr (100MHz, dmso-d_6, $40^{\circ}C$) δ1.34 (d, ^{3}J7.0Hz, 3H, ala_2Me), 1.37 (d, ^{3}J7.4Hz, 3H, ala_1Me), 2.31 (s, 3H, tosylMe), 4.40 (m, ^{3}J7.2Hz, 1H, ala_1CH), 4.48 (m, ^{3}J7.2Hz, 1H, ala_2CH), 5.16 (s, 2H, benzylCH_2), 7.13 (d, ^{3}J7.7Hz, 2H, tosyl), 7.38 (m, 5H, benzyl) 7.51 (d, ^{3}J8.3Hz, 2H, tosyl), 8.08 (

---

[2] ^{1}H nmr (100MHz, $CDCl_3$, $30^{\circ}C$) δ4.60 (s, 2H, benzylCH_2), 7.35 (m, 5H, benzyl).

[3] ^{1}H nmr (100MHz, $CDCl_3$, $30^{\circ}C$) δ1.18 (d, ^{3}J7.1Hz, 3H, ala_2Me), 1.25 (d, ^{3}J7.0Hz, 3H, ala_1Me), 3.41 (m, ^{3}J7.0Hz, 1H, ala_1CH), 3.55 (m, J7.0Hz, 1H, ala_2CH), 4.60 (s, 2H, benzylCH_2), 7.32 (m, 5H, benzyl).

broad, 2H, ala_2NH), 8.78 (d, ^3J7.0Hz, 1H, ala_1NH)

TLC in 10% methanol in chloroform eluant produced a single spot, R_F0.20.

8.1.9 D-ALANYL-D-ALANINE BENZYL ESTER - 2

A solution of D-ala-D-ala benzyl ester p-toluene sulphonic acid salt (100mg) in water (0.5ml) was adjusted to pH9 by the addition of sodium hydrogen carbonate. After 45 minutes the dipeptide free base was extracted into diethyl ether and dried over anhydrous magnesium sulphate. Removal of the solvent produced an oil which was identified by its ^1H nmr spectrum to be essentially starting material.

8.1.10 L-ALANINE BENZYL ESTER HYDROCHLORIDE

The conversion of L-alanine benzyl ester p-toluene sulphonic acid salt (3.5g) into the hydrochloride was effected by dissolving the former in chloroform (15ml) at 0^o-5^oC, triethylamine (1g) was then slowly added with stirring. The absence of water at this stage was found to be imperative for successful reaction and was readily checked using nmr. The reaction was allowed to proceed for 1 hour and then dry diethyl ether (50ml) was added to precipitate the ammonium tosylate by-product which was subsequently filtered off. Dry hydrogen chloride gas was bubbled through the solution to cause precipitation of L-ala benzyl ester hydrochloride which was filtered and washed with dry diethyl ether. Recrystallisation from methanol/diethyl ether proved unsuccessful.

Yield: 1.27g (59%)

^1H nmr (100MHz, dmso-d_6, 30^oC) δ 1.46 (d, ^3J7.1Hz, 3H, alaMe), 4.18 (m, ^3J7.2Hz, 1H, alaCH), 5.26 (s, 2H, benzylCH_2), 7.42 (m, 5H, benzyl), 8.59 (broad, 1H, alaNH).

8.1.11 N,N'-DI-ACETYL-L-LYSINE

L-lysine hydrochloride (0.88g) was dissolved in water (5ml) and acetic anhydride (5ml) was added. Reaction proceeded for 1 hour then rotary-evaporation was used to remove the solvents, leaving an oil. ^1H nmr

analysis of this oil identified L-lysine starting material and acetic acid.

The most obvious reason for reaction failure was the possible protonation of the primary amino groups when present as the hydrochloride salt. Therefore L-lysine hydrochloride (1g) was dissolved in water (2ml) and potassium carbonate added to adjust to pH10 (from pH7). Acetic anhydride (3ml) was added and reaction allowed to proceed for 6 hours, dilute hydrochloric acid (3M) was then added to adjust to pH1. Extraction into diethyl ether or chloroform proved unsuccessful, as did crystallisation from methanol/diethyl ether.

Yield: 1.09g oil

^1H nmr showed secondary splitting (2Hz) of the lys-CH proton indicating that racemization had probably occurred about this centre.

TLC in BWA eluant gave three spots, R_F 0.7, 0.3 and 0.0, presumably from the diacetyl, monoacetyl and unprotected lysine respectively.

8.1.12 DI-t-BOC-L-LYSINE

L-lysine hydrochloride (0.73g), t-butyl-oxycarbonyloxyimino-2-phenylacetonitrile (2.71g), triethylamine (1.05ml), 1,4-dioxane (3ml) and water (3ml) were mixed together, a further amount of 1,4-dioxane (6ml) was necessary in order to dissolve the components. The solution changed colour from yellow to brown after stirring for 20 minutes of the 3 hours at 40°C. The di-t-BOC-L-lysine was isolated from the oxime by-product by diluting with water (6ml) followed by the addition of ethyl acetate (8ml). The aqueous layer, containing the protected amino acid, was separated and washed with further portions of ethyl acetate. Acidification to pH1 with dilute hydrochloric acid (3M) was followed by extraction into ethyl acetate. The volume of ethyl acetate was reduced by rotary-evaporation. Crystallisation, by the addition of n-hexane, was unsuccessful.

Yield: 0.55g (36%)

Analytical TLC, eluting with 10% methanol in chloroform, gave a single spot, R_F0.80. However, in BWA three spots were obtained, R_F0.80, 0.40 and 0.00, presumably due to di-protected, mono-protected and un-protected L-lysine. The estimated conversion was 50% to the di-protected L-lysine. The nmr spectrum showed many impurities, further purification was therefore necessary.

The dicyclohexylcarbodiimide (DCC) derivative of di-t-BOC-L-lysine was thought likely to give a crystalline product. However upon reaction of the crude di-t-BOC-L-lysine oil, dissolved in diethyl ether, with a slight excess of ethereal DCC, only unchanged crystalline DCC was recovered. Purification of this derivative was not pursued further; the purchase of N,N′-di-CBZ-L-lysine was considered more pertinent to the ultimate synthetic goal.

8.1.13 DI-t-BOC-L-LYSINE SUCCINIMIDE ESTER

A crude preparation of di-t-BOC-L-lysine (0.5g) was dissolved in ice-cold 1,2-dimethoxyethane (10ml). N-hydroxysuccinimide (0.17g) was then added followed by dicyclohexylcarbodiimide (0.31g). The solution was stored at 3°C for 42 hours during which time the urea by-product precipitated from solution. Filtration and rotary-evaporation at 50°C of the filtrate produced an oil.

Yield: 0.46g (73%)

Analytical TLC in BWA eluant gave four spots, R_F0.92, 0.68, 0.48 and 0.00; in 10% methanol in chloroform five spots were obtained, R_F0.73, 0.61, 0.36, 0.15 and 0.00.

^{1}H nmr showed the major component of the oil to be the crude di-t-BOC-L-lysine starting material.

8.1.14 N,N′-DI-CBZ-L-LYSINE SUCCINIMIDE ESTER

N-hydroxysuccinimide (0.57g) was added to a solution of N,N′-di-CBZ-L-lysine (2.0g) in 1,2-dimethoxyethane (5ml), which in turn was chilled and added to a dispersion of dicyclohexylcarbodiimide (1.30g) in 1,2-

dimethoxyethane (15ml) and chloroform (4ml) - this solvent system was found to be preferable to 1,4-dioxane. The urea by-product precipitated within minutes and was filtered off to give a clear filtrate. Rotary-evaporation to remove the solvents produced an oil which crystallised from methanol/diethyl ether. Vacuum filtration and drying over phosphorous pentoxide/sodium hydroxide gave a white crystalline product.

Yield: 1.88g (76%) Melting Point: $113^{o} \pm 0.5^{o}C$

^{1}H nmr (100MHz, dmso-d_6, $30^{o}C$) δ1.44 (broad, 4H, lysCH_2), 1.80 (broad, 2H, lysCH_2), 2.83 (s, 4H, succinimide), 3.01 (q, ^{3}J5.8Hz, 2H, lysCH_2), 4.43 (q, ^{3}J6.8Hz, 1H, lysCH), 5.03 (s, 2H, benzylCH_2), 5.09 (s, 2H, benzylCH_2), 7.23 (t, 1H, lysNH), 7.36 (m, 5H, benzyl), 7.37 (m, 5H, benzyl), 8.05 (d, ^{3}J7.2Hz, 1H, lysNH).

The ^{1}H nmr spectral parameters of di-CBZ-L-lysine under the same conditions are given below for comparison.

^{1}H nmr δ1.25 (broad, 1H, lysCH_2), 1.36 (broad, 4H, lysCH_2), 1.64 (broad, 1H, lysCH_2), 2.97 (q, ^{3}J6.0Hz, 2H, lysCH_2), 3.75 (q, ^{3}J5.9Hz, 1H, lysCH), 5.02 (s, 4H, benzylCH_2), 7.24 (t, 1H, lysNH), 7.35 (m, 11H, benzyl+lysNH).

TLC using 10% methanol in chloroform produced a single spot with R_F0.77.

8.1.15 N,N'-DI-CBZ-L-LYS-D-ALA BENZYL ESTER

A solution of di-CBZ-L-lys succinimide ester (143mg) in 1,2-dimethoxyethane (1ml) was added to a dispersion of D-ala benzyl ester p-toluene sulphonic acid salt (50mg) in 1,2-dimethoxyethane (1ml). A precipitate formed immediately and was subsequently identified as the lysine starting material. A slightly modified experimental procedure was found to be successful. The D-ala benzyl ester p-toluene sulphonic acid salt (75mg) was dissolved in water (0.5ml) containing sodium hydrogen carbonate (84mg). This solution was then added to a solution containing di-CBZ-L-lys succinimide ester (214mg) dissolved in 1,2-dimethoxyethane (1.7ml). Combination of the two solutions resulted in immediate precipitation. The residue from filtration was dried over phosphorous pentoxide/sodium hydroxide to give a white solid.

Yield: 152mg (63%) Melting Point: $160^{\circ} \pm 2^{\circ}C$

^1H nmr (100MHz, CD_2Cl_2, $30^{\circ}C$) δ1.40 (d, ^3J7.0Hz, 3H, alaMe), 1.0-2.0 (broad, 6H, lysCH_2), 3.18 (q, ^3J6.0Hz, 2H, lysCH_2), 4.15 (q, ^3J6.0Hz, 1H, lysCH), 4.57 (m, ^3J7.0Hz, 1H, alaCH), 5.08 (s, 2H, benzylCH_2), 5.12 (s, 2H, benzylCH_2), 5.18 (s, 2H, benzylCH_2), 6.57 (d, 1H, alaNH), 7.35 (m, 10H, benzyl), 7.37 (m, 6H, benzyl+lysNH).

m/e 575 (M^+); calc. 575.

8.1.16 N,N′-DI-CBZ-L-LYS-D-ALA-D-ALA BENZYL ESTER

The dipeptide D-ala-D-ala benzyl ester p-toluene sulphonic acid salt (0.5g) was dissolved in water (2ml) and sodium hydrogen carbonate added to adjust to pH9. Immediate precipitation resulted upon the addition of a solution of di-CBZ-L-lys succinimide ester (0.61g) in 1,2-dimethoxyethane (5ml). Filtration and drying of the residue over phosphorous pentoxide/sodium hydroxide produced a light white powder.

Yield: 0.75g (98%) Melting Point: $159^{\circ} \pm 1^{\circ}C$

TLC using 10% methanol in chloroform as eluant produced a single spot, R_F0.79; using BWA a single spot was also obtained with R_F0.89.

^1H nmr (100MHz, dmso-d_6, $30^{\circ}C$) δ1.16 (d, ^3J8.0Hz, 3H, alaMe), 1.32 (d, ^3J8.0Hz, 3H, alaMe), 1.0-1.8 (broad, 6H, lysCH_2), 2.97 (q, ^3J6.0Hz, 2H, lysCH_2), 3.50 (broad, 1H, alaCH), 4.00 (q, ^3J7.0Hz, 1H, lysCH), 4.34 (m, ^3J7.0Hz, 1H, alaCH), 5.02 (s, 2H, benzylCH_2), 5.13 (s, 2H, benzylCH_2), 7.14 (d, 1H, alaNH), 7.36 (m, 10H, benzyl), 7.38 (m, 6H, benzyl+lysNH), 8.02 (d, ^3J8.0Hz, 1H, lysNH), 8.26 (d, ^3J7.0Hz, 1H, alaNH).

8.1.17 N,N′-AC_2-L-LYS-D-ALA-D-ALA

A solution of di-CBZ-L-lys-D-ala-D-ala benzyl ester (0.84g) was dissolved in concentrated aqueous acetic acid (80%, 100ml) and then hydrogenated for a minimum of 6 hours in the presence of palladium (10%) on charcoal (1.3g) catalyst. Filtration followed by rotary-evaporation at $60^{\circ}C$ produced a clear, partially crystalline oil (1.33g) which was then dissolved in water (1ml) and acetylated by reaction for 1 hour with acetic

anhydride (3ml). Rotary-evaporation at 70°C, until all traces of acetic acid had been removed, resulted in an oil. Several crystallisation systems were tried, including i-propanol/acetone, ethyl acetate/carbon tetrachloride, i-propanol/carbon tetrachloride, ethanol/petroleum ether (boiling range 40°-60°C) and ethanol/n-hexane. The last mentioned of these systems had been successfully employed for this purpose by Nieto and Perkins during their extensive binding studies on vancomycin and ristocetin, however in this laboratory it was found to be as unsuccessful as the others. The one system which could be used was ethanol/diethyl ether, the problem being that the precipitated product was found to be exceedingly soluble in ethanol, and unless excess ether was present during filtration resolvation occurred with concommitant loss of product. The white powder was dried over phosphorous pentoxide/sodium hydroxide.

Yield: 0.31g (64%)

TLC in BWA eluant produced a single spot, R_F0.16, in 10% methanol in chloroform a single spot with R_F0.08 was obtained. A further solvent system which proved particularly sensitive in this experiment was chloroform/t-amyl-alcohol/methanol/acetic acid in the ratio 40:30:30:3, producing a single spot with R_F0.25. On occasion trace impurities of mono-acetyl tripeptide were detected in which case it was found expedient to pass the preparation, dissolved in dilute acetic acid (6%), down an ion-exchange column (Amberlite IR-120, H^+ form, BDH Ltd.).

^1H nmr, figure 8.2(coupling constants from 100MHz, shifts from 400MHz, dmso-d_6, 30°C) δ 1.19 (dd, ^3J6.7 and 7.0Hz, 6H, alaMe's), 1.25 (m, 2H, lys γ CH_2), 1.36 (m, 2H, lys δ CH_2), 1.52 and 1.58 (m, 1H+1H, lys $\beta$$CH_2$), 1.79 (s, 3H, AcMe), 1.86 (s, 3H, AcMe) ,2.99 (q, ^3J6.3Hz, 2H, lys ε CH_2), 3.83 (m, ^3J7.0Hz, 1H, ala_1CH), 4.23 (m, 2H, lysCH + ala_2CH), 7.64 (d, ^3J7.0Hz, 1H, ala_2NH), 7.95 (t, ^3J6.2Hz, 1H, lys ε NH), 8.06 (d, ^3J7.5Hz, 1H, lys α NH), 8.17 (d, ^3J7.5Hz, 1H, ala_1NH).

Further characterisation was obtained from mass spectral evidence. The electron impact spectrum at 200°C of the permethylated tripeptide produced a m/e 442(M^+), 326(M^+-ala), 241(M^+-ala-ala), 178 m^*(326→241). The spectrum of the perdeuteriomethylated tripeptide produced a similar

FIGURE 8-2 Ac_2-L-lys-D-ala-D-ala, dmso-d_6, 30°C, 400 MHz

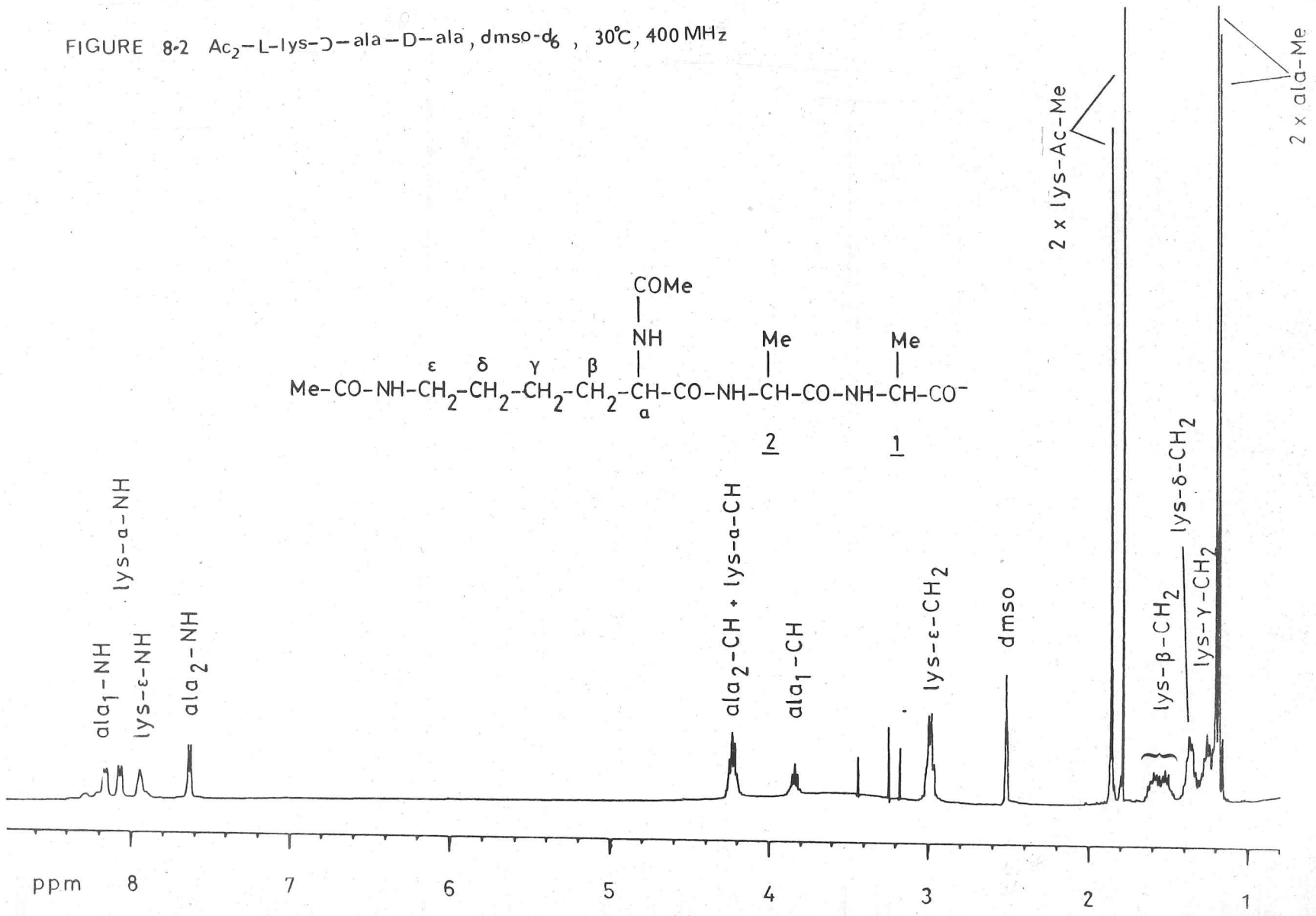

fragmentation pattern, m/e 457(M^+), 335(M^+-ala), 247(M^+-ala-ala).

8.1.18 RISTOCETIN IODIDE SALT

Ristocetin A (0.18g), supplied as the hydrogen sulphate salt, was dissolved in water (3ml) and a solution of barium iodide (0.12g) in water (4ml) was added. A white precipitate formed immediately. The suspension was centrifuged (~1000xg, 20 minutes) to give a clear supernatant which was readily decanted from a hard white pellet of barium sulphate. Freeze-drying of the supernatant produced a pale yellow, light powder of ristocetin A iodide salt (confirmed by standard chemical tests).

8.1.19 RISTOCETIN-Ψ-AGLYCONE

Ristocetin A (300mg) was heated under reflux in methanolic hydrogen chloride (5%, 15ml) for one hour. The volume was reduced to near-dryness (~0.5ml) and the residue redissolved in water (10ml). A solution of potassium carbonate (1M) was added to adjust to pH 7.5, at which point precipitation of crude Ψ-aglycone occurred. The precipitate was separated by centrifugation, redissolved in a minimum volume of aqueous acetic acid (6%) and applied to a gel-filtration (Sephadex G-25) column (1x120cm). The column was eluted with acetic acid (6%, 18ml/hour). An ultra-violet absorbing (280nm) component was eluted after 7.5 hours.

The eluate was freeze-dried to give the required product (80mg) which was found to be pure by TLC (BWA, R_F 0.55) and by HPLC (Bondapak C_{18} column, eluted with 0.05M KH_2PO_4/MeCN, 3:1, 2ml/minute).

8.2.1 TECHNIQUES

Of the techniques generally available[78] two in particular were used extensively and are described below.

(1) The Layering Method

A suitable precipitant was placed in a tube and then, with the aid of a hypodermic needle and syringe, a small amount of sample was very slowly injected beneath the precipitant layer. The latter had to be less dense than the sample solution and miscible with it. A ratio of 1:4 sample solution:precipitant was typically used, with sample volumes of 0.2ml. The tube was sealed and left undisturbed for various periods of time. Diffusion of the precipitant into the sample produced, if successful, crystals at the interface of the two solutions. An alternative method of applying the precipitant directly to the surface of the sample solution produced excessive disturbance of the interface.

(2) Vapour Diffusion

The principle is essentially the same as for the layering method but the precipitant is allowed to diffuse into the solution from the vapour phase. The sample solution (usually 0.2ml) was placed in an unsealed vial (0.5dram) which in turn was placed in a larger vial (3dram), containing the volatile precipitant, which was then sealed. Crystal formation was slower than for the layering method but improved crystal quality was often attained with this method. The main parameters which were varied were temperature, concentration of antibiotic and of course the solvent system.

8.2.2 VANCOMYCIN

Vancomycin is soluble in water and dmso, sparingly soluble in ethanol and methanol, and insoluble in chloroform and carbon tetrachloride. Experiments were therefore performed with solutions of vancomycin in either water or dmso.

Vancomycin (50mg) was dissolved in water (1ml) and a duplicate sample in dmso (1ml). Five equal portions of each of these solutions were used for vapour diffusion experiments with various solvents. The results after one week are shown in table 8.1.

Table 8.1 Vancomycin Crystallisation Experiments

Sample Solvent	Precipitant	Result
water	acetone	pptn
water	methanol	pptn
water	ethanol	pptn
water	i-propanol	pptn
water	DME	pptn
dmso	acetone	pptn+amres
dmso	$CHCl_3$	pptn
dmso	CH_2Cl_2	pptn+amres
dmso	CCl_4	oily residue

Abbreviations: pptn=precipitation, amres=amorphous residue, DME=1,2-dimethoxyethane.
All experiments were performed at 20°C.

8.2.3 VANCOMYCIN/AC-D-ALA-D-ALA

Vancomycin (73mg) and Ac-D-ala-D-ala (10mg) were dissolved in water (1ml). A viscous solution (pH2.4) was obtained which precipitated above pH3. Incubation under conditions similar to those which produced the crystals of CDP-I were tried (80°C for 16 hours) but produced a gel only. A similar result was obtained with a more dilute solution of vancomycin (28mg) and Ac-D-ala-D-ala (4mg).

Vancomycin (25mg) and Ac-D-ala-D-ala (3mg) were dissolved in water (1ml). a duplicate sample was dissolved in dmso (1ml). Each solution was divided into five equal portions which were then used for vapour diffusion experiments (25°C) with various solvents. The results obtained after two weeks are shown in table 8.2.

Table 8.2 Vancomycin/Ac-D-ala-D-ala Crystallisation Experiments

Sample Solvent	Precipitant	Result
water	acetone	pptn
water	80% acetone	neg
water	methanol	pptn
water	i-propanol	pptn
water	CH_2Cl_2	pptn
dmso	acetone	pptn
dmso	80% acetone	neg
dmso	methanol	pptn
dmso	CCl_4	amres
dmso	CH_2Cl_2	amres

Abbreviations: pptn=precipitation, neg=no residue, amres=amorphous residue.
All experiments were performed at 20°C.

8.2.4 RISTOCETIN A

Ristocetin A was found to be soluble in 95% methanol or 70% ethanol or 70% acetone. In addition, aqueous solutions with ristocetin concentrations of up to 20% were readily prepared. The results of many experiments, performed at 20°C unless otherwise stated, are shown in table 8.3.

Table 8.3 Ristocetin A Crystallisation Experiments

Risto(mg)	Sample Solvent	Precipitant	Method	Result(days)
5	70%acetone	acetone	VD	pptn(21)
5	70%EtOH	acetone	VD	amres(21)
5	95%MeOH	acetone	VD	amres(21)
5	water	acetone	VD	pptn(7)
5	70%acetone	95%EtOH	VD	neg(40)
5	70%EtOH	95%EtOH	VD	neg(40)
5	95%MeOH	95%EtOH	VD	neg(40)
5	water	95%EtOH	VD	neg(40)
15	70%EtOH	95%EtOH	L	neg(7)
5	70%EtOH	95%EtOH	L	neg(24)
5	70%EtOH	acetone	L	neg(24)
5	95%MeOH	EtOAc	L	neg(91)
5	70%EtOH	EtOAc	L	pptn(91)
5	water	EtOAc	L	neg(91)
5	70%acetone	EtOAc	L	neg(91)
5	95%MeOH	acetone	VD	pptn(5)
50	water	95%EtOH	VD	amres(11),5°C
50	water	95%EtOH	VD	amres(7)
50	water	acetone	VD	pptn(10),5°C
50	water	acetone	VD	pptn(7)
50	water	MeOH	VD	pptn(11),5°C
50	water	MeOH	VD	pptn(7)
50	water	75%acetone	VD	cryst(10)
50	water	MeOH	VD	amres(21)
50	water	95%EtOH	VD	pptn(21)
5+S	water	75%acetone	VD	cryst(2)
5	water	75%acetone	VD	cryst(4)
10+S	water	75%acetone	VD	cryst(2)
25	water	75%acetone	L	cryst(3)
10	water	75%acetone	VD	cryst(4)

Table 8.3 Continued

Risto(mg)	Sample Solvent	Precipitant	Method	Result(days)
10	water/MPD(3:1)	MPD	VD	cryst(11)
50	water/MPD(4:1)	MPD	VD	cryst(12)
50	water/MPD(2:1)	MPD	VD	cryst(12)
50	water/MPD(4:3)	MPD	VD	cryst(11)
50	water/MPD(1:1)	MPD	VD	cryst(12)
50	water/MPD(4:5)	MPD	VD	cryst(12)
50	water/MPD(2:3)	MPD	VD	cryst(12)
10	water	75%EtOH	VD	neg(7)
10	water	80%EtOH	VD	neg(7)
10	water	95%EtOH	VD	neg(7)
10	70%EtOH	75%acetone	VD	pptn(7)
10	water	EtOAc/EtOH(9:1)	L	amres(7)
10	water	EtOAc/EtOH(7:3)	L	amres(7)
10	water	EtOAc/EtOH(1:1)	L	amres(7)
10	water	EtOAc/EtOH(3:7)	L	amres(7)
10	water	EtOAc/EtOH(1:9)	L	amres(7)
10	water	EtOAc/EtOH(1:99)	L	amres(7)
20	water/MeOH(6:1)	75%acetone	VD	cryst(5)
20	water/EtOH(6:1)	75%acetone	VD	cryst(5)
20	water/TFA(6:1)	75%acetone	VD	cryst(5)
20	water/i-PrOH(6:1)	75%acetone	VD	cryst(5)
20	water/n-BuOH(6:1)	75%acetone	VD	cryst(5)
20	water/DMF(6:1)	75%acetone	VD	cryst(5)
20	water/t-AmOH	75%acetone	VD	cryst(5)
20	water	75%acetone	VD	cryst(13)
600	water	75%acetone	VD	cryst(38)

Abbreviations: pptn=precipitation, amres=amorphous residue cryst=crystals, neg=no residue, S=seeded, VD=vapour diffusion, L=layering, MPD=2-methylpentan-2,4-diol, TFA=trifluoroacetic acid, DMF=dimethylformamide, t-AmOH=t-amyl alcohol, i-PrOH=i-propanol, EtOAc=ethyl acetate, EtOH=ethanol, MeOH=methanol, n-BuOH=n-butanol, Risto=ristocetin A.

Several systems produced crystalline residues although none except for the water/75% acetone system were considered of suitable quality for x-ray analysis. The crystals obtained from the water/75%acetone solvent system were generally in the form of multiple clusters. The size of these

clusters was reduced by using more dilute solutions of ristocetin A but single crystals (suitable for x-ray analysis) were not routinely produced. All crystallisations performed up to this point had used commercial ristocetin without further purification, however improved crystals were obtained with purified ristocetin. The multiple crystals of ristocetin A were harvested by decanting the mother liquor, dissolving in water, pooling many samples and then freeze-drying. The whole cycle was repeated a further time and produced a white fluffy powder (commercial ristocetin A is pale brown in colour) which was used in subsequent crystallisations. The purified ristocetin A routinely produced single crystals from the water/75% acetone system and in greatly reduced times (within 2 days) although a further two weeks was usually necessary in order to obtain crystals of suitable size. Further crystallisation experiments using this purified material are shown in table 8.4, although none produced crystals superior in quality to those from the water/75%acetone system.

Table 8.4 Ristocetin A (purified) crystallisation Experiments

Risto(mg)	Precipitant	Result(days)
5	75%acetone	cryst(2)
5+S	75%acetone	cryst(1)
3	ethanol	pptn(34)
3	95%ethanol	pptn(34)
3	85%ethanol	pptn(34)
3	methanol	neg(34)
3	95%methanol	neg(34)
3	80%acetone	cryst(14)
3	75%acetone	cryst(14)
3	80%i-propanol	cryst(14)
3	EtOAc	neg(34)

Abbreviations: Risto=ristocetin A, S=seeded, pptn=precipitation, cryst=crystals, neg=no residue, EtOAc=ethyl acetate.
All experiments were performed at 20°C in aqueous solution with vapour diffusion of the precipitant.

Ristocetin A crystals from water/75%acetone - Crystal Data

The crystals were rhombic platelets which grew in stacks, often from a common edge. They were unstable in air and had to be enclosed in a glass capillary with some mother liquor present. The x-ray diffraction data was observable in part to $\sim 90^{\circ}$ with confirmed intensities at $2\theta = 86^{\circ}$. The crystals were not amenable to isomorphous replacement and posed severe mounting problems. $C_{95}H_{110}N_8O_{44}$, monoclinic, space group $P2_1$, a=26.68(1), b=27.77(1), c=20.48(1), β=101.88(1)°, V=14,899$\mathring{A}^3$.

The ristocetin A iodide salt was soluble in water, dimethylformamide, dmso, methanol, ethanol, 80% acetone$_{(aq)}$, 90% i-propanol$_{(aq)}$, 75% n-butanol in methanol, 40% ethyl acetate in methanol, 40% chloroform in methanol,30% carbon tetrachloride in methanol and was insoluble in diethyl ether. The results of crystallisation studies are presented in table 8.5.

Table 8.5 Ristocetin A Iodide Salt Crystallisation Experiments

Sample Solvent	Precipitant	Result(days)
water	75%acetone	neg(60)
water	85%acetone	neg(60)
water	95%acetone	amres(25)
water	95%i-propanol	neg(60)
water	n-BuOH/MeOH(4:1)	amres(25)
water/MPD(2:1)	MPD	pptn(25)
MeOH	n-BuOH	amres(6)
MeOH	ethanol	pptn(6)
MeOH	acetone	pptn(6)
DMF	diethyl ether	amres(6)
water	ethanol	neg(11)
water	i-propanol	neg(11)
water	n-BuOH	pptn(6)
water	chloroform	pptn(6)

Abbreviations: amres=amorphous residue, neg=no residue, pptn=precipitation, MPD=2-methyl-2,4-pentandiol n-BuOH=n-butanol, DMF=dimethylformamide, MeOH=methanol. All experiments were performed using 5mg ristocetin A iodide salt at 20°C with vapour diffusion of the precipitant.

Crystallisation by 'salting out' was performed as follows. Glass tubing (6cm long x 0.35cm i.d.) was sealed at one end with restricted-pore dialysis tubing (prepared by soaking Visking dialysis tubing in acetic anhydride/pyridine, 1:1, for 10 minutes), filled with aqueous ristocetin A solution (10%) and the other end sealed with a stopper. The tube was then immersed in a saturated salt solution (either ammonium sulphate or potassium dihydrogen phosphate). Both of the salts used produced clusters of very fine needle-like crystals but they were not suitable for x-ray analysis.

8.2.5 RISTOCETIN-Ψ-AGLYCONE

Crystal studies were also performed on the Ψ-aglycone derivative of ristocetin A which was soluble in water, methanol and ethanol, sparingly soluble in i-propanol and insoluble in acetone, diethyl ether, n-hexane, chloroform and methylene chloride. The results are presented in table 8.6.

Table 8.6 Ristocetin Ψ-Aglycone Crystallisation Experiments

Sample Solvent	Precipitant	Result(days)
water	acetone	pptn(5)
water	CH_2Cl_2/MeOH(1:1)	pptn(5)
water	$CHCl_3$/MeOH(1:1)	pptn(5)
MeOH	diethyl ether	pptn(5)
MeOH	Et_2O/MeOH(3:1)	pptn(5)
MeOH	Et_2O/MeOH(1:1)	pptn(5)
MeOH	acetone/MeOH(1:1)	neg(5)

Abbreviations: pptn=precipitation, neg=no residue, Et_2O=diethyl ether, MeOH=methanol.
All experiments used 5mg ristocetin Ψ-aglycone at 20°C with layering of the precipitant.

The vapour diffusion experiment was modified in order to reduce the rate at which the precipitant condensed on the surface of the sample. The inner sample vial was sealed with a plastic cap which had a small hole pierced in it, thus limiting the rate of diffusion of the volatile solvent into the small vial. The results are presented in table 8.7.

Table 8.7 Ristocetin Ψ-Aglycone Crystallisation Experiments - 2

Sample Solvent	Precipitant	Result(days)
methanol	diethyl ether	pptn(7)
methanol	chloroform	pptn(7)
methanol	acetone	pptn(7)
methanol	pet. ether*	pptn(25)

Abbreviations: pptn=precipitation, pet. ether=petroleum ether (boiling range 60°-80°C).
All experiments used 5mg antibiotic and vapour diffusion at 20°C.

8.2.6 RISTOCETIN A/PEPTIDE

Experiments were also performed with ristocetin A and Ac-D-ala-D-ala or Ac_2-L-lys-D-ala-D-ala in solution together in order that crystals of the complex formed between them could be obtained. The results are presented in table 8.8.

Table 8.8 Ristocetin A/Peptide Crystallisation Experiments

Peptide	Sample Solvent	Precipitant	Result(days)
dipep	water	80%ethanol	cryst(115)
dipep	water	75%acetone	cryst(115)
dipep	water	90%methanol	amres(115)
dipep	water/MPD(1:1)	MPD	pptn(115)
dipep	water	75%acetone	cryst(7)
tripep	water	75%acetone	cryst(7)

Abbreviations: dipep=Ac-D-ala-D-ala, tripep=Ac_2-L-lys-D-ala-D-ala, cryst=crystals, pptn=precipitation, amres=amorphous residue, MPD=2-methyl-2,4-pentandiol.
All experiments used 10.3mg antibiotic and either 1.0mg dipeptide or 1.8mg tripeptide and vapour diffusion at 20°C.

The crystals obtained from ristocetin A/tripeptide were not stable upon storage and decomposed within 2-3 days of being formed. On the other hand, the crystals of ristocetin A/dipeptide (from water/75%acetone) were of high quality. Preliminary x-ray analysis of the latter complex has

shown the crystals to be cubic with 24 trimer units per unit cell. The cell volume was correspondingly large ($\sim$140,000$\mathring{A}^3$).

8.3 NMR EXPERIMENTS

All nmr experiments were performed with 0.4-0.6ml samples in 5mm tubes. Three machines were used for the studies (exclusively proton) described in this dissertation.

A Varian XL-100-15 (100MHz) machine was operated in the Fourier transform mode with a spectral width of 1000Hz (10.0ppm), a 90° pulse width of 0.07 seconds and 8192 data points (producing an acquisition time of 4 seconds). Most of the 100MHz experiments were used for analysis only and with sufficient sample available that few transients (typically 16 or less) were necessary in order to obtain acceptable signal to noise in the spectrum.

The conformational and mode of action studies were performed at higher field which resulted in spectral simplification. A Bruker WH-270 (270MHz) with associated Nicolet software was operated in the Fourier transform mode with quadrature detection and phase alternation. A spectral width of 3000Hz (11.1ppm) was used, except when peptide was present in the binding studies on vancomycin in which case 3500Hz (13.0ppm) was used. A pulse width of around 0.008 seconds was used in conjunction with 8192 data points and an acquisition time of 1.37 or 1.17 seconds (for 3000Hz or 3500Hz respectively). Finally, a Bruker WH-400 (400MHz) with associated Bruker software was operated in the Fourier transform mode with quadrature detection and phase alternation. Sensitivity enhancement was usually employed to reduce the effect of noise on the spectrum. A spectral width of 4000Hz (10.0ppm) was used, except for the vancomycin binding studies in the presence of peptide when 5200Hz (13.0ppm) was used. A 90° pulse of around 0.008 seconds was used in addition to 8192 data points and an acquisition time of 1.02 or 0.79 seconds (for 4000Hz or 5200Hz respectively). The 400MHz reference spectra (not the spectra obtained from double

irradiation) displayed in this thesis were enhanced by multiplication of the free induction decay by a Gaussian function, typically using a line broadening constant of -2 or -3 and a Gaussian factor (actually the fraction of the FID containing useful information) of 0.3-0.35. A non-Gaussian sensitivity enhancement was usually employed with all other spectra. This distinction between the enhancement methods arose because in practice the Gaussian function, although generally considered superior for sensitivity enhancement in most applications compared to the usual negative exponential function, was very time consuming to operate, typically taking 3-4 minutes for the data manipulation of 8192 data points compared to the 3-5 seconds for the simpler alternative. Obviously as the software improves this situation may change.

Difference spectra were obtained by the simultaneous accumulation of a reference spectrum, in which part of the spectrum void of any resonances was irradiated, and a series of spectra (typically up to 20) in which one resonance was irradiated in each. The standard Bruker microprograms were used throughout. Transients were accumulated up to a maximum of 2000 (usually less than 400) in multiples of 8 or 16. Typical decoupler power settings used were 5-9L for spin-decoupling experiments and 15-19L for nOe experiments. The following amounts of compound were used for the nmr studies. Triostin A (1μmole, 1mg), aglucovancomycin (10μmoles, 11.5mg), vancomycin (10μmoles, 15.0mg) and the corresponding multiples of peptide, Ac-D-ala-D-ala (10μmoles, 2.0mg) and Ac_2-L-lys-D-ala-D-ala (10μmoles, 3.8mg).

9. REFERENCES

1. M.H.McCormick, W.M.Stark, G.F.Pittenger, R.C.Pittenger and G.M.McGuire, Antibiotics Annual, 1955-1956, 606.

2. M.G.Brazhnikova, N.N.Lomakina, M.F.Lavrova, I.V.Tolstykh, M.S.Yurina and L.M.Klyueva, Antibiotiki, 1963, **8**, 392.

3. M.P.Kunstmann, L.A.Mitscher, J.N.Porter, A.J.Shay and M.A.Darken, Antimicrobial Agents Annual, 1968, 242.

4. V.A.Shorin, S.D.Yudnitsev and I.A.Kunrat, Antibiotiki, 1957, **5**, 44.

5. K.H.Michel and M.DeBono, Abstracts, 17th Interscience Conference, Antimicrob. Ag. Chemother., New York, 1977.

6. M.R.Bardone, G.Tuan and C.Coronelli, Abstracts, 11th International Symposium on Chemistry of Natural Products, Golden Sands, Bulgaria.

7. R.L.Hamill, W.M.Stark and D.C.DeLond, US Patent 4115552, 1978.

8. A.P.Raun, US Patent 3816618, 1974.

9. D.W.Ziegler, R.N.Wolfe and J.M.McGuire, Antibiotics Annual, 1956-1957, 612.

10. F.Tedesco, R.Markham, M.Gurwith, D.Christie and J.G.Bartlett, Lancet, 1978, 226.

11. M.R.B.Keithley, D.W.Burdon, Y.Arabi, J.Alexander-Williams, H.Thompson, D.Youngs, M.Johnson, S.Bentley, R.H.George and G.A.G.Mogg, Brit. Med. J., 1978, 1667.

12. W.E.Grundy, Antibiotics Annual, 1956-1957, 687.

13. J.E.Philip, J.R.Schenck and M.P.Hargie, Antibiotics Annual, 1956-1957, 699.

14. D.H.Williams, V.Rajananda and J.R.Kalman, J. Chem. Soc., Perkin Trans. 1, 1979, 787.

15. H.A.Lechevalier and M.P.Lechevalier, Annual Review Microbiology, 1967, **21**, 71.

16. J.E.Philip, J.R.Schenck, M.P.Hargie, J.C.Holper and W.E.Grundy, Antimicrob. Ag. Chemother., New York, 1960, 10.

17. B.S.Coller, W.B.Lundberg and H.R.Gralnick, Thromb. Diath. Haemorrh., 1975, **34**, 83.

18. M.A.Howard, R.A.Hutton and R.M.Hardisty, Brit. Med. J., 1973, 586.

19. E.F.Mammen, Semin. Thromb. Hemostasis., 1971, **2**, 61.

20. M.A.Howard and B.G.Firkin, Thromb. Diath. Haemorrh., 1971, **26**, 362.

21. S.S.Kuwahara and W.T.Chambers, Experientia, 1978, **34**, 532.

22. J.Shoji and K.Katagiri, J. Antibiotics, Ser. A (Tokyo), 1961, **14**,335.

23. W.Keller-Schierlein, M.L.Mihailovic and V.Prelog, Helv. Chim. Acta, 1959, **42**, 305.

24. W.Y.Chen, M.L.Hsu and R.K.Olsen, J. Org. Chem., 1975, **40**, 3110.

25. T.L.Ciardelli and R.K.Olsen, J. Am. Chem. Soc., 1977, **99**, 2806.

26. M.A.Viswamitra, O.Kennard, W.B.T.Cruse, E.Egert, G.M.Sheldrick, P.G.Jones, M.J.Waring, L.P.G.Wakelin and R.K.Olsen, Nature, 1981, **289**, 817.

27. J.S.Lee and M.J.Waring, Biochem J., 1978, **173**, 115.

28. M.J.Waring, in 'Antibiotics', Vol. 5, Pt. 2, ed. F.E.Hahn, Springer, Heidelberg, 1979, p.173.

29. F.J.Marshall, J. Med. Chem., 1965, **8**, 18.

30. C.R.Johnson, Ph.D. thesis, University of Illinois, 1962.

31. P.J.Roberts, O.Kennard, K.Smith and D.H.Williams, J. Chem. Soc., Chem. Commun., 1973, 772.

32. D.H.Williams and J.R.Kalman, Tetrahedron Lett., 1976, 4829.

33. W.D.Weringa, D.H.Williams, J.Feeney, J.P.Brown and R.W.King, J. Chem. Soc., Perkin Trans. 1, 1972, 443.

34. A.W.Johnson, R.M.Smith and R.D.Guthrie, J. Chem. Soc., Perkin Trans. 1, 1972, 2153.

35. K.A.Smith, D.H.Williams and G.A.Smith, J. Chem. Soc., Perkin Trans. 1, 1974, 2369.

36. G.A.Smith, K.A.Smith and D.H.Williams, J. Chem. Soc., Perkin Trans. 1, 1975, 2108.

37. D.H.Williams and J.R.Kalman, J. Am. Chem. Soc., 1977, **99**, 2768.

38. G.M.Sheldrick, P.G.Jones, O.Kennard, D.H.Williams and G.A.Smith, Nature, 1978, **271**, 223.

39. M.G.Brazhnikova, N.N.Lomakina, F.Sztaricskai, M.M.Puskas, S.Makleit and R.Bognar, Kem. Kozlem., 1967, **27**, 143.

40. N.N.Lomakina, L.I.Muravyeva and M.Puskas, Antibiotiki, 1968, **13**, 867.

41. F.Sztaricskai, R.Bognar and M.M.Puskas, Acta chim. Acad. Sci. Hung., 1975, **84**, 75.

42. M.P.Williamson and D.H.Williams, Tetrahedron Lett., 1980, 4187.

43. F.Sztaricskai, A.Neszmelyi and R.Bognar, Tetrahedron Lett., 1980, 2983.

44. F.Sztaricskai, I.Pelyvas and R.Bognar, Tetrahedron Lett., 1975, 1111.

45. N.N.Lomakina, R.Bognar, M.G.Brazhnikova, F.Sztaricskai and L.I.Muravyeva, 7th International Symposium on the Chemistry of Natural Products, Riga, 1970.

46. J.R.Fehlner, R.E.J.Hutchinson, D.S.Tarbell and J.R.Schenck, Proc. Nat. Acad. Sci. USA, 1972, **69**, 2420.

47. T.M.Harris, J.R.Fehlner, A.B.Raabe and D.S.Tarbell, Tetrahedron Lett., 1975, 2655.

48. C.M.Harris, J.J.Kibby, J.R.Fehlner, A.B.Raabe, T.A.Barber and T.M.Harris, J. Am. Chem. Soc., 1979, **101**, 437.

49. V.Rajananda, A.F.Norris and D.H.Williams, J. Chem. Soc. Pakistan, 1979, **1**, 29.

50. D.H.Williams, V.Rajananda, G.Bojesen and M.P.Williamson, J. Chem. Soc., Chem. Commun., 1979, 906.

51. J.R.Kalman and D.H.Williams, J. Am. Chem. Soc., 1980, **102**, 897.

52. H.Otsuka and J.Shoji, Tetrahedron, 1967, **23**, 1535.

53. T.J.Blake, J.R.Kalman and D.H.Williams, Tetrahedron Lett., 1977, 2621.

54. J.R.Kalman, T.J.Blake, D.H.Williams, J.Feeney and G.C.K.Roberts, J. Chem. Soc, Perkin Trans. 1, 1979, 1313.

55. H.T.Cheung, J.Feeney, G.C.K.Roberts, D.H.Williams, G.Ughetto and M.J.Waring, J. Am. Chem. Soc., 1978, **100**, 46.

56. E.Cundliffe, E.F.Gale, P.E.Reynolds, M.H.Richard and M.J.Waring, 'The Molecular Basis of Antibiotic Action', Wiley, 1972.

57. C.H.Wallas and J.L.Strominger, J. Biol. Chem., 1963, **238**, 2264.

58. P.E.Reynolds, Biochim. Biophys. Acta, 1961, **52**, 403.

59. D.C.Jordan, Biochem. Biophys. Res. Commun., 1961, **6**, 167.

60. H.R.Perkins, Biochem. J., 1969, **111**, 195.

61. M.Nieto and H.R.Perkins, Biochem. J., 1971, **123**, 773.

62. M.Nieto and H.R.Perkins, Biochem. J., 1971, **123**, 789.

63. M.Nieto and H.R.Perkins, Biochem. J., 1971, **124**, 845.

64. J.P.Brown, J.Feeney and A.S.V.Burgen, Mol. Pharmacology, 1975, **11**,119.

65. J.P.Brown, L.Terenius, J.Feeney and A.S.V.Burgen, Mol. Pharmacology, 1975, **11**, 126.

66. O.Convert, A.Bongini and J.Feeney, J. Chem. Soc., Perkin Trans. 2, 1980, 1262.

67. J.R.Kalman and D.H.Williams, J. Am. Chem. Soc., 1980, **102**, 906.

68. E.Schnabel, Liebigs Ann. Chem., 1967, **702**, 188.

69. M.Itoh, D.Hagiwara and T.Kamiya, Tetrahedron Lett., 1975, 4393.

70. B.F.Erlanger and R.M.Hall, J. Am. Chem. Soc., 1954, **76**, 5781.

71. L.Zervas, M.Winitz and J.P.Greenstein, J. Org. Chem., 1957, **22**, 1515.

72. G.W.Anderson, J.E.Zimmerman and F.M.Callahan, J. Am. Chem. Soc., 1964, **86**, 1839.

73. D.H.Williams and D.W.Butcher, J. Am. Chem. Soc., 1981, in press.

74. D.H.Williams, personal communication.

75. W.B.T.Cruse, personal communication.

76. M.P.Williamson and D.H.Williams, J. Chem. Soc., Chem. Commun., 1981, 165.

77. R.C.Pandey, R.Misra and K.L.Rinehart, J. Chromatog., 1979, **170**, 498.

78. P.G.Jones, Chem. in Brit., 1981, **17**, 222.

APPENDIX 1

SELECTED BIBLIOGRAPHY

(1) **BACTERIAL CELL WALL**

(a) P.M.Meadow, in 'Companion to Biochemistry - Selected Topics for Further Study', eds. A.T.Bull, J.R.Lagnado, J.O.Thomas and K.F.Tipton, Longman, 1974, ch.10.

(b) J-M.Ghuysen and G.D.Shockman, in 'Bacterial Membranes and Walls', ed. L.Leive, Marcel Dekker Inc., New York, 1973, ch.2.

(c) P.M.Blumberg and J.L.Strominger, Bacteriol. Rev., 1974, **38**, 291.

(2) **MODES OF ACTION OF ANTIBIOTICS**

(a) T.J.Franklin and G.A.Snow, 'Biochemistry of Antimicrobial Action', 3rd Edn., Chapman and Hall, 1981.

(b) E.F.Gale, E.Cundliffe, P.E.Reynolds, M.H.Richmond and M.J.Waring, 'The Molecular Basis of Antibiotic Action', Wiley, 1972.

(3) **THE VANCOMYCIN GROUP OF ANTIBIOTICS**

D.H.Williams, V.Rajananda, M.P.Williamson and G.Bojesen, in 'Topics in Antibiotic Chemistry', Vol.5, ed. P.Sammes, Ellis Horwood, 1980, p119.

(4) **THE QUINOXALINE ANTIBIOTICS**

M.J.Waring, in 'Antibiotics', Vol.5, Pt.2, ed. F.E.Hahn, Springer, Heidelberg, 1979, p173.

(5) NMR SPECTROSCOPY

(a) H.Gunther, 'NMR Spectroscopy', Wiley, 1980.

(b) D.H.Williams and I.Fleming, 'Spectroscopic Methods in Organic Chemistry', 2nd Edn., McGraw-Hill, 1973, ch.3.

(c) T.C.Farrar and E.C.Becker, 'Pulse and Fourier Transform NMR - Introduction to Theory and Methods', Academic Press, 1971.

(d) D.Shaw, 'Fourier Transform NMR Spectroscopy', Elsevier, 1976.

(e) J.W.Cooper, in 'Transform Techniques in Chemistry', ed. P.R.Griffiths, Plenum, 1978, ch.4.

(f) T.C.Farrar, ibid., ch.8.